

國立臺灣大學工學院機械工程學系

碩士論文

Department of Mechanical Engineering

College of Engineering



National Taiwan University

Master Thesis

以機率模型預測都會區路口的駕駛行爲

Probabilistic Modeling of Driver Behaviors

at Urban Crossroads

劉員成

Yuan-Cheng Liu

指導教授：詹魁元博士

Advisor: Kuei-Yuan Chan, Ph.D.

中華民國 108 年 7 月

July, 2019

國立臺灣大學
機械工程學系

碩士論文

以機率模型預測都會區路口的駕駛行爲

劉員成 撰

國立臺灣大學碩士學位論文

口試委員會審定書

以機率模型預測都會區路口的駕駛行爲

Probabilistic Modeling of Driver Behaviors

at Urban Crossroads

本論文係劉員成君 (R06522616) 在國立臺灣大學機械工程
學系完成之碩士學位論文，於民國 108 年 7 月 19 日承下列考
試委員審查通過及口試及格，特此證明

口試委員：


(簽名)

(指導教授)

劉達

鄭宇和

系主任、所長

董文娟

(簽名)



© YUAN-CHENG LIU 2019

All Rights Reserved



For all the people



ACKNOWLEDGEMENTS

首先要感謝所有口試委員給我在這篇碩士論文上的建議，這些建議使得這篇論文變得更加完整。這其中最需要特別感謝我的指導老師，詹魁元教授，不但在研究過程中給了我許多有趣且具啟發性的想法，也在生活歷練與待人處世上給了許多寶貴的經驗。

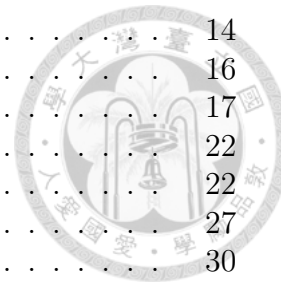
感謝 SOLab 的所有夥伴在學習與生活上的砥礪，謝謝彥智提供無限的圖書資源與紮實而謙遜的知識。謝謝盈樺在剛進實驗室時幫助與建議；顯主在計畫上的教導與支援；穎寬無私的奉獻與所帶來不自覺的歡樂。謝謝心婷那直率而精確的態度；還有柏宇教會我吃素的藝術。謝謝中信這個強而有力的幫手；世哲、峻廷、旻憲、路寧、奕憲、怡平與宥廷時而邂逅的美好。感謝期璟與柏賢的幫助，讓我們能夠心無旁騖。感謝所有專業的車手，尤其是柏賢與冠頓貢獻出寶貴的無數時光。

感謝瑄瑄與阿姨，讓我也能專心的寫論文。最後感謝家人們作爲我最堅強的後盾，謝謝你們。



TABLE OF CONTENTS

口試委員會審定書	i
DEDICATION	v
ACKNOWLEDGEMENTS	vi
LIST OF FIGURES	ix
LIST OF TABLES	xiv
LIST OF ABBREVIATIONS	xv
摘要	xvi
ABSTRACT	xvii
CHAPTER	
I. Introduction	1
1.1 Motivation	1
1.2 Thesis Structure	4
II. Background and Literature Review	7
2.1 Introduction	7
2.2 Physics-Based Models	7
2.3 Driver Behavior Models	9
2.4 Interactive Models	10
2.5 Explicit Driver Behavior Models	11
2.6 Summary	12
III. Human Driver Modeling at Crossroads	13
3.1 Time to Collision and Time for Action	14



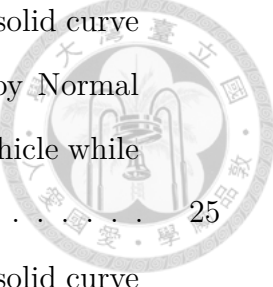
3.1.1	Crossroad Modeling	14
3.1.2	Time to Collision	16
3.1.3	Time for Action	17
3.2	The TFA Distribution	22
3.2.1	TFA Distribution	22
3.2.2	TFA Probability Density Function	27
3.3	Probability of Yielding	30
3.3.1	TFA Distribution Modeling	31
3.3.2	The Model for Probability of Yielding Estimation .	37
3.4	Driver Intentions Prediction with Probability of Yielding . .	44
3.4.1	Urban Crossroads in Simulated Environment	44
3.4.2	Experimental Results in Simulated Environment . .	49
3.4.3	Validation for Experiments in Simulated Environment	57
IV.	Model Parameters Identification	61
4.1	Characteristic Parameters	61
4.2	Objective Function and Constraints for Optimization	67
4.3	Optimization Using Simulated Annealing	71
V.	Applications	81
5.1	Crash Examinations in the Simulated Crossroad	81
5.1.1	Crashing Likelihood Using TFA Distributions	82
5.1.2	TTC differences and POYs	87
5.2	POY Estimation at Urban Crossroads	91
5.3	Procedures for Autonomous Vehicle	96
VI.	Conclusions and Future Works	101
6.1	Conclusions	101
6.2	Future Works	102
BIBLIOGRAPHY		103



LIST OF FIGURES

Figure

1.1	A crossroad with no signal.	3
1.2	Thesis structure.	5
2.1	Physics-Based Model.	8
2.2	Driver Behavior Model.	10
2.3	Interactive Model.	11
3.1	Demonstration of the proposed scenario and relevant variables. . .	15
3.2	Illustrations of TTC and TFA.	18
3.3	History of time to collision when brake is applied.	19
3.4	The host driver estimate the possible position of the oncoming vehicle depending on its current states. To avoid the potential collision, the host driver adjust the time to brake as if the oncoming vehicle is at the intersection.	21
3.5	Example of TFA of general people and TTC of the host agent. . .	23
3.6	TFA results of participant 1 displayed in histogram. The solid curve is the TFA distribution of participant 1 approximated by Normal distribution ($\mu = 2.35, \sigma = 0.29, N = 97$). Speed of the vehicle while braking was set to 5 m/s.	25



3.7	TFA results of participant 2 displayed in histogram. The solid curve is the TFA distribution of participant 2 approximated by Normal distribution ($\mu = 2.37, \sigma = 0.35, N = 47$). Speed of the vehicle while braking was set to 5 m/s.	25
3.8	TFA results of participant 3 displayed in histogram. The solid curve is the TFA distribution of participant 3 approximated by Normal distribution ($\mu = 2.05, \sigma = 0.21, N = 47$). Speed of the vehicle while braking was set to 5 m/s.	26
3.9	TFA results of participants are displayed in histogram. The solid curve is the TFA distribution of combined data of participants approximated by Normal distribution ($\mu = 2.37, \sigma = 0.35, N = 197$). Speed of the vehicle while braking was set to 5 m/s.	27
3.10	Example of TFA of general people and TTC of the host agent.	29
3.11	Example of TFA distribution of general people.	30
3.12	Decomposing the distance left before action (apply the brake).	31
3.13	The TFA scatter plot of Participant 1 under various velocities.	34
3.14	The TFA scatter plot of Participant 3 under various velocities.	34
3.15	The R_{min} scatter plot of combined data under various velocities.	35
3.16	The a_{dec} scatter plot of combined data under various velocities.	36
3.17	History of TTC as the vehicle accelerating through the node.	39
3.18	The probability before the weighting parameter A_t is 0.5	42
3.19	The probability after the weighting parameter A_t is 0.97	42
3.20	The simulated crossroad scenario in the Gazebo simulator.	45
3.21	Front camera from driver seat in the simulated environment.	46
3.22	Left camera from driver seat in the simulated environment.	47
3.23	Right camera from driver seat in the simulated environment.	47
3.24	First driver in the simulated crossroad interaction experiment.	48

3.25	Second driver in the simulated crossroad interaction experiment.	48
3.26	Illustration of TTC and probability of stopping along with concerning variables.	49
3.27	Trial #003 where car_0 was yielding and car_1 was passing with little interaction.	50
3.28	Trial #003 using POY without weighting parameter A (α).	52
3.29	Trial #003 using POY without acceleration threshold.	53
3.30	Trial #077 where car_0 and car_1 were confused about what action the other one might take.	55
3.31	Trial #063 where car_0 yielded first but then passed due to the deceleration of car_1	56
3.32	CARate of the POY using all data sets.	58
3.33	Trial #039 where car_1 begun to accelerate before car_0 passed the node, causing the false prediction.	59
4.1	Trial #003 with POY using average parameters and parameters of Participant 1.	63
4.2	Trial #077 with POY using average parameters and parameters of Participant 1.	64
4.3	The R_{min} scatter plot of Participant 1 under various velocities.	65
4.4	The R_{min} scatter plot of Participant 3 under various velocities.	65
4.5	The a_{dec} scatter plot of Participant 1 under various velocities.	66
4.6	The a_{dec} scatter plot of Participant 3 under various velocities.	66
4.7	CARate curve of POY using average parameters and characteristic parameters are compared.	68
4.8	CARate curve of POY using characteristic parameters and the parameters set of another participant are plotted.	69

4.9	Optimized parameters of R_{min} are compared with characteristic parameters.	74
4.10	Optimized parameters of a_{dec} are compared with characteristic parameters.	75
4.11	CARate curve of POY using characteristic parameters and optimized parameters are plotted.	76
4.12	Trial #003 using the optimized parameters and the characteristic parameters.	78
4.13	Trial #077 using the optimized parameters and the characteristic parameters.	79
5.1	The velocities and displacements versus POYs of a normal case where no collision happened.	83
5.2	TFA distributions of Participant 1, 2 and average of a normal case where no collision happened.	84
5.3	The velocities and displacements versus POYs of a normal case where a collision did happened.	85
5.4	TFA distributions of Participant 1, 2 and average of a normal case where a collision did happened.	86
5.5	Situation where vehicles attempting to cross the intersection passed without any collision. Note that the TTC differences rose before POYs.	89
5.6	Situation where vehicles attempting to cross the intersection collided with each other. Note that the TTC differences rose way after POYs.	90
5.7	Using video analysis tool to track vehicles driven by humans.	91
5.8	The corresponding POY curve at a crossroad in real world (Case I). car_0 had the dominance position and passed at the end.	93
5.9	The corresponding POY curve at a crossroad in real world (Case II). car_1 had the dominance position but yield at the end.	94

5.10	Both drivers yielded at the beginning of the interaction.	96
5.11	Flow chart for autonomous vehicle to deal with the interactions with human drivers.	97
5.12	The POYs during the interaction between human driver and au- tonomous vehicle (computer driver) in the simulated environment. .	99
5.13	The scene of interaction between human driver and autonomous ve- hicle with navigation algorithm in the simulated environment. . . .	100



LIST OF TABLES

Table

3.1	Table for parameters used in TFA distribution model.	37
4.1	Table for characteristic and average parameters.	67
4.2	Table for results of the proposed optimization problem.	73
4.3	Table for parameters used in the Simulated Annealing.	74



LIST OF ABBREVIATIONS

TTC Time to Collision

TFA Time for Action

Q-Q Plots Quantile Quantile Plots

POY Probability of Yielding

CARate Classification Accuracy Rate

SA Simulated Annealing



摘要

以機率模型預測都會區路口的駕駛行爲

劉員成 著作

無人車與人類駕駛的互動與溝通，將會在不遠的將來成為主要的議題。在這篇論文中，本論文將研究聚焦於最仰賴互動的無交通號誌十字路口。為了研究駕駛是如何進行決策來安全通過路口，本論文首先定義了路口的重要參數，包括了互動車輛的速度與離路口的距離，並定義了一個駕駛決策行爲。藉由研究此決策行爲，本論文得到了互動車輛煞車讓道的機率，以及駕駛行爲的機率模型。為了驗證此模型，本論文在模擬環境中進行測試，並蒐集真人駕駛的數據進行分析。所得到的驗證結果證明，所提出模型的預測準確率與現有方法接近，且具有更廣泛的應用，同時此預測模型也能夠反映出不同駕駛特徵參數的差異。接著，本論文嘗試使用最佳化方法，藉由所蒐集數據進行駕駛行爲的特徵參數回推。儘管此參數辨認的準確率尚有改進空間，目前所得到結果證明了所提出模型在此應用上的可行性。同時，為了驗證此模型在實際路口的可行性，本論文蒐集了真實路口的車輛數據並使用所提出模型進行行爲預測，所得結果與模擬環境中的結果一致。最後，本論文將所提出模型應用在無人車的決策行爲上並與人類駕駛進行互動，初步結果證明無人車的駕駛行為能夠更順暢的與人類駕駛進行互動。

關鍵字：混流，無人駕駛，機率模型，駕駛行爲，十字路口，互動模型，避障。



ABSTRACT

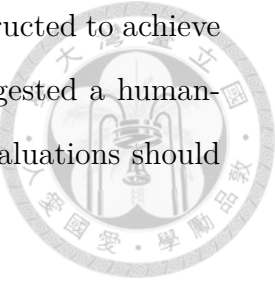
Probabilistic Modeling of Driver Behaviors at Urban Crossroads

by

YUAN-CHENG LIU

The interactions with human drivers is one of the major challenges for autonomous vehicles in the near future. In this work we consider urban crossroads without signals where driver interactions are indispensable. Crossroad parameters are defined and how drivers passing the crossroad while maintaining a desired speed without collision is studied. A point of action is defined for incoming vehicles from different directions and a probability of yielding for each car is proposed as a function of vehicle speed and the distance-to-intersection for both vehicles. Driver behaviors with these probability models are also proposed. The method is then analyzed and validated by data collected from human drivers in the simulated environments. The result shows comparable prediction accuracy to the state of the art method, where characteristic parameters of drivers are also shown to be critical for the behavior predictions. Afterwards, parameters representing driving styles of drivers are attempted to identify using the optimization approach. In spite of the limited accuracy of parameter identifications, important attributes of the proposed model as well as possible modification are pinpointed. The proposed model is also applied at the urban crossroads to evaluate the applicability in real world. The prediction results are analogous to

those acquired in virtual environments. Finally, a procedure is constructed to achieve smoother interactions with human drivers. Preliminary results suggested a human-like computer driver is born while more instances and aspects of evaluations should be accomplished in the future work.



Keywords: mixed-fleet, autonomous vehicle, probabilistic model, driver behavior, crossroad, interaction model, collision avoidance.



CHAPTER I

Introduction

Complex interactions between drivers are often observed at urban crossroads, especially those without traffic signals. In this thesis, the human driver behaviors at crossroads are modeled in a probabilistic way. In the Chapter II, techniques for motion planning are reviewed. Similar topics regarding the behavior prediction at the crossroad are also brought out. The central idea of this thesis is introduced in Chapter III, where the cognitive states during the interaction are examined and modeled. The parameters representing the driving styles of drivers are attempted to identify in Chapter IV. In Chapter V, possible applications of the proposed model are explored and verified. Finally, the conclusions and future works are discussed and listed in Chapter VI.

1.1 Motivation

Since 2006, the year when the concept of autonomous vehicles came alive and into urban environments, the autonomous vehicle industry has been growing rapidly [1]. Before the end of 2018, Waymo's self-driving vehicles had driven more than 10 million miles in 25 cities across the United States. Besides Waymo, 47 autonomous vehicle companies are also testing their self-driving cars in the urban area of California. Those optimistic predictions claim that by 2030, most of the human driving vehicles

will be replaced by autonomous vehicles, and that it will be a solution to congestion, accidents due to human errors and air pollution. However, it doesn't seem to be so simple.

First, according to the work of Bansal et al. [2], fully autonomous vehicles are unlikely to be ready by 2030. They also use a simulation-based fleet evolution framework to predict long-term (year 2015-2045) adoption rates of connected and autonomous vehicles (CAVs) under different scenarios. The result suggests that the vehicle fleet is likely to have only 24.8% level 4 (which is level 5 using the current definition of US Department of Transportation [3]) autonomous vehicle penetration by 2045. McKinsey & Company and Frost and Sullivan also forecast that only 15% of passenger vehicles will be fully autonomous by 2030 and that level 3 and level 4 are expected to account for approximately 0.8% and 2.3% by 2023.

Apart from the fact that the technology itself is still at a preliminary stage where there is no commercially available level 4 vehicles exist in the market. The amount of autonomous vehicles needs to reach a certain threshold for more practical discussions, such as policy, legislation, infrastructure and consumer acceptance [4]. Before these four key components and the technology itself are well prepared, it is not possible to see fully autonomous vehicle being adopted by 100%. As a consequence, it is foreseeable that the human-driving and computer-driving *mixed traffic flow* will comprises the major part of the traffic flow during the transition stage that might last more than 30 years. Therefore, the major challenge during this stage would be the interaction between human drivers and computer drivers.

In most of urban traffic scenarios, such as merging into lanes, entering roundabouts and crossing over crossroads without signals, drivers rely heavily on interactions with surrounding agents to blend in the traffic. For example, in Fig. 1.1 an unsignalized crossroad in central Taiwan is shown. Colored arrows represent the velocity vectors of the traffic participants. In the scene, interactions among traffic participants are



Figure 1.1: A crossroad with no signal.

based on their perception of others' intentions, and their capability in presenting their own. For example, at an unsignalized intersection, human drivers usually slow down (but not entirely stopped) or do some gesture if they intend to yield. Autonomous vehicles, on the other hand, might pose a threat to road traffic safety due to the lack of the ability to perceive the intentions of surrounding agents. According to the report of traffic collision involving autonomous vehicles published by the state of California Department of Motor Vehicles (DMV) [5], autonomous vehicles being rear-ended accounts for 18 of the 33 filed reports in 2019 (as of June 17, 2019). Even though there is not much detailed documentation describing how the accident happened, we still can learn the fact that most of the accidents (over 60%) happened while the autonomous vehicle was yielding to someone. Autonomous vehicles are designed to drive conservatively for the cause of safety, but when those behaviours are not understandable to human drivers, autonomous vehicles become a potential threats to other road users.

This research presents and initial attempt to comprehend the intentions of human drivers at an unsignalized intersection, where drivers, no matter humans or computers, are required to have more intense interaction than those at other intersections with signals or explicit rules. The targeted driver behavior model should enable the

computer driver to understand and interact with human drivers smoothly so as to eliminate the potential threats in human-computer mixed traffic flow. Primary goals as well as the process of the model construction are listed as follow:



1. Driver decision making process

How human drivers perceive and react to the traffic participants at the crossroad is required to be identified.

2. Driver behaviors modeling in a probabilistic way

Based on the current states of the target driver, a probabilistic model that accounts for the behaviors is needed.

3. Driver parameters identification

Characteristic parameters representing the driving styles of the driver should be defined.

4. Procedure for complex interaction

Based on the proposed model, a procedure should be defined for autonomous vehicle to handle complex interaction with human drivers.

1.2 Thesis Structure

The structure of this thesis and the objectives of each chapter is listed below (as shown in Fig. 1.2).

- Chapter I : Introduction

The motivation and the objectives of this thesis are introduced.

- Chapter II : Background and Literature Review

Researches regarding the driver behaviors are reviewed.

- Chapter III : Human Driver Modeling at Crossroads
A probabilistic driver behaviors model is proposed and verified.
- Chapter IV : Model Parameters Identification
Parameters representing driving styles are discussed and attempted to identify.
- Chapter V : Applications
Possible application based on the proposed model are explored.
- Chapter VI : Conclusions and Future Works
Conclusions of this thesis and future research directions are delivered.

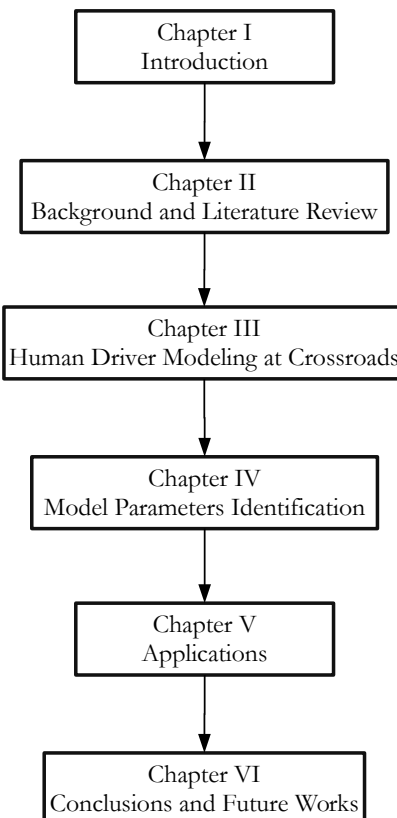
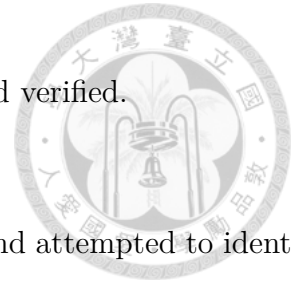


Figure 1.2: Thesis structure.





CHAPTER II

Background and Literature Review

2.1 Introduction

Techniques for autonomous vehicles in motion planning have been studied extensively in recent years [6]. Various algorithms are developed for optimized and collision-free trajectories. However, these algorithms tends to assume the future trajectories of other agents to be known, while in fact we have only limited knowledge about how other surrounding vehicles will behave. Without in-traffic direct communications or high-level traffic commands, this over-simplified assumption will result in unrealistic and often over-cautious reaction to avoid collisions. In the following section, based on the method employed, motion prediction models are classified into three main categories : Physics-Based Models, Driver Behavior Models and Interactive Models.

2.2 Physics-Based Models

Predicting surrounding vehicles' movements enables more active and more practical traffic studies. In the literature, physics-based motion predictions, as shown in Fig. 2.1, use dynamic or kinematic models governed by simple physics laws as surveyed in [7]. These models requires less computational power, are easier to con-

struct, and also have decent accuracy in short-term predictions[8, 9]. Nevertheless, the original functions do not account for uncertainties in real traffic, as a result, have only limited ability to interact with other human drivers. Zhan et al. use probability model of yielding/passing actions at a crossroad in the traffic optimization study in [10]. Other prediction models such as the work of Ruf et al. [11] use a cost map with probabilistic values on each path to optimize the global planner of vehicle movements. Despite Physics-Based Model are easy to be applied and demand low computational power, they still suffer from poor long-term predictions which means they are unable to anticipate the future paths of surrounding agents. In other words, there will be only minimum interaction between the ego vehicle and other traffic participants.

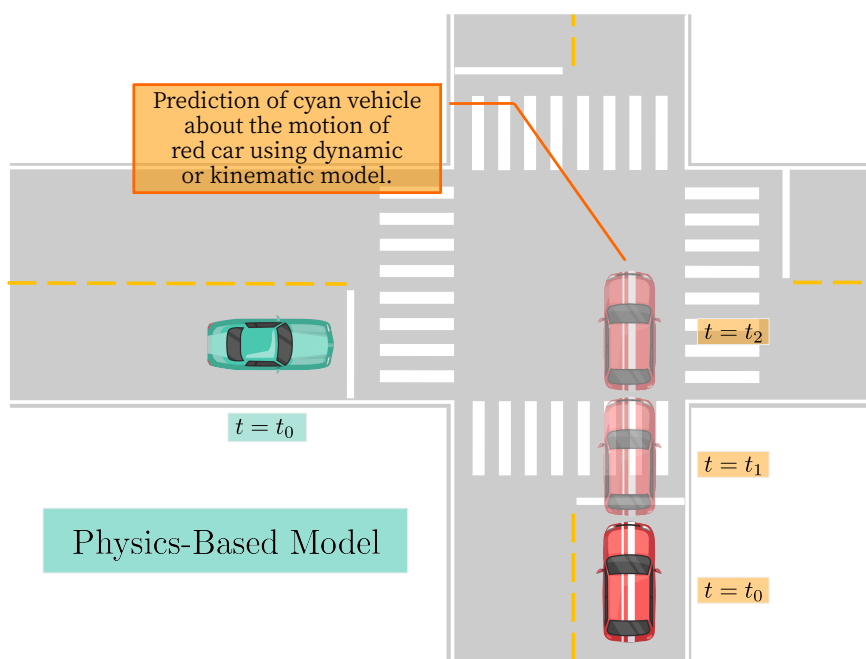


Figure 2.1: Physics-Based Model.

2.3 Driver Behavior Models

A behavior could be a single action (e.g. braking, accelerating) or a series of actions (e.g. drive along a path require a series of actions). The motion prediction with Driver Behavior model is the intent recognition process based on the previous and current states of the target agent (as in Fig. 2.2). If the intent of the driver is identified, we can then predict the future behavior of the target vehicle. When handling the uncertainty of human behaviors, probabilistic method like Bayesian networks or Hidden Markov Model (HMM) are often used.

From the motion of the vehicle and the layout of the intersection, Lefevre et al. [12] estimate the chance of a vehicle violating a stop sign with Dynamic Bayesian Network (DBN). In this work, the probability of the intention and expectation do not match is estimated. The intention stands for the intention to stop and the expectation is the necessity for the driver to stop given the circumstances (i.e. speed, turn signal and pose of the vehicle). Without the need to perform trajectory prediction, the proposed method is computationally efficient and flexible to different situations.

Similar method is also used in literature where driver behaviors are predicted and recognized with DBN. Dagli et al. [13] construct a vehicle following and lane change models which form the basics for the behavior recognition. DBN is used to handle the uncertainty in sensor data gathering and human driver behaviors. The performance of this model is assessed in a simulated lane change experiment where the driver behaviors is recognized 1.5 seconds earlier than the actual lane change. Combining the manually formulated models and models learned with random forest tree, Gindele et al. [14] use DBN to estimate and predict the driver behaviors of two cars passing the intersection. Online learning is possible in the proposed method where the model would be able to adapt to new environments.

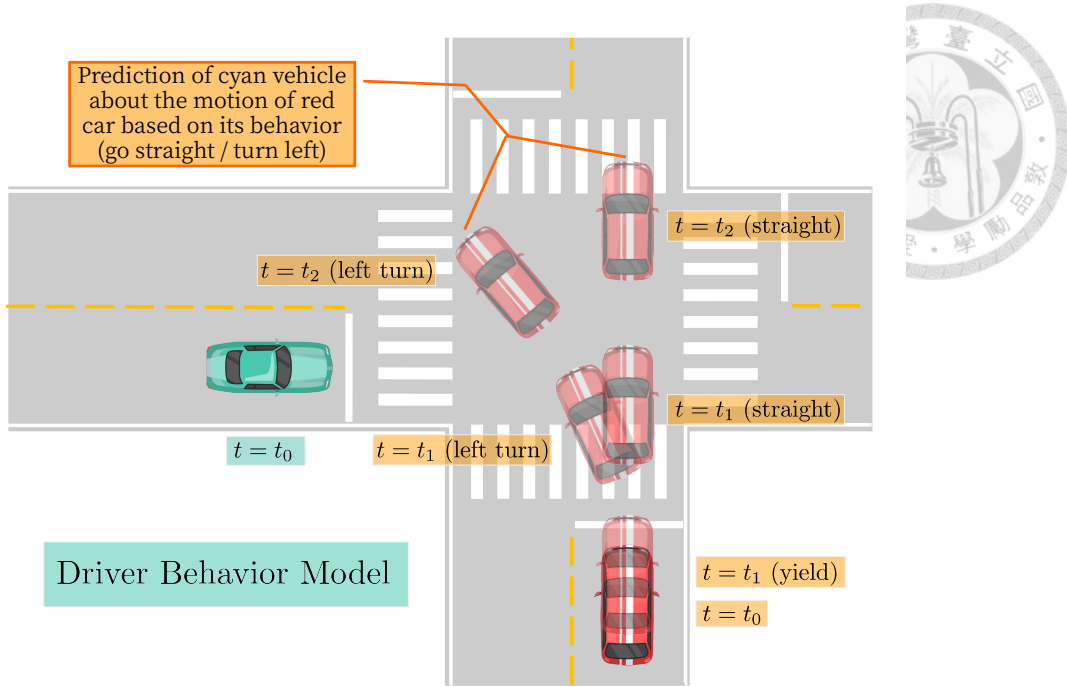


Figure 2.2: Driver Behavior Model.

2.4 Interactive Models

To achieve a better long-term prediction while considering the joint behaviors between traffic participants, interactive models are used . In these models, all the motions and behaviors of a vehicle is considered having a causal relationship with surrounding agents (as in Fig. 2.3). Hence a better behavior prediction or recognition results could be acquired. In order to generate interactive models, probabilistic methods such as partially observable Markov decision process (POMDP) have been applied. POMDP can decide the actions of the host agent while interacting with other traffic participants by predicting their future states and taking their current state into account. Navigation and obstacle avoidance are solved in a probabilistic manner using POMDP by Foka et al. [15]. Hubmann et al. [16] also use POMDP to evaluate the possible maneuvers of other agents and optimize the actions of the

host agent. Despite the advantages, POMDP is typically solved off-line, which means it's intractable for large state spaces. Its large demand for computational power also making it struggle to do the prediction in real-time. Driver behavior models, on the other hand, have no need to predict the whole future trajectory of the target vehicle, thus are able to solve this problem.

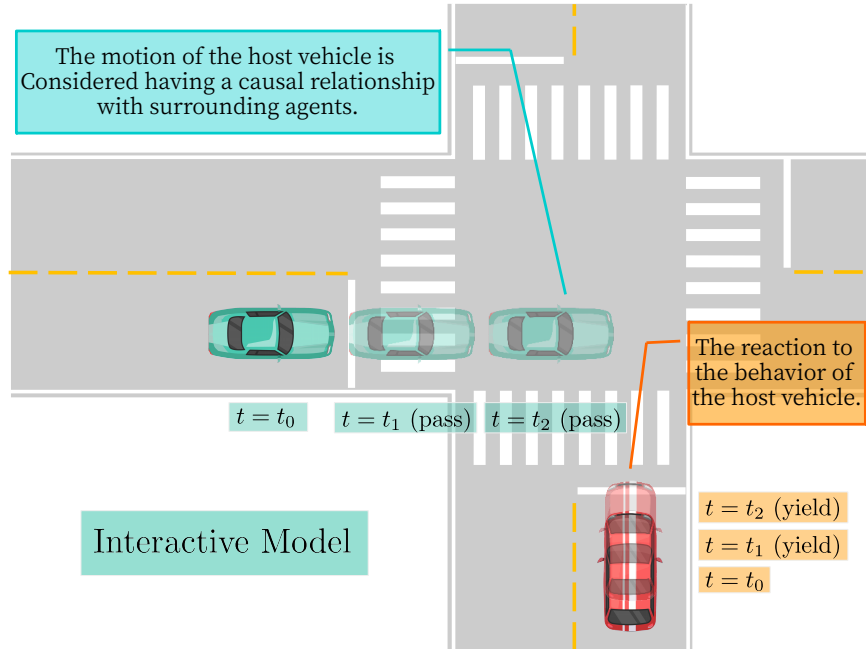


Figure 2.3: Interactive Model.

2.5 Explicit Driver Behavior Models

Driver intent prediction for urban intersection has been a basic requirement for Advance Driver Assistance System (ADAS). To predict turn and stop maneuvers, Liebner et al. [17] use the Intelligent Driver Model (IDM) to model probability of turning and car-following behaviors in a simple Bayes net. The resulting probabilities of four different intentions are compared. The proposed method could be applied to arbitrary intersection if a more generalized desired velocity profiles are used.

For the purpose of overcoming the changing driver behavior at site-specific intersections, Graf et al. [18] extract important features from participants (e.g. speed, distance to the intersection) then put them in the process of Case-Based Reasoning (CBR). The main idea of CBR is to identify a case from experience that is similar to the current one, and use the result to predict the behavior of the driver. However, the results learned from one intersection still do not perform well at other intersections. Drivers with different driving style also affect the prediction accuracy significantly.

Despite the Driver Behavior Model has the advantage of better long-term estimation than Physics-Based Models as mentioned in 2.2 and better the computational efficiency than Interactive Models in 2.4, most of the models using pre-trained model are only applicable to designated situations and environments where the training data is extracted. To overcome this problem, more general and explicit driver behavior models is needed.

2.6 Summary

Despite the explicit formulation and general applicability, physics-based models can not account for states changes of the subject, which results in the poor long-term prediction. Considering joint behaviors of surrounding agent, the interactive models do achieve a better long-term prediction, but they are computationally expensive and intractable for large state spaces. In this thesis, the driver behavior model is chosen for its better long-term prediction and computational efficiency compared to the other two models. Yet, being pre-trained models, most of the behavior models in the literature are restricted to specific traffic scenario or certain driving styles. Hence, in the following chapters, an explicit driver behavior models will be developed to account for driver behaviors at various traffic scenarios.



CHAPTER III

Human Driver Modeling at Crossroads

When we are driving, unless no other traffic participants nearby, interactions between drivers happen much more frequent than we realize. Autonomous vehicles, or computer driven vehicles, nowadays are quite adept at driving between lines, make a turn or avoid an obstacles. They are also capable of reacting to humans' behavior, but more often than not, those reactions are not what we expected. This is owing to their incapability of interacting with human. Autonomous vehicles can't communicate with us if they can't understand our gesture or how we usually react to some specific situation. To solve this, we need to develop a model that is able to account for human driver behaviors. The unsignalized crossroads is chosen as the scenario that the model build around for the fact that it is the most communication-requiring traffic scenario, where the other participant's intention to pass or yield is required.

In the following sections, the concepts of time to collision and time for action will be introduced in Section 3.1. Time to collision and time for action are both key elements for the proposed method, which define the mechanism drivers employed to avoid the potential collision from happening. In Section 3.2, time for action is transformed into a distribution to estimate the chance of braking, and based on this idea, a probabilistic evaluating model is proposed in Section 3.3. Finally, to verify and validate the proposed model, experiments at both simulated and real crossroad

are conducted in Section 3.4.



3.1 Time to Collision and Time for Action

When crossing an unsignalized crossroad, the longitudinal speed is decided empirically by human. Drivers observe the oncoming vehicle in a short amount of time and estimate the next possible position, speed and direction it might be, mostly by experience. Then the speed is adjusted accordingly: accelerate to pass the vehicle if drivers **believe** that arrive at the crossroad before the other participant is possible; or decelerate to yield if a collision is anticipated. Since humans don't perceive the world numerically, researchers have suggested that instead of calculating the distance and the speed directly to define the time to hit an object, more cognitive and abstract methods are used [19]. In this section, we first introduce the crossroad model. Then, to make driver behavior predictable for computer driven vehicle, researches regarding such mechanism are studied and applied. Finally, a probabilistic model of driving behavior is then developed.

3.1.1 Crossroad Modeling

A crossroad model where the whole scenario based on is introduced before digging deeper into the driver decision mechanism at the crossroads. Fig. 3.1 illustrates a human driver (on the left, heading to the right) and an autonomous vehicle (on the bottom heading upward) crossing a perpendicular crossroad with no signal. Under this circumstance, to reduce the dimensionality of the state space, only on the longitudinal states of concerning vehicles are considered. Also, to prevent confusions, only the interactions between two vehicles are studied at the beginning. In this scenario, **the node** represents the intersection of the extended lines of movement of two traffic agents and would be represented by the symbol like the node in figure Fig. 3.1.

the node is used as the origin of the coordinate system. The positive x direction is

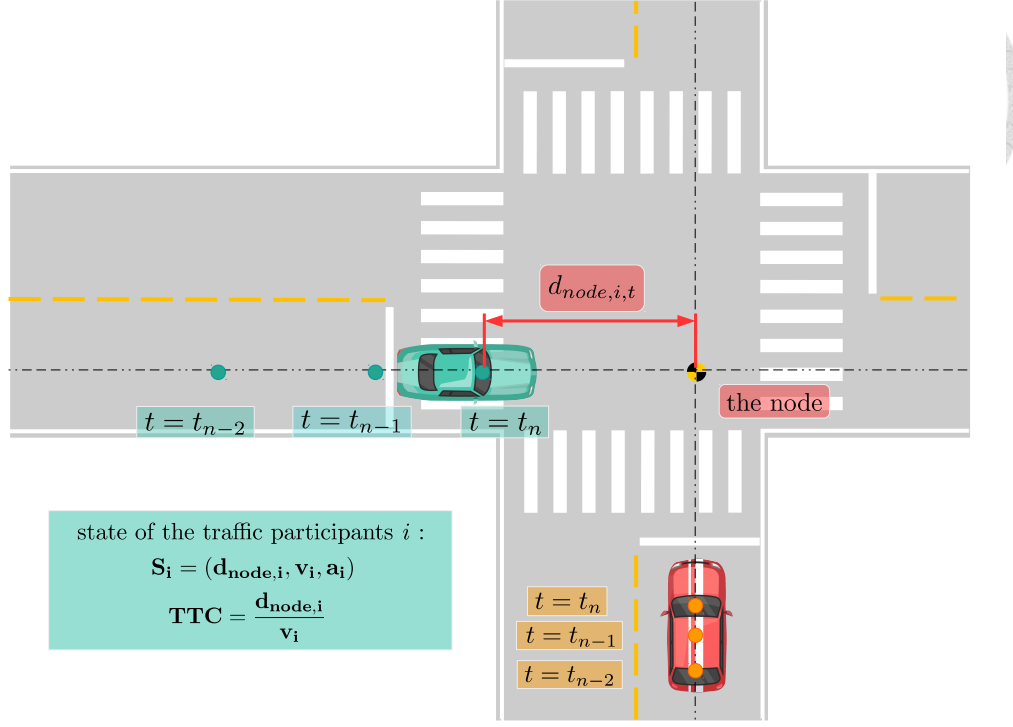


Figure 3.1: Demonstration of the proposed scenario and relevant variables.

same as the vector of velocity of the first approaching vehicle, and positive y direction as the vector of velocity of the other vehicle. The state of the i th vehicle is defined as :

$$\mathbf{S}_{i,t} = \begin{pmatrix} \mathbf{d}_{\text{node},i,t} \\ \mathbf{v}_{i,t} \\ \mathbf{a}_{i,t} \end{pmatrix}, \text{ where } i = \{0, 1, 2, \dots, N\} \quad (3.1)$$

where $d_{node,i,t}$ is the displacement from the position of the i th vehicle to that of the node, $v_{i,t}$ and $a_{i,t}$ are the speed and the acceleration of the i th vehicle at time t respectively. Given that \mathbf{S}_0 is the state of the ego vehicle, N is the number of its surrounding vehicles. Note that they are all one-dimensional.

As mentioned previously, what is interesting is how the human driver interact

with another moving vehicle as he or she proceeding towards the the node. To focus on this topic, the crossroad model is simplified : only one lane per direction, and one participant driving on each direction. As a consequent, the maneuvers of drivers are reduced to linear motion involving hitting the braking and the gas pedal. In the following section, the resulting crossroad model is used to determine the mechanism behind the decisions making process of potential collision avoidance.

3.1.2 Time to Collision

How human decide when is the moment to start braking to avoid collision with a stationary obstacle or another moving vehicle has been a popular topic since a couple decades ago [20]. Time to Collision (TTC), or time to contact, is a crucial method for human to predict the time it will take to reach the obstacle and take necessary measure to prevent potential collisions from happening. Being an efficient safety measure in traffic safety assessment for decades, TTC was described as “the time required for two vehicles to collide if they continue at their present speed and on the same path.” by Hayward in [21]. This concept was usually applied to deal with car following problem, but in this research, it is used to handle vehicle interactions at the crossroad.

The original definition was specified by an optic variable τ_{optic} , which is the inverse of the rate of dilation of the object relative to the observer as shown in Eqn. (3.2).

$$TTC = \frac{\theta_1}{(\theta_2 - \theta_1)/(t_2 - t_1)} \quad (3.2)$$

In the Eqn. (3.2), θ_1 and θ_2 are the angular distances of the obstacle’s image on the retina at times t_1 and t_2 separately. Hence the $(\theta_2 - \theta_1)/(t_2 - t_1)$ would be the expansion rate of the obstacle as the observer approaches. However, there are intense disputations over whether τ_{optic} provides necessary TTC information, since both empirical results and analyses suggest that the hypothesis is false, as described

in [22].

There also exist another potential way to describe TTC involving the information of the speed and the distance to the target object, as described in Eqn. (3.3).

$$TTC = \frac{\text{distance to obstacle}}{\text{speed}} \quad (3.3)$$

Also known as cognitive or computational strategy, this method takes account of the distance from the obstacle (the target object) and the speed assessed by the driver. To verify this idea, Cavallo et al. [23] conduct a series of experiments in real driving condition. Volunteers of different ages, genders and experience levels in driving were asked to estimate the time it would take to collide with the obstacle. The results suggested that both speed and distance information are taken into account in TTC estimation.

Since the TTC definition in Eqn. (3.3) is more applicable and also verified in the literature, in this research the speed and the distance to the intersection are used as variables to describe the human driver behaviors in proposed model.

3.1.3 Time for Action

TTC provides a way to imitate the method used by human drivers when facing a potential collision event. However, the goal is to predict the other participant's decision, that is, to pass or to yield, and the mechanism of this decision is still unclear. To explain the decision making process, we will introduce the new term "Time for Action (TFA)".

To fully understand the role of TFA in braking decision, first the definition of TTC is used to explain how the braking decision is made : under a given speed, the driver decides to brake to avoid collisions when a certain distance is left between the car and the obstacle. As shown in Fig. 3.2, a car is approaching from the left while a red obstacle is on its path. At point P_A , the car is cruising with constant speed V_0 .

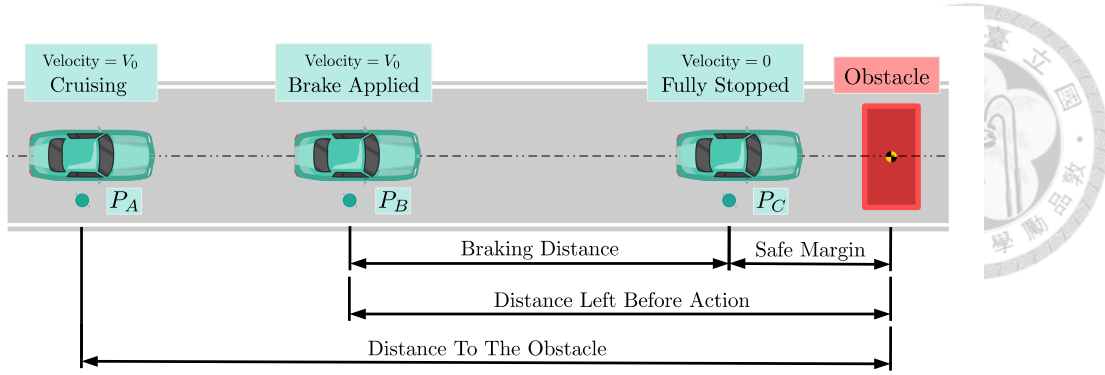


Figure 3.2: Illustrations of TTC and TFA.

The driver should have already observed the obstacle but he or she feels no pressure to brake at this point. As the car keeps moving forward, the driver realizes that if he or she does not brake here, the vehicle might collide with the red obstacle. After the brake being applied at P_B , the car begins to slow down and finally comes to a stop with the speed equals to 0 at point P_C .

In this scenario, TTC decreases as the distance to the obstacle is getting shorter. Finally at point P_B , the driver decides to brake to keep a safe margin from the vehicle to the obstacle when the car is fully stopped. The distance from point P_B to the obstacle is the "distance left before action", which is the minimum distance required to stop in front of the obstacle and keep the safe margin in between. Now we divide this distance by the speed at point P_B , we get this TTC where the driver take the action to avoid the collision. We call this TTC "Time for Action (TFA)".

The time-history of TTC and the dependent variables depicted in Fig. 3.2 are put together and presented in Fig. 3.3. The figure used here is similar to the time-history of braking presented in the work of Winsum et al. [24]. The motion of the vehicle cruising from point P_A to P_B in Fig. 3.2 results in the TTC drops from $t = 0$ to $t = t_0$ in Fig. 3.3. This is due to the decrease of the distance to the obstacle while the speed of the vehicle is constant. Then the driver brakes at point P_B in Fig. 3.2 as the driver

brakes at time t_0 in Fig. 3.3.

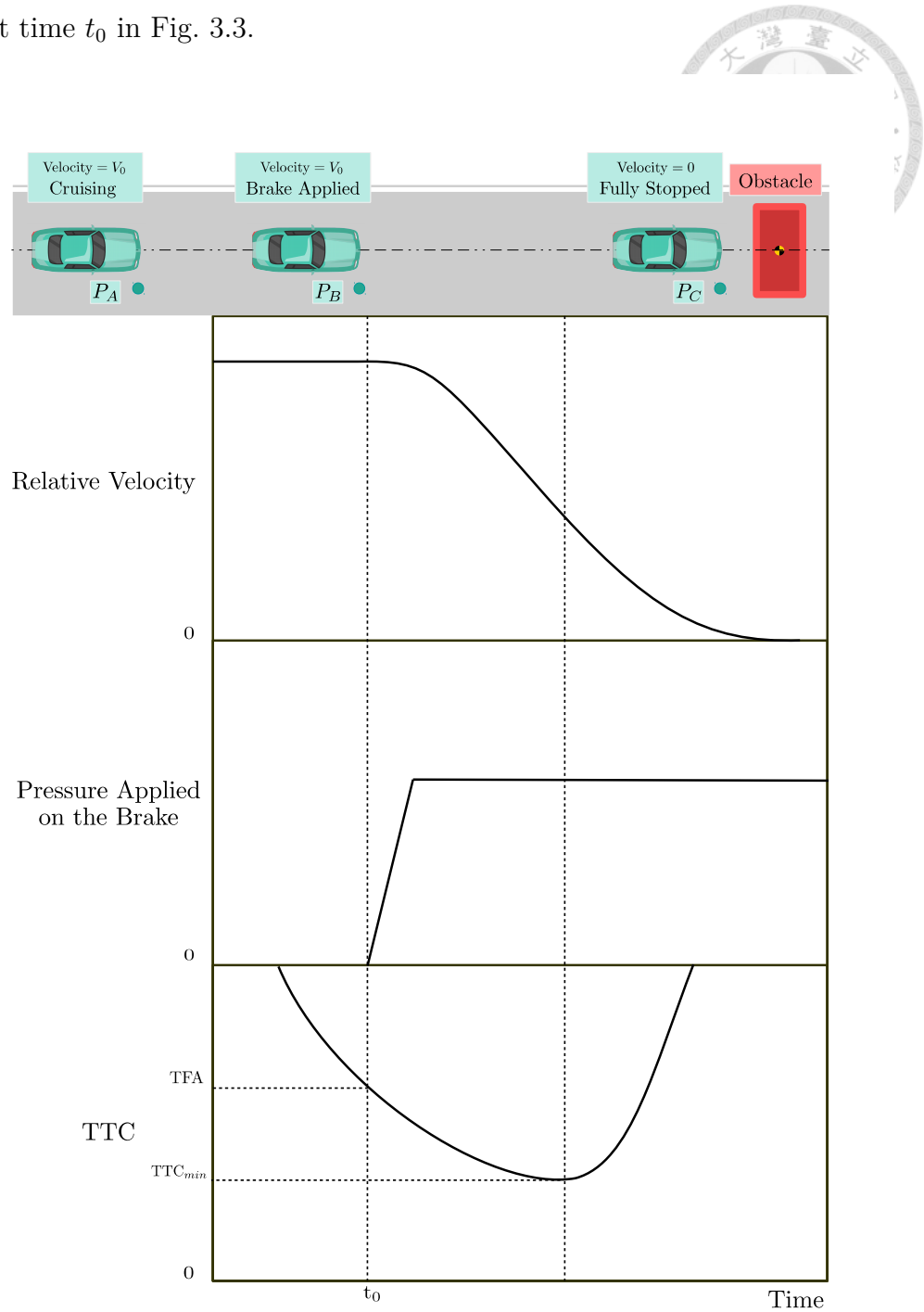


Figure 3.3: History of time to collision when brake is applied.

The TTC value at this instance should equal to TFA of the driver under this speed by definition since this is the TTC he or she believes that a collision would

happen if the brake is applied any later. During the braking, TTC drops to its lowest point labeled as TTC_{min} and then rises. The rise is due to the speed decreasing rate (i.e. acceleration) being higher than the rate of the distance decrease (i.e. the speed). Note the TFA is the minimum TTC that drivers start to hit the brake to avoid collision, not the minimum TTC during the whole process (which is the TTC_{min} in Fig. 3.3).

From the above paragraph we know that not solely speed or distance is utilized in the decision of braking, it is the TTC which formulated using the combined information of both variables that driver perceived take parts in the mechanism. In the crossroad scenario, when a vehicle is about to arrive at the crossroad at the same time as the host vehicle, the host vehicle driver subconsciously imagines the future position of the oncoming vehicle, which turns out to be a real obstacle exist at the point of intersection due to the fact that the only location of the potential collision is at the intersection of two perpendicular paths (as shown in Fig. 3.4). Despite there is not really an obstacle lying right in the middle of the crossroad, we tend to prevent the worst case from happening by estimating the next possible position of the oncoming vehicle with the tangential path. We can adjust our speed accordingly to avoid the potential collision.

Now let us bring TTC and TFA into our crossroads scenarios. Since TTC here can be estimated using the distance to the intersection and the current speed of the vehicle while the TFA is the same as in the situation which a real obstacle exists at the intersection, combining Eqn. (3.1) and Eqn. (3.3) we have :

$$TTC = \frac{d_{node,i}}{v_i} \quad (3.4)$$

In this case, at the moment the host driver sees the oncoming vehicle and thinks that it might collide with him, he or she would put the foot on the brake while the TTC is dropping. Then, the brake would finally be applied at the instance that the

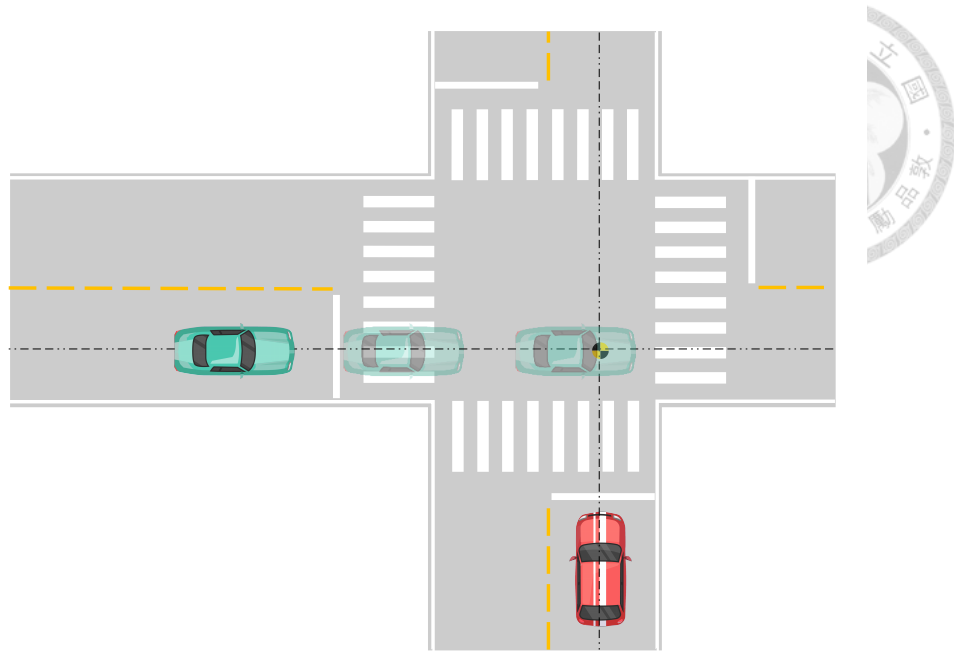
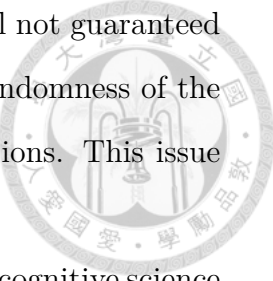


Figure 3.4: The host driver estimate the possible position of the oncoming vehicle depending on its current states. To avoid the potential collision, the host driver adjust the time to brake as if the oncoming vehicle is at the intersection.

TTC he cognized is equivalent to his TFA, so the potential collision at the node (the intersect of two routes) would be avoided. Note that the $\mathbf{d}_{\text{node},i}$ here represents the *displacement* instead of the distance for the purpose of distinguishing two opposite sides of the node, in other words, the displacement is adopted to separate the states before and after passing the node. So, the direction the host vehicle faces would always be the positive on the coordinate system. Throughout this research, the use of displacement and distance are interchangeable since the situations that we are interested in happen before the node (i.e. the displacement is always positive).

It is clear until now that the particular moment of decision making at the crossroad is accessible if both TTC and TFA are able to be determined. The TTC can be calculated without effort by dividing the displacement to the node by the speed of the subjective vehicle. However, there is little discussion about the concept of TFA in the literature. Also, even if the access to the very TFA of the driver is possible,

which in fact only an approximated value could be acquired, it is still not guaranteed that the driver will hit the brake at that exact moment since the randomness of the human perception and the resulting errors while generating the actions. This issue will be addressed thoroughly in the following section.



In the previous sections, the literature concerning psychology and cognitive science is investigated to determine the deciding component (i.e. TTC and TFA) in human drivers' braking event. Then, both variables are applied in the crossroad scenarios as illustrated in 3.1.1. In the next section, an assumption that is capable of explaining the stochastic character of TFA will be established. Then a probabilistic model of drivers behavior based on the concepts of TTC and TFA will be proposed to handle the stochastic decision process of human at the crossroad.

3.2 The TFA Distribution

In this section, the concept of TFA distribution is described. TFA distribution is the fundamental idea to this research an it is what the proposed model is built upon. Following this concept, we are able to obtain the probability density function of TFA from which the probability of the vehicle yielding could be determined using the proposed model.

3.2.1 TFA Distribution

From the above paragraph we know that the definition of TFA is the minimum TTC (or the minimum distance left before braking at the current speed) that drivers start to hit the brake to avoid potential collision. This decision making process will differ from person to person since each of us has our own risk threshold to decide the braking timing. For example, a young driver with a high performance sports car might have a relatively low TFA because of his personality and the great braking performance of the car allowed the driver to go closer before braking. On the contrary,

an older driver driving an aged passenger sedan might have a higher TFA since the driver is more cautious and the car requires longer distance to stop.

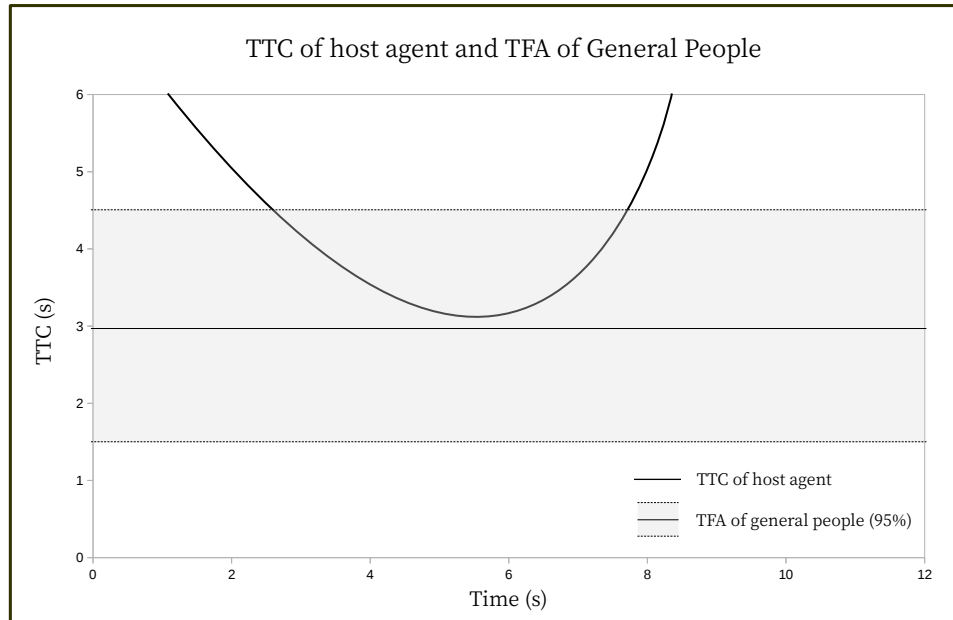


Figure 3.5: Example of TFA of general people and TTC of the host agent.

This idea is illustrated in Fig. 3.5. In Fig. 3.5, grey area is drawn to illustrate the distribution of TFA of general people (95% of people's TFAs are within the area) while solid line is indicating the TTC changing with time of host agent, which is similar as in Fig. 3.3. The distribution of TFA can be explained as "within this range of TTC, 95% of drivers will initiate the action (hit the brake) if potential collisions exist". So in the crossroad scenario where two vehicles are about to reach the intersection at the same time, when the TTC of one of the drivers is getting lower, we can infer that his or her chance of braking to yield is getting higher because more and more people in the distribution start braking as it goes.

In fact, not only is the TFA of different people a distribution, but the TFA of a person under different personal or environmental conditions also is a distribution. However, there is rarely any literature conducted such experiments, so the assumption

that TFA distributions are normally distributed is made. The reason behind this assumption is that even if the distributions of the perception and the motion during the action process (which is braking in this context) are not normally distributed, the combined outcome of these independent random variables would still approximate a Normal distribution, given large enough samples.

In spite of the fact that this idea is supported by the Central Limit Theorem, experiments are conducted to support the assumption. Both Relative Judgement tasks or Prediction-motion tasks are often employed in the literature to estimate the ability of the participant to derive TTC information . In Relative Judgement tasks, subjects are required to indicate the first arriving moving target from two approaching ones. In the Prediction-motion tasks, on the other hand, subjects are asked to predict the time of the moving object arrive at a specified position after the moving object disappeared from the view. In these tasks, subjects are making decisions while watching a pre-recorded film.

However, it is hardly possible for subjects to identify the TFA without knowing how the vehicle will response while the brake is applied. Consequently, to make it more similar to the driving scenario in real world, a simulated crossroad environment is constructed. Detailed discussion regarding the simulated crossroad as well as how the experiments are conducted will be delivered in the following sections where model validation is conducted. For now, the focus is put on the distribution of TFA.

In the experiments, three volunteers are asked to drive toward a static vehicle with constant speed and apply the brake when they believe that the collision will happen if it is applied any later. TFAs in this scenario would be the displacement from the host vehicle to the static vehicle divided by speed of the host vehicle at the moment which brake is applied. Results are shown in Fig. 3.6, Fig. 3.7 and Fig. 3.8. Noted that the distribution of TFA might varies under different speed, but only the parameters of the distribution are changed, not the type of the distribution. The focus now is on

whether the TFA could be modeled as a normal distribution ,the property of TFA distributions under different speed will be discussed later.

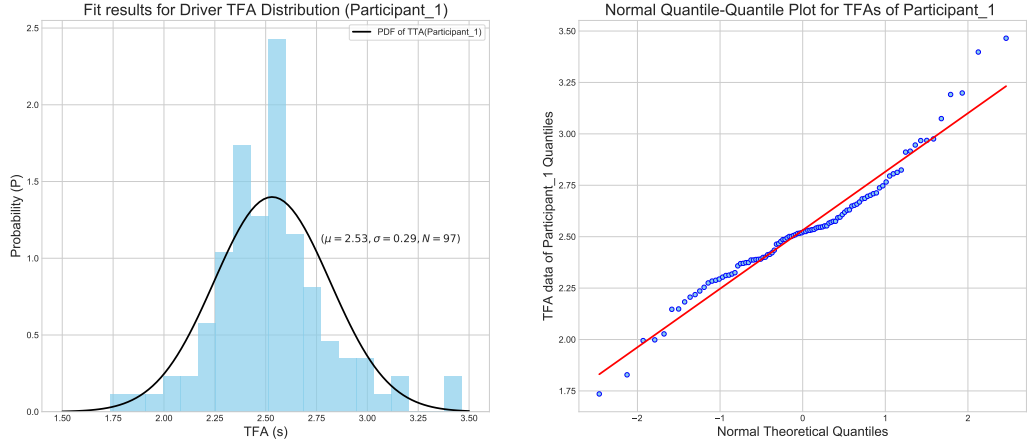


Figure 3.6: TFA results of participant 1 displayed in histogram. The solid curve is the TFA distribution of participant 1 approximated by Normal distribution ($\mu = 2.35, \sigma = 0.29, N = 97$). Speed of the vehicle while braking was set to 5 m/s.

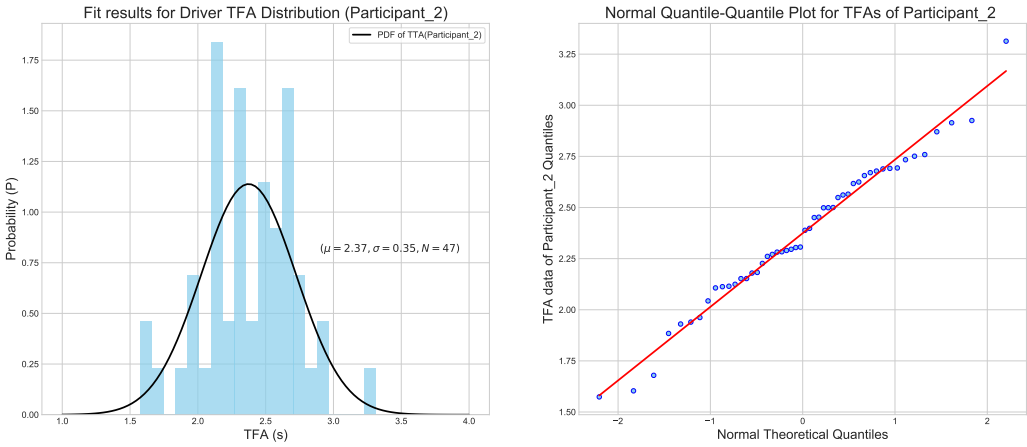


Figure 3.7: TFA results of participant 2 displayed in histogram. The solid curve is the TFA distribution of participant 2 approximated by Normal distribution ($\mu = 2.37, \sigma = 0.35, N = 47$). Speed of the vehicle while braking was set to 5 m/s.

In Fig. 3.6, Fig. 3.7 and Fig. 3.8, sub-figures on the left are experimental TFA results plotted in histograms while sub-figures on the right are Quantile Quantile

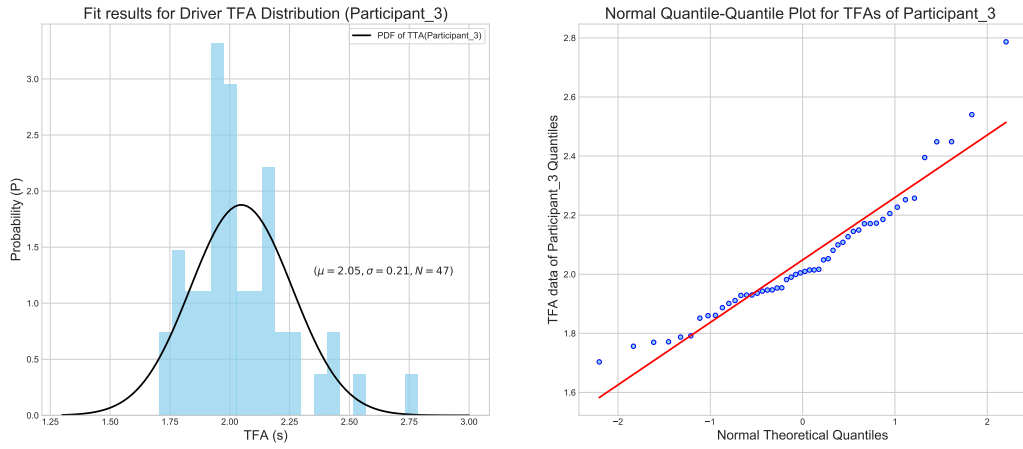


Figure 3.8: TFA results of participant 3 displayed in histogram. The solid curve is the TFA distribution of participant 3 approximated by Normal distribution ($\mu = 2.05$, $\sigma = 0.21$, $N = 47$). Speed of the vehicle while braking was set to 5 m/s.

Plots (Q-Q Plots) using the same sets of TFA data. Q-Q plot is a graphical tool that can be used to examine the plausibility of the examined data coming from a theoretical distribution which is the Normal distribution in our case. One should note that Q-Q plots are merely a visual checking method that can give us an idea of how close the distribution of sampling data is comparing to theoretical one. Red solid lines in each figures are standard lines representing the theoretical results if the subject distribution is also a Normal distribution, in other words, closer the points to the red line higher chance the subject data is normally distributed.

What we can learn from the figures is that TFA distribution of a single driver can be approximated by the Normal distribution if given large enough number of samples. To examine whether the TFA of general people is also normally distributed, all TFA data of participants are combined together in Fig. 3.9. Although the number of volunteers is not large enough, we can still learn from Fig. 3.9 that combined distribution of drivers' TFA can also be approximated by Normal distribution. This result is actually unsurprising providing that all three individual TFA distributions

are normally distributed.

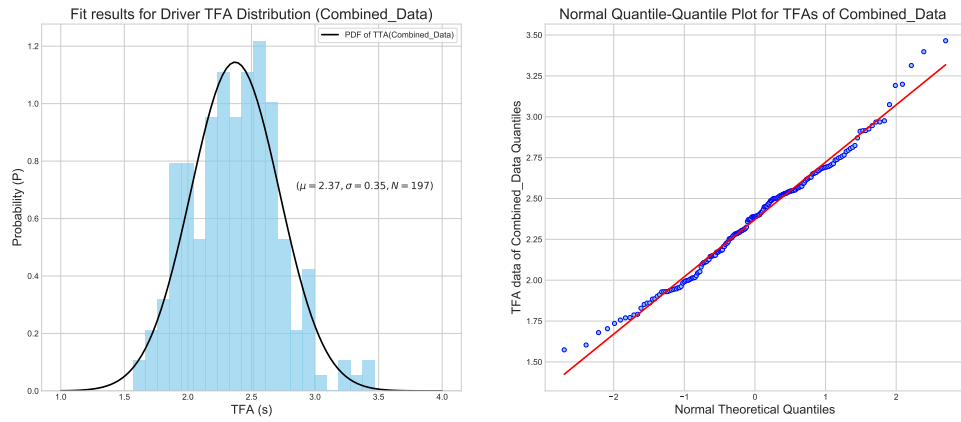


Figure 3.9: TFA results of participants are displayed in histogram. The solid curve is the TFA distribution of combined data of participants approximated by Normal distribution ($\mu = 2.37, \sigma = 0.35, N = 197$). Speed of the vehicle while braking was set to 5 m/s.

Knowing the TFA distribution for both individual and general people can be approximated by Normal distribution, the probability of a driver braking could be inferred effortlessly using the probability density function of the Normal distribution.

3.2.2 TFA Probability Density Function

From the previous section, the distribution of TFA is identified. In order to describe the human decision making process in a probabilistic way, the probability density function (PDF) of the TFA distribution is used. PDF is a function that defines the continuous random variables. A point on the PDF represents the *likelihood* that the value of the random variable equals the sample value. Hence, an area under the curve of PDF would stand for the *probability* of the random variable falling within that range.

We can turn the grey area in Fig. 3.5 into a PDF as in Fig. 3.11. In this case, when a certain value of TTC within the PDF of TFA of general people is reached, the

area under the PDF and right to this value represents the probability of the brake being applied. To make it clearer, let us assume the TTC of a vehicle driving towards a crossroad now is 3. At this instance, the probability for the driver to brake would then be the area under the PDF and right to the value 3, which is 50% since 3 is also the mean value of the TFA distribution in Fig. 3.11. Drivers with TFA greater than 3 would have braked before the TTC reached 3 because the TTC drops as the host vehicle is driven toward the crossroad and the displacement to the node is decreasing according to Eqn. 3.4. The concept behind using the area under the PDF and right to the current TTC as the probability to brake combines elements introduced in the previous sections, including using TTC as to indicate the time for braking (i.e. TFA) and approximating the TFA distribution with Normal distribution.

What should be noted here is that since whether the driver brakes or not, the displacement to the node during that time is always decreasing. According to Eqn. 3.4, if constant speed is maintained, the value of TTC will fall down as the vehicle is driven toward the node. On the other hand, if the brake is applied, the TTC rises parabolically as shown in Fig. 3.3. Hence, before the brake is applied, the TTC used to calculate the probability is the TTC at the moment. The TTC used to calculate the probability after the brake is applied should then be the lowest TTC that occurs on the TTC curve of the host agent since the intention to brake during the braking process remains the same as the beginning of the action. We will use Fig. 3.10 and 3.11 to further explain this idea.

In Fig. 3.10, the dashed lines indicated by colored shapes (including squares, triangles and circles) on both sides represent the sampled moments during the braking process. Red squares indicating the TTC at 3 seconds on the time line, blue triangles at around 5.5 seconds and magenta circles at around 7 seconds. The corresponding moments are also labeled on the TFA distribution in Fig. 3.11. At 3 seconds (red square connected with dashed line, using red line in short) the TTC of the host

agent is around 4.2 seconds. We can then estimate from the PDF in Fig. 3.11 that the probability of the vehicle stopping is 0.0013, which is the area right side of the red line. This result is reasonable since the TTC at this moment is still far from the TFA average which is 3. Similarly, when the time is at 5.6 seconds (blue line) the TTC at the time is around 3.1, so the probability of the vehicle stops rise to 0.401. As it comes to the time at 7 seconds (magenta line) the TTC becomes larger due to the brake, but as mentioned before, the rising of TTC indicates the agent is slowing down, which does not lower the probability to brake. So the probability of the host agent braking is still calculated using the lowest TTC value on the TTC curve which is 3.1, so the probability to brake is still 0.401.

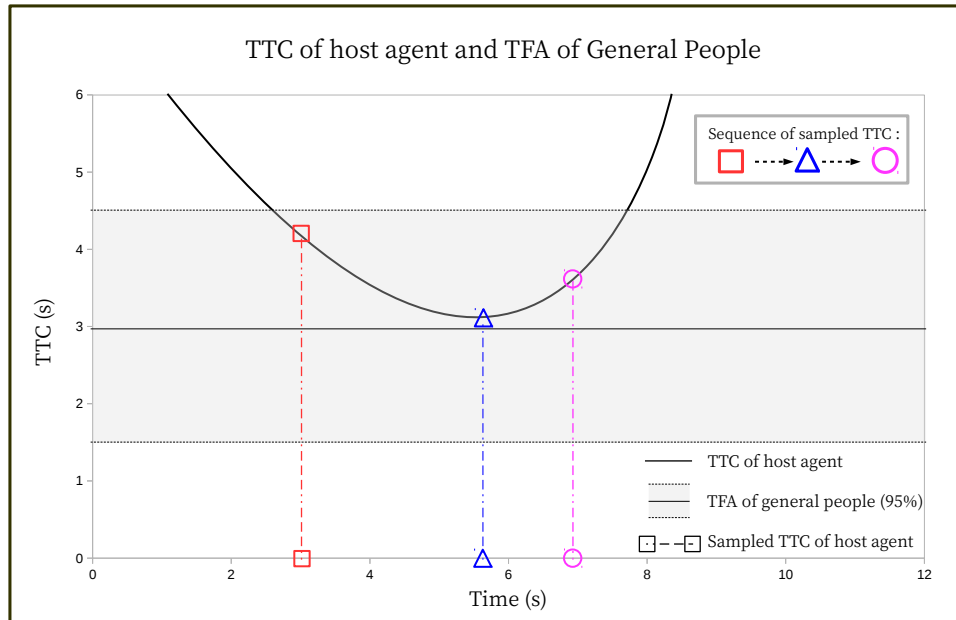


Figure 3.10: Example of TFA of general people and TTC of the host agent.

So far we learned that the probability for the driver to brake is the integral of the PDF from the current, or the lowest in case the brake is applied, to the $+\infty$. The probability to brake mentioned in the above paragraph refers to the intention that the driver brake to avoid potential obstacles. In the next section, the probability

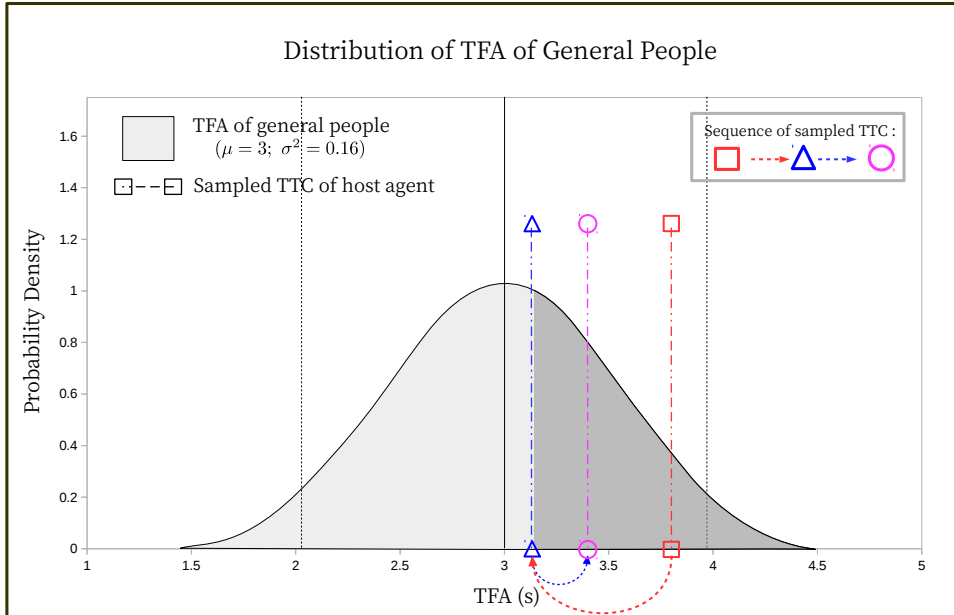


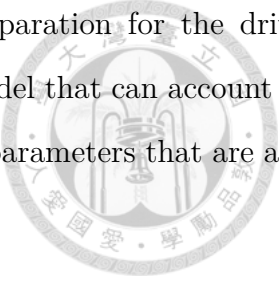
Figure 3.11: Example of TFA distribution of general people.

estimation method illustrated in this section will be used to evaluate the probability for the driver to yield to other traffic participants at the crossroad described in section 3.1.1.

3.3 Probability of Yielding

To this moment, the probability for a driver to brake can be calculated using the PDF of TFA of general people, but merely integrating the PDF is still inadequate to explain the probability for the driver to yield. For example, assuming a driver drives towards the node without decelerating. Throughout the whole operation, the TTC of the host agent decreases, resulting the rising of the Probability of Yielding (POY) (increasing area right to the current TTC and under the TFA distribution), which is a contradiction to our goal. Additionally, the TFA distribution for a driver is a function of the speed, hence the distribution Fig. 3.9 represents the TFA distribution

of general people (combined data of participants). In preparation for the driver yielding model at crossroads, firstly the TFA distribution model that can account for the distributions under different speed is required, secondly parameters that are able to explain all possible circumstances should be included.



3.3.1 TFA Distribution Modeling

In this work, we focus on the crossroad scenario described earlier where two drivers drive toward the node (the intersection of their courses) on the paths perpendicularly to each other at the same time. The term $d_{node,i,t}$ in Eqn. (3.4) denotes the displacements to the node that change along with time. In other words, at the moment that the driver has the intention to yield, this term will then represent the distance required for the vehicle braking and keeping a distance between the vehicle and the node when fully stopped which is the *distance left before action* in Fig. 3.12 .

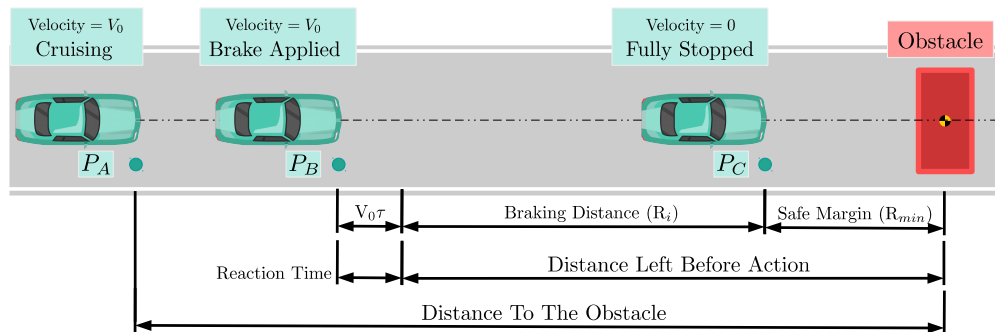
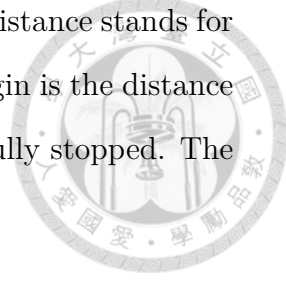


Figure 3.12: Decomposing the distance left before action (apply the brake).

The distance left before action is broken down into three parameters in Fig. 3.12, which are reaction time, braking distance and the safe margin (i.e. the distance left when fully stopped). The reaction time is the combination of the human perception-reaction delay and the vehicle actuation delay, i.e., these are the time that drivers need from seeing a potential threat to hitting the brake and the time the brake system need

to decelerate the vehicle after the applying the brake. The braking distance stands for the distance the vehicle need to be fully stopped. And the safe margin is the distance left between the host vehicle and the obstacle when the vehicle is fully stopped. The reaction time can be expressed as



$$\text{Reaction Time} = v_i \tau \quad (3.5)$$

where v_i is the speed of the subject vehicle at the very moment when the brake is applied and τ is the combination of system and driver delays as mentioned earlier. The second parameter is the braking distance, denoting as

$$R_i = \frac{v_i^2}{2a_{dec}} \quad (3.6)$$

where v_i is same as the one in Eqn. 3.5 which stands for the speed of the vehicle at that moment while a_{dec} represents the average deceleration applied during the braking. What should be noted here is that Eqn. 3.6 is based on the assumption that the constant deceleration is applied throughout the entire braking process. The last parameter, safe margin, is denoted as R_{min} which stands for the safe distance that the driver left after the vehicle is fully stopped. For the sake of making data extraction easier, the R_{min} is defined as distance from the center of one vehicle to another. Combining these three parameters we have the distance left for braking as

$$\text{Distance Left Before Braking} = R_i + v_i \tau + R_{min} \quad (3.7)$$

One should have been aware of the fact that the meaning of this distance is exactly the distance term in Eqn. 3.4 when the TTC at this moment equals the TFA of the driver, since Eqn. 3.7 is the estimated distance needed for the driver if he or she attempts to yield at this moment. So dividing Eqn. 3.7 by the speed of the subject vehicle v_i we will have

$$\text{TFA}_{est} = \frac{R_i + v_i \tau + R_{min}}{v_i} \quad (3.8)$$

where TFA_{est} represents the estimated TFA of the driver. This TFA_{est} is then applied as the mean value of the TFA distribution under the vehicle speed v_i . Combining all the element, the TFA distribution is now described as

$$\text{TFA} \sim \mathcal{N}(\text{TFA}_{est}, \sigma_{est}^2). \quad (3.9)$$

and the value of the variance σ^2 is defined as

$$\sigma_{est} = \gamma \cdot \text{TFA}_{est} \quad (3.10)$$

where γ is the coefficient for standard deviation, which is obtained from the ratio of μ and σ obtained from the approximated normal distribution of TFA.

As mentioned in Section 3.2.1, the TFA distribution is suggested to vary under different velocity. It seems more plausible using the TFA distribution described in Eqn. 3.8. To confirm this idea, the experiments similar to the one conducted in Section 3.2.1(to prove the TFA distribution is normally distributed) is repeated but under different velocity at the moment of the brake. The velocity varies from 2.5 to 5 m/s using 0.5 as the step. Results of two participants are shown in Fig .3.13 and Fig .3.14.

In Fig .3.13 and Fig .3.14, the blue dots are the collected data while the red line represents the curve fitting using hyperbolic equation. The reason for choosing hyperbolic equation is to provide evidence of how accurate the proposed TFA_{est} equation is. It turns out that the TFA varies under different velocity following the hyperbolic equation, which is similar to the relation in Eqn. 3.8.

Now the TFA_{est} is identified to be a function of v_i as described in Eqn. 3.8, there are only three parameters left to be identified before completing the TFA distribution

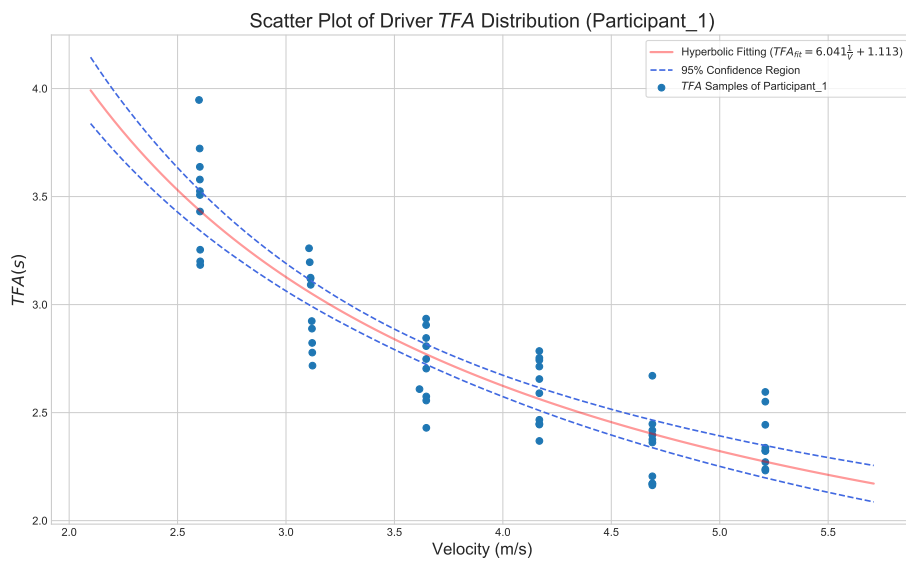


Figure 3.13: The TFA scatter plot of Participant 1 under various velocities.

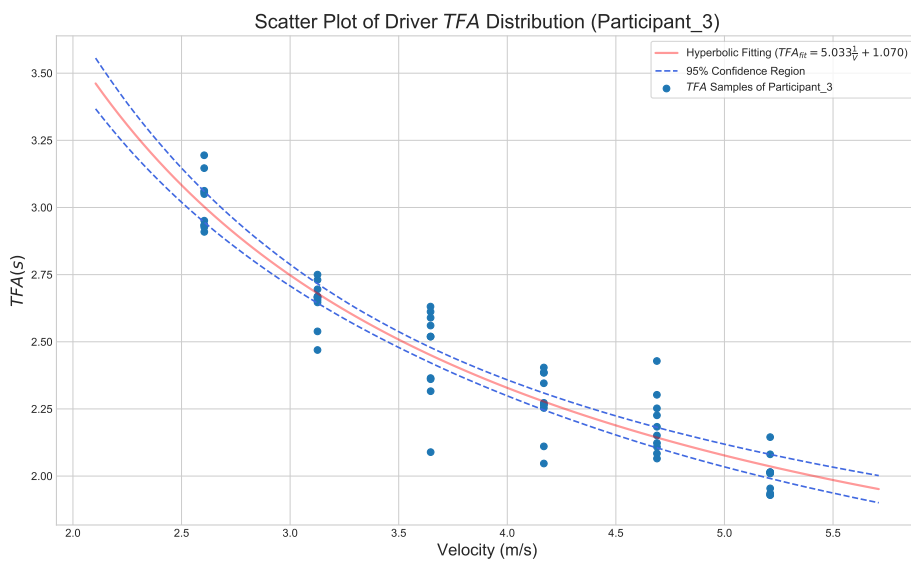


Figure 3.14: The TFA scatter plot of Participant 3 under various velocities.

model. Since τ represents the reaction time of the driver which is biological trait, it can be considered as a constant under different speed. R_{min} and a_{dec} on the other hand, are functions of velocity due to different possible consequences at different velocities. For instance, people might have more aggressive actions when at lower speed (e.g. smaller R_{min} for closer distance to the other vehicle after stopped) since everything is under control (i.e. the severity of the collision is low). While at high speed, however, drivers tend to act more conservatively (e.g. larger R_{min} to keep a "safer margin") to avoid the serious collision. Experiments are conducted and shown to confirm the idea.

To estimate the parameters needed for TFA distribution of average drivers, data collected from participants are combined and analyzed in Fig. 3.15 and Fig. 3.16. The corresponding linear equation defining R_{min} and a_{dec} under various velocity are also presented.

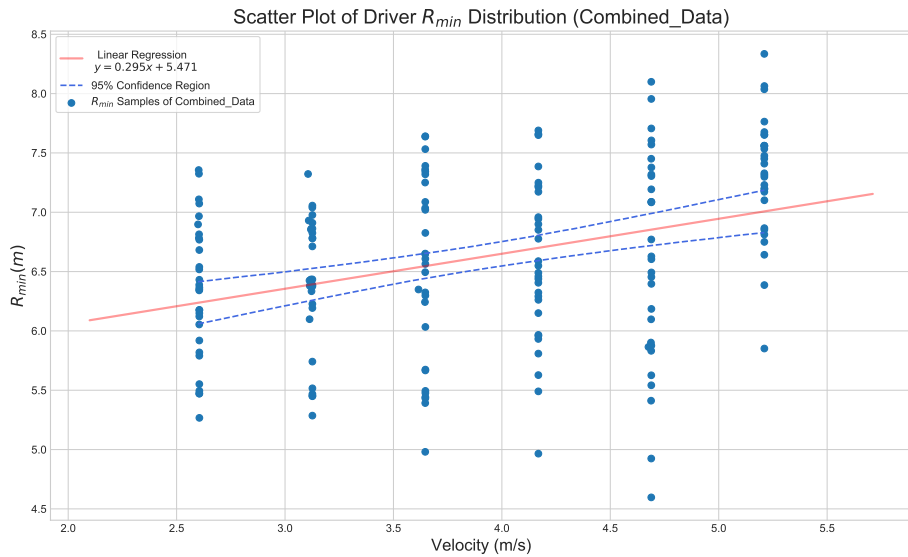


Figure 3.15: The R_{min} scatter plot of combined data under various velocities.

where the approximated equations for R_{MIN} and a_{dec} are

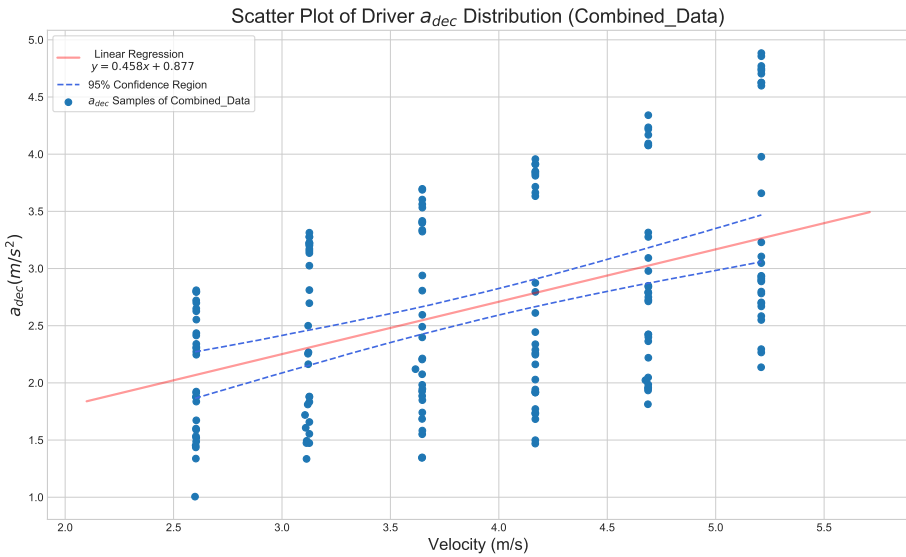


Figure 3.16: The a_{dec} scatter plot of combined data under various velocities.

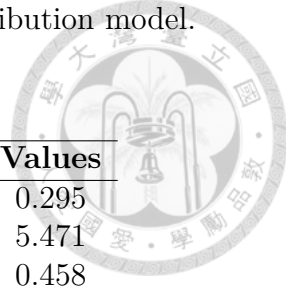
$$R_{min} = 0.295v_i + 5.471 \quad (3.11)$$

$$a_{dec} = 0.458v_i + 0.877 \quad (3.12)$$

We can see that the R_{min} does get higher linearly as the velocity rises which is the same as predicted. The same trends happen to the a_{dec} as the velocity ascends, which suggests that drivers brake slowly at low velocity and rapidly at high velocity. This is also reasonable since more urgent the situation is when the velocity is high. Therefore, the R_{min} and a_{dec} in Eqn. 3.8 are also functions of v_i which can be approximated by linear equation. Now we have all the elements needed, the required TFA distribution under different speed can now be estimated using TFA_{est} . Parameters used in the proposed TFA distribution estimation are listed in Table 3.1.

where Safe Margin Coefficient ($C1_{Rmin}$), Safe Margin Constant ($C2_{Rmin}$), Deceleration Coefficient ($C1_{a_{dec}}$), and Deceleration Constant ($C2_{a_{dec}}$) standing for the co-

Table 3.1: Table for parameters used in TFA distribution model.



Parameters	Values
Safe Margin Coefficient ($C1_{Rmin}$)	0.295
Safe Margin Constant ($C2_{Rmin}$)	5.471
Deceleration Coefficient ($C1_{a_{dec}}$)	0.458
Deceleration Constant ($C2_{a_{dec}}$)	0.877
Reaction Time (τ)	0.6 s
Standard Deviation Parameter (γ)	0.148

efficients and constants of the linear equation of R_{min} and a_{dec} . R_{min} and a_{dec} are formulated in Eqn. 3.13 and Eqn. 3.14.

$$R_{min} = C1_{Rmin}v_i + C2_{Rmin} \quad (3.13)$$

$$a_{dec} = C1_{a_{dec}}v_i + C2_{a_{dec}} \quad (3.14)$$

Finally, the model to estimate the TFA distribution of general people is completed. The TFA distributions are proved to be normally distributed and the formulated TFA_{est} can also account for the hyperbolic growth in the TFA data collected. In the next section, the TFA distribution will be used as the core of the proposed probabilistic model.

3.3.2 The Model for Probability of Yielding Estimation

So far, the problem concerning the model for TFA distribution is solved by considering the distance needed for the driver to yield. Then the distance is divided by the speed at the instance and turned into the TFA_{est} . Before the TFA distribution is brought into the probability evaluation method proposed in section 3.2.2, few improvements are required because the proposed model is unable to account for all the

situations yet.

For example, the situation where a vehicle is accelerating through the node is described in Fig. 3.17. Three sub-figure from the top to the bottom are the velocity, the displacement to the node and the TTC versus the time respectively. Note that in this example, the acceleration of the vehicle is constant, so the line of velocity rise linearly while the displacement to the node and TTC are a parabolic and the curve consisting of reciprocal and linear function separately. In this figure, as the velocity of the vehicle is accumulating, the displacement to the node drops in a parabolic curve since the vehicle is moving closer. The resulting TTC curve, defined by Eqn. 3.4, is also decreasing and even goes beneath 0. In the cases like this one, the POY using merely the integral from the TFA distribution, as in Fig. 3.11, would causing the increase of the POY as the TTC keeps decreasing.

To overcome this problem, few adjustments are needed to be performed. First, the influence of the acceleration on the probability of stopping should be considered. As described in the above example, besides the integral acquired from the TFA distribution, the current states of acceleration are also important. After some trials for different possibilities, the first order derivative of TTC is chosen. By assuming constant acceleration while braking, the $d_{node,i,t}$ can be expressed as

$$d_{node,i,t} = d_{node,i,0} - \left(v_0 t + \frac{1}{2} a t^2 \right) \quad (3.15)$$

where $d_{node,i,0}$ is the displacement at the beginning of the brake, v_0 is the speed and a the acceleration. Then, combining Eqn. 3.15 and Eqn. 3.4, the derivative of TTC is determined

$$TTC' = \frac{d}{dt} \frac{d_{node,i,t}}{v_t} = -1 - a \cdot d_{node,i,t} \cdot v_t^{-2} \quad (3.16)$$

As a dimensionless weighting parameter, TTC' takes not only acceleration bit also

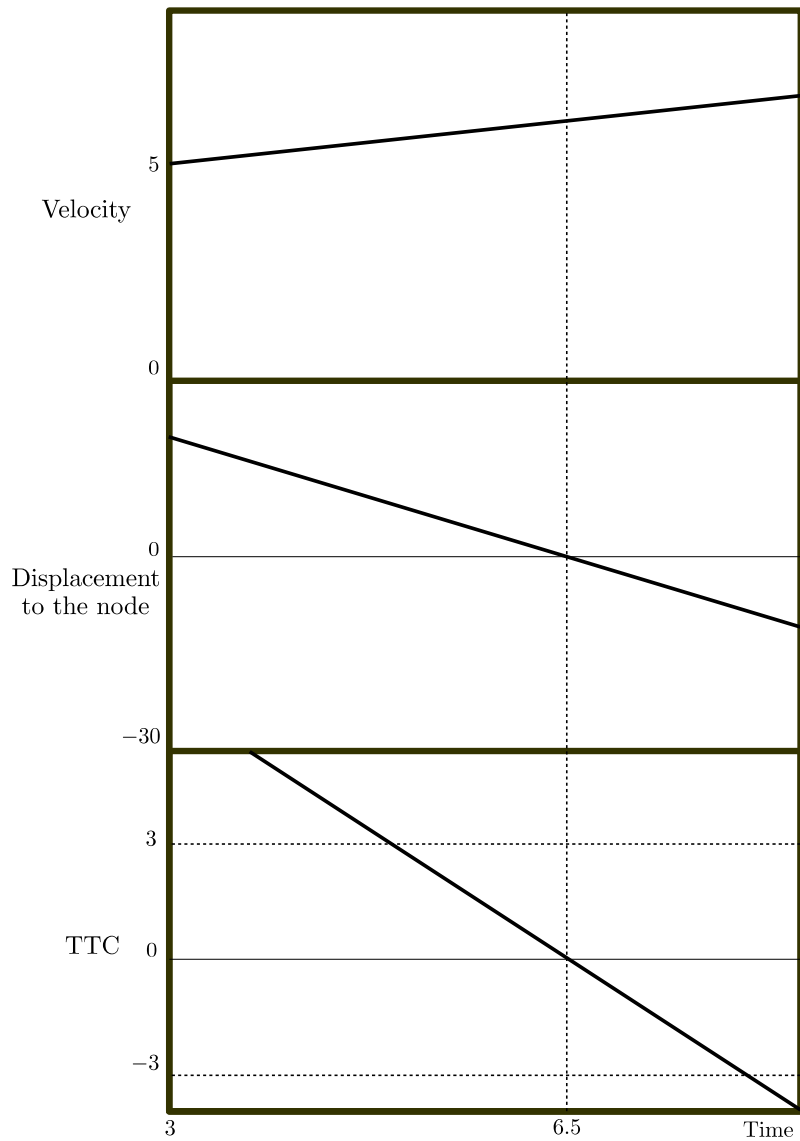


Figure 3.17: History of TTC as the vehicle accelerating through the node.

displacement and the speed into account. For instance, when a constant deceleration is applied, the higher the speed of the vehicle implies the smaller chance this vehicle will yield and vice versa. So this weighting parameter is capable of punishing those with low TTC while accelerating or at high speed and rewarding those with deceleration or low speed. Now, the last step is to add this weighting on the proposed model.

In order to increase the POY in those circumstances such as the deceleration or the low vehicle speed, the mean value of TFA_{est} should be elevated. Similarly, to decrease the POY while the vehicle is accelerating or driving with high speed, the mean value of TFA_{est} is reduced. However, chances are the brake is not applied to yield but to adjust the speed, or it is not acceleration but simply some sensor errors, which all could lead to bumpy probabilities of yielding. To bring down the number of the results affected by false positive, the following adjustments are made

$$P_{yield,t} = \left(1 - \Phi_{\mu,\sigma^2}(minTTC_t)\right) \quad (3.17)$$

where $P_{yield,t}$ is the proposed probability of yielding at time t , Φ_{μ,σ^2} is the CDF of the TFA distribution $\mathcal{N}(\mu, \sigma^2)$, μ is defined by $TFA_{est,t} + A_t$ which represents the adjusted mean value of the TFA distribution and $\sigma_{est,t}$ is the resulting adjusted mean value of the TFA distribution.

The weighting parameter A_t is defined as

$$A_t = \begin{cases} \alpha_t & \text{if } |\alpha - \alpha_{t-1}| < 1.67 \cdot \sigma_{est,t} \\ 1.67 \cdot \sigma_{est,t} & \text{otherwise} \end{cases} \quad (3.18)$$

where α_t in Eqn. 3.18 is dominated by the acceleration. From Eqn. 3.16, we can see that the TTC' equals -1 when the acceleration is 0. So the TTC' value is greater than -1 when the subject vehicle is decelerating, and less than -1 when accelerating.

In order to account for the acceleration as well as the velocity, α_t is defined as

$$\alpha_t = \begin{cases} \beta_t \cdot \ln((|TTC'_t| + 1) \cdot e) & \text{if } TTC'_t > -1 \\ -\beta_t \cdot \ln((|TTC'_t| + 1) \cdot e) & \text{if } TTC'_t < -1 \\ \alpha_{t-1} & \text{otherwise} \end{cases} \quad (3.19)$$

where

$$\beta_t = \max(|minTTC_t - TFA_{est,t}|, \sigma_{est,t}) \quad (3.20)$$

As described in Eqn. 3.17, the weighting A_t is applied to increase the mean value of the TFA distribution. When the A_t is positive, meaning that the POY will increase under the same TTC, which is due to the larger integral of that area under TFA distribution, and vice versa for the negative A_t values. This is illustrated in Fig. 3.18 and Fig. 3.19. In Fig. 3.18, the current TTC equals the mean of the TFA distribution so the resulting POY is 0.5. However, since the vehicle is decelerating, the mean value of the TFA distribution is adjusted according to Eqn. 3.19. The POY, which is the area under the TFA distribution and right to the current TTC, becomes 0.97, as illustrated in Fig. 3.19.

In Eqn. 3.19, the magnitude of α_t is adjusted depending on the greater one between $|minTTC_t - TFA_{est,t}|$ and $\sigma_{est,t}$ (as shown in Eqn. 3.20). By doing so, the increase or decrease of the mean value of the TFA distribution will be in direct proportion to the difference between $minTTC_t$ and $TFA_{est,t}$ if $|minTTC_t - TFA_{est,t}|$ is larger. Within those situations where the $|minTTC_t - TFA_{est,t}|$ is too small or even equals to 0, $\sigma_{est,t}$ is used instead. Either way, the resulting β_t value allows the proposed model to have more immediate response to the situation at the moment. (Noted that in Eqn. 3.19, $|TTC'_t|$ in both conditions are added by 1 and times e , so the outcome of the natural logarithm will be greater than 1 at all times.)

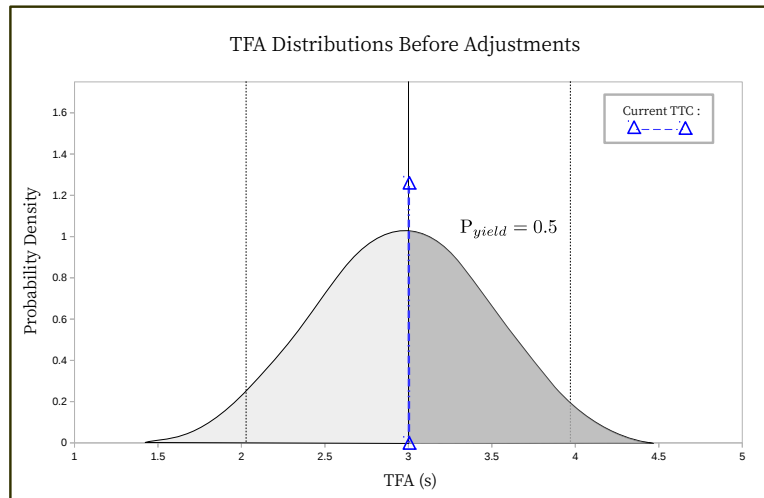


Figure 3.18: The probability before the weighting parameter A_t is 0.5 .

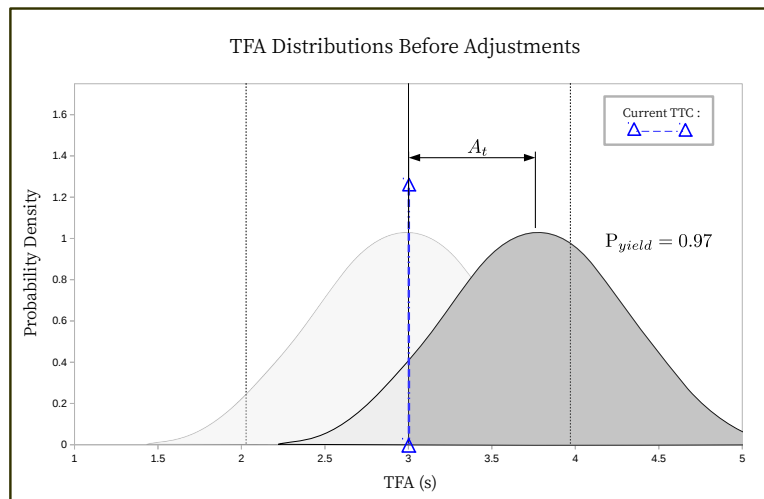


Figure 3.19: The probability after the weighting parameter A_t is 0.97 .

However, jagged POY curve might be shown if the response is "too immediate", in other word, if the value of α_t is too large, the resulting POY curve would be too cluttered. For example, if the current POY is 0.97 as depicted in Fig. 3.19, and the α_t at the moment is minus four standard deviation. In the next moment, the POY then drop rapidly from 0.97 to 0.0 . If situations like this keep repeating, there will be too many spikes for people to understand the real intention of the other driver. As a result, the maximum value of A_t is set to 1.67 standard deviation to suppress the value and prevent the POY from rising or dropping too rapidly.

Another reason for spikes on the POY curves is that, the throttles or brakes are sometimes applied for speed adjustments, not yielding or passing. To prevent the POY curve from making response to situations like this, the change of sign in A_t would only be accepted when the acceleration introducing the change last for longer than 0.2 sec, i.e., when the vehicle starts braking, the A_t brought by this brake would only be applied when the deceleration lasts longer than 0.2 sec. Even though the sensitivity to the yielding or passing cases might be diminished if the threshold is set too large, this can effectively reduce the number of cases falsely detected as the other intention.

Up till now, the driver behaviors at the crossroad is modeled in a probabilistic way. The proposed probabilistic of yielding is able to anticipate the decision of drivers at the crossroad. With this functionality, the proposed method can help autonomous vehicle understand the intentions of other traffic participants and make the mixed-fleet safer before the fully autonomous vehicles are adopted by 100%.

The intents of drivers at simulated and real crossroad are predicted and shown using the proposed model. Then, the verification is conducted using the classification accuracy rate, and the results are also compared with other methods from the literature.

3.4 Driver Intentions Prediction with Probability of Yielding

In Section 3.3, the POY is proposed to evaluate the intentions of drivers at crossroads probabilistically. To verify the outcomes of the proposed model, experiments are conducted in both virtual and real environments. The states required in the proposed model are extracted from the data and send into the model. Finally, the predicted behaviors are compared to the actual behaviors and the discussion is also made.

3.4.1 Urban Crossroads in Simulated Environment

The simulated environment (as shown in Fig. 3.20) is constructed in Gazebo which is an open source, 3 dimensions robotics simulator. Gazebo has been used in varius technical challenges and competitions including DARPA Robotics Challenge (2012-2015), NASA Space Robotics Challenge (2016-2017) and Toyota Prius Challenge (2016-2017). This simulator is known for its accuracy and the powerful, robust physics models that can simulate the world to the extent that most of the data output required for the model is available. Despite only the displacement from the subject vehicle to the the node and the speed of the vehicle is required, the realistic rendering of the constructed environment can minimize the differences between virtual and real crossroads. Also, here are a few advantages of using simulated world. First, collecting the data from experiments becomes easier. The required states of targets can be directly extracted form the simulator. Second, different scenarios can be employed with little efforts. Thirdly, it is both time and cost efficient.

The simulated vehicle in the virtual world are controlled using Gazebo ROS Controller which is a part of ROS packages names gzebo_ros_pkgs. This package provide the necessary modules and interfaces to simulate a robot (a vehicle in our case) in Gazebo which is taking orders from ROS messages and services. ROS is the short for

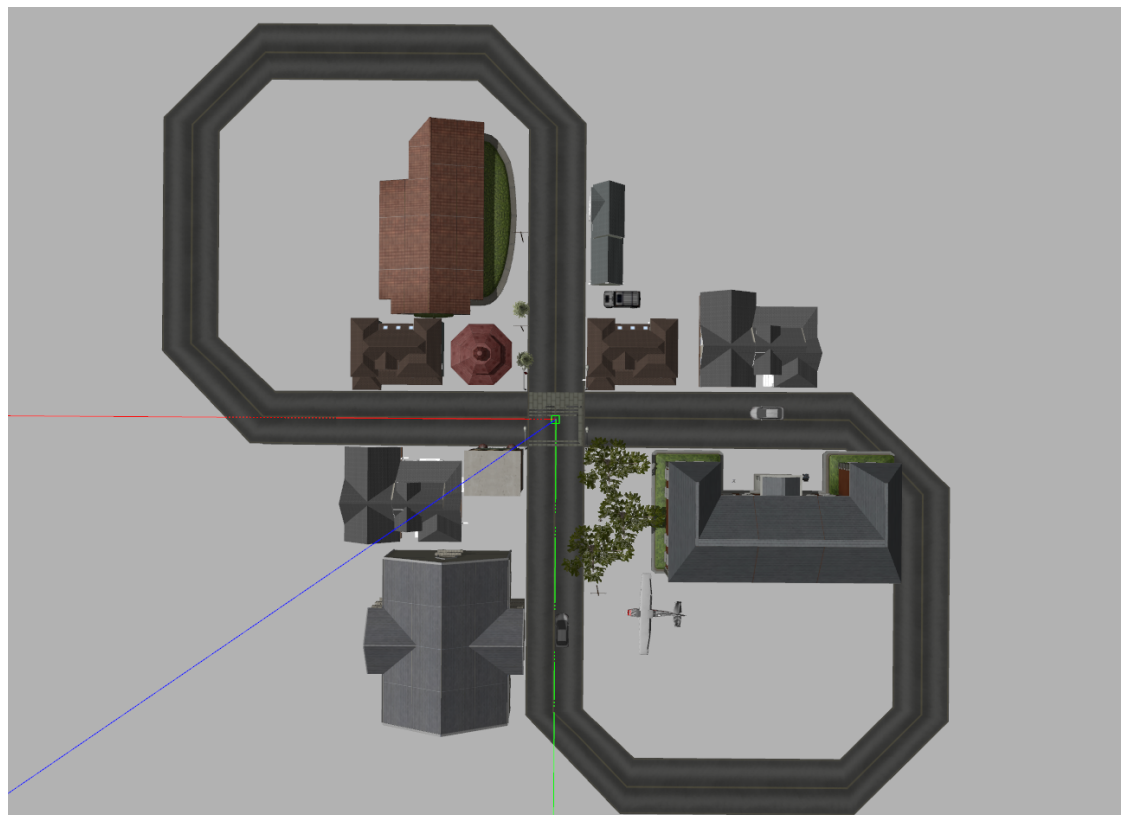


Figure 3.20: The simulated crossroad scenario in the Gazebo simulator.

"Robot Operating System" which is a robotics middleware that provide users with integrated packages, services and tools. The reusability for codes, implemented in multiple languages and continuous support from its community are all the benefits of ROS.

The front, left and right views from the driver seat are directly projected onto the screens when driving in simulated world. (Fig. 3.21, Fig. 3.22 and Fig. 3.23 respectively.) Control commands from the volunteers are sent from the joysticks to ROS node (a single process under ROS). Then the command velocity calculated according to the movement of the joystick is finally sent from the ROS node to the simulated vehicle in Gazebo. In every set of interaction experiments, a pair of volunteers (as shown in Fig. 3.24 and Fig. 3.25) are asked to drive across the intersection without collision. The displacements to the node and the speed of vehicles for both driver are recorded with the time resolution of 0.01 sec.



Figure 3.21: Front camera from driver seat in the simulated environment.



Figure 3.22: Left camera from driver seat in the simulated environment.

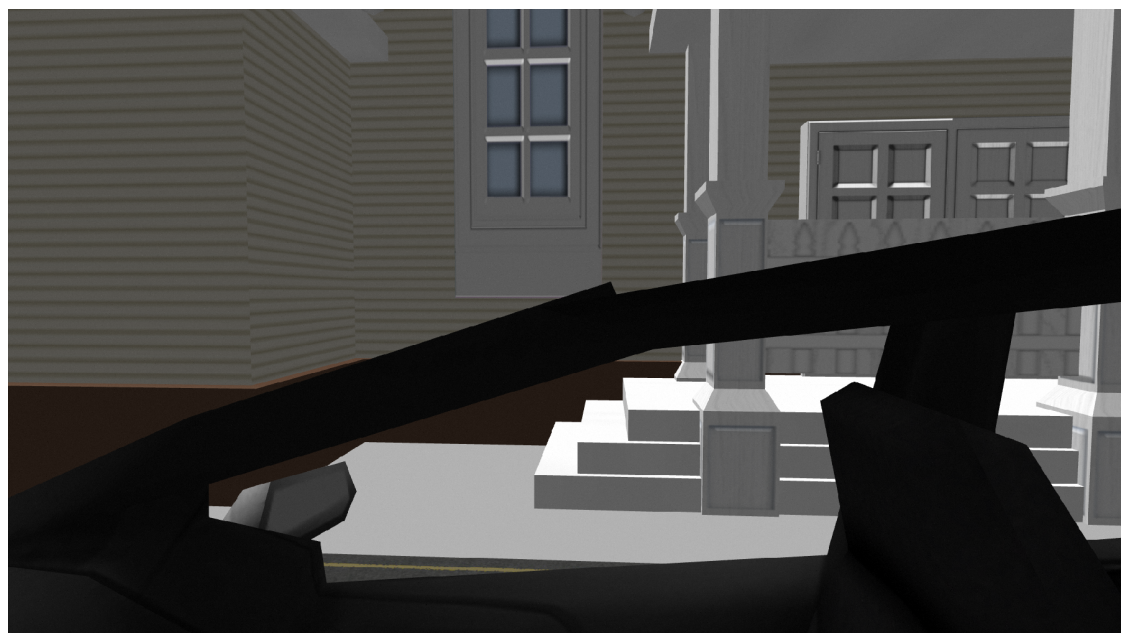


Figure 3.23: Right camera from driver seat in the simulated environment.



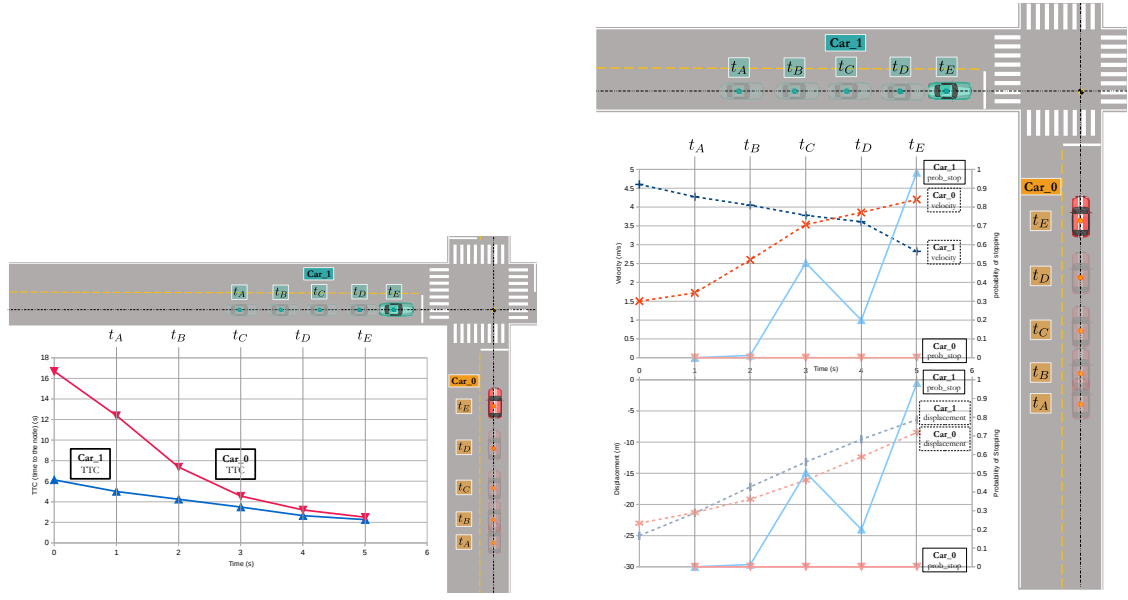
Figure 3.24: First driver in the simulated crossroad interaction experiment.



Figure 3.25: Second driver in the simulated crossroad interaction experiment.

3.4.2 Experimental Results in Simulated Environment

Since there are three participants who are asked to participate in pair, and about 50 repetitions were conducted each pair, so there will be about 150 sets of data in total. Within these trials, some will be explained in detail to demonstrate the performance of the proposed model. Then the classification accuracy rate will be evaluated using all data sets for validation.



(a) Illustration of calculated TTC of each vehicle. (b) Illustration of probability of stopping together with velocity and displacement.

Figure 3.26: Illustration of TTC and probability of stopping along with concerning variables.

We start the analysis by calculating the corresponding TTC of Car_0 (in red) and Car_1 (in cyan), as illustrated in Fig. 3.26a. TTCs correspond to t_A , t_B , t_C , t_D and t_E are shown in the chart of the figure. Afterward, the probability of stopping for each car is calculated using the proposed method and is plotted together with the velocity and the displacement in two separate figures, as illustrated in Fig. 3.26b. The data collection begins when both of the displacements to the node is smaller than 18 meters where drivers are able to see each other, and ends when the node is reached

by one of the participants. We then analyze how the probability of stopping can give assistance to the traffic participants using these figures.

Next, some of the experiments results will be presented to evaluate the performance of the proposed model. There will also be further explanations about the importance of parameters in the model. In the experiment conducted, trials are labeled with number (e.g. #001, #002, ...). The first interaction observed is trial #003.

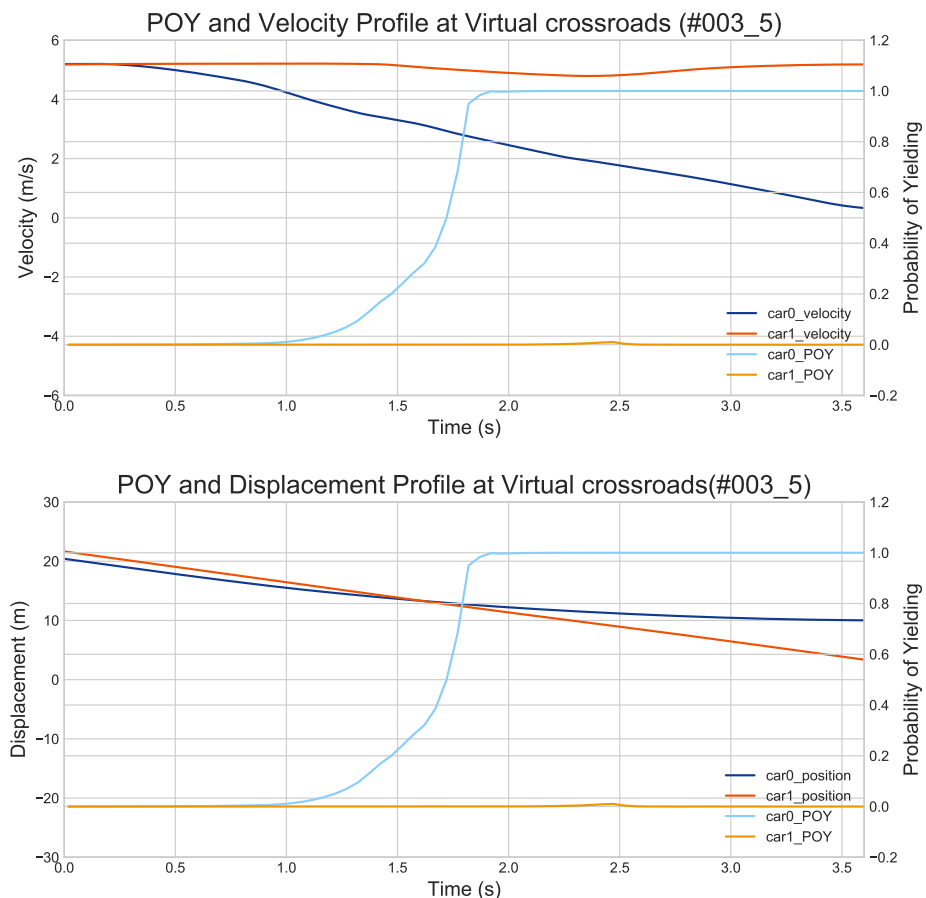
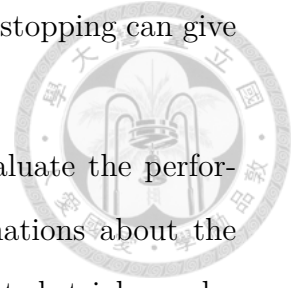


Figure 3.27: Trial #003 where car_0 was yielding and car_1 was passing with little interaction.

In this case, both yielding and passing types of drivers were included in this scene. Yielding type of drivers are those who will stop relatively early before the node, and slowly approach the intersection. They would only pass when the other agent is yielding. The passing type is the opposite, where there will be almost zero braking applied during the whole process.

As presented in Fig. 3.27, driver of car_0 was the yielding type because the deceleration started as soon as they could see each other in the sight (displacement at around 15 to 18 meters), and the driver of car_1 was the passing type. During 0.8 to 1.8 sec, the POY of car_0 was rising mainly due to the decreasing of the TTC at the moment, which was becoming smaller than the TTA_{est} and resulted in more and more areas were under the TFA distribution and right to the TTC. The small spike on the POY curve of car_1 around 2.5 was owing to the braking applied at about the same moment. In the next but one figure, this little bump will be elaborated. In this figure, the outcome suggests that the proposed model can correctly estimate the intention of the driver on other moving vehicles about 2 secs earlier.

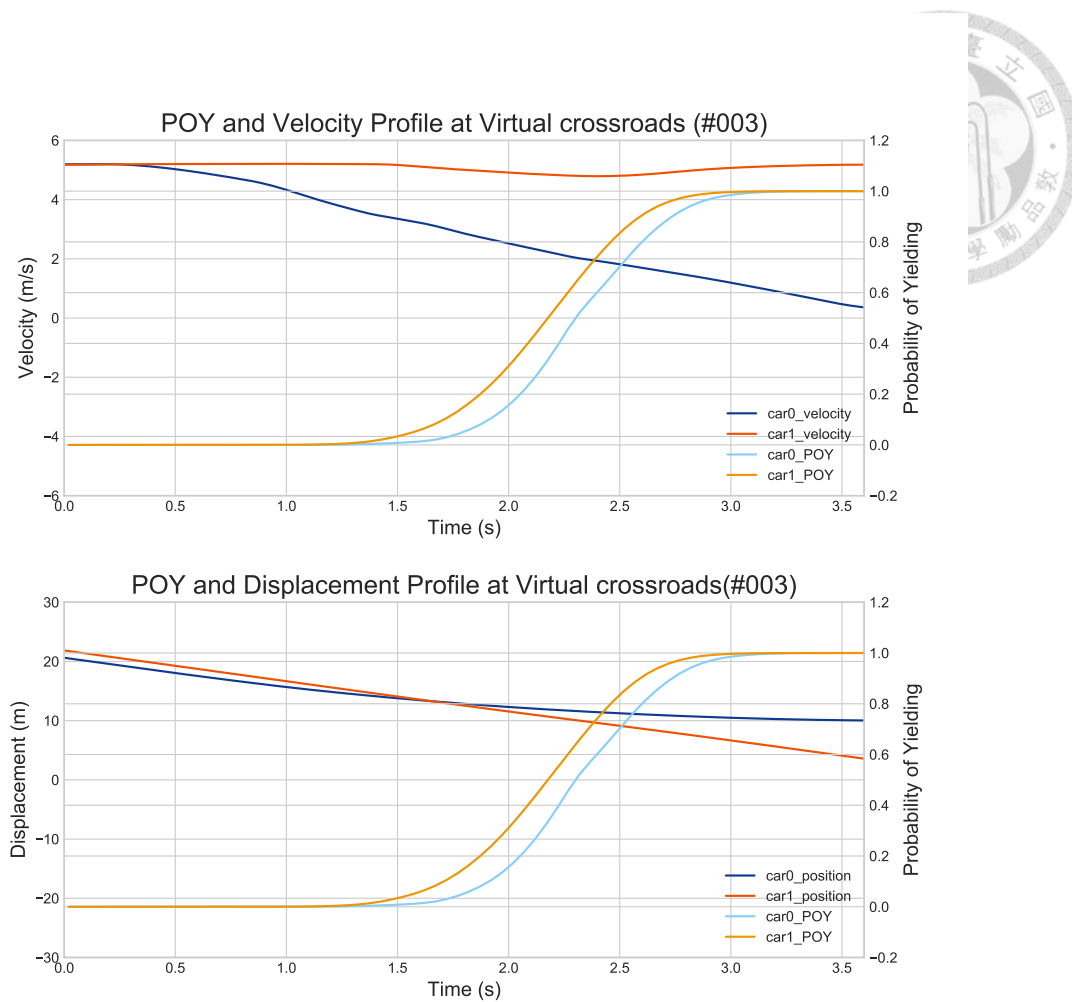


Figure 3.28: Trial #003 using POY without weighting parameter A (α).

To demonstrate the importance of the weighting parameter A (α), which was formulated in Chapter III, the same trial (trial #003) was evaluated again using the proposed POY model, but without the parameter A (α). Results are shown in Fig. 3.28. Note that the POY of both vehicles rose to 1.0 from 1 to 3 sec. The main factor in this scenario was the displacement to the node which affected the TFA_{est} and the $minTTC$. The plot showed that the closer the vehicle to the node, the higher the POY will be if it only depends on the displacement. Without the parameter A (α) being able to account for the acceleration and velocity and provide adjustments

accordingly, the POY is unable to predict accurately.

The conditions in Eqn. 3.19 were also proved to be indispensable for the proposed model to produce a stable result in Fig. 3.29. The huge spike occurred on the curve of car_1 POY around 1.2 to 2.5 secs was the consequence of the proposed model being too "sensitive" about some small changes in acceleration that usually do not imply the intention to yield. Constraints such as the maximum deviation for the TFA distribution (as formulated in Eqn. 3.18) or the threshold for acceleration longer than 0.2 sec are employed to prevent the POY from being too sensitive to accelerations.

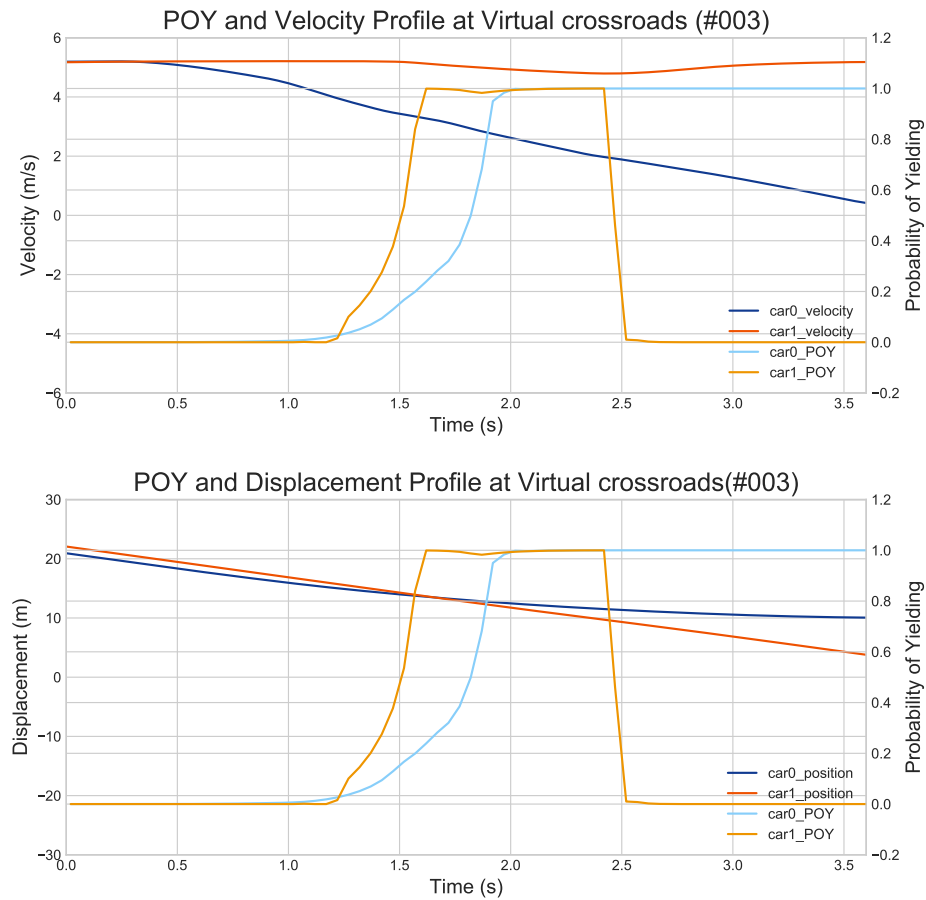


Figure 3.29: Trial #003 using POY without acceleration threshold.

The second case of interaction is more interactive than trial #003. In trial #077, both drivers were indecisive, since both participants were quite even at their states and no one was in dominant position. In the most extreme cases, it will take both drivers quite a long time before one of them decides to pass or yield. In trial #077, however, it did not take them too long before car_0 finally decide to pass. At the beginning of the interaction, POYs of both vehicles rose due to their deceleration. And from 1.5 to 3.2 secs, the POYs were kept at high level for car_0, while car_1 had the intention to pass, which resulted in the drop of POY. But right after car_1 accelerated, so did car_0 with very small time difference (0.5 sec). And after about a second, they both decelerated together again, but this time car_1 was determined to yield and car_0 finally passed. During this time, human drivers had no information about what actions the other one intended to take, so they waited until one of them did something. Yet, if one could utilize the proposed model which could estimate the TFA distribution of the driver and generate a probability from his or her current states, this stand-off-like situation could have been avoided.

The final case presented can again show how one can benefit from the proposed model. In Fig. 3.31, car_0 was a bit closer to the node and it yielded to let car_1, who was farther but had no intention to yield, passed first. However, car_1 did not think that the deceleration of car_0 was intended to yield, so it chose to yield too and car_0 then accelerated to pass. Again, this situation could have been avoided if the proposed method is referenced by the driver.

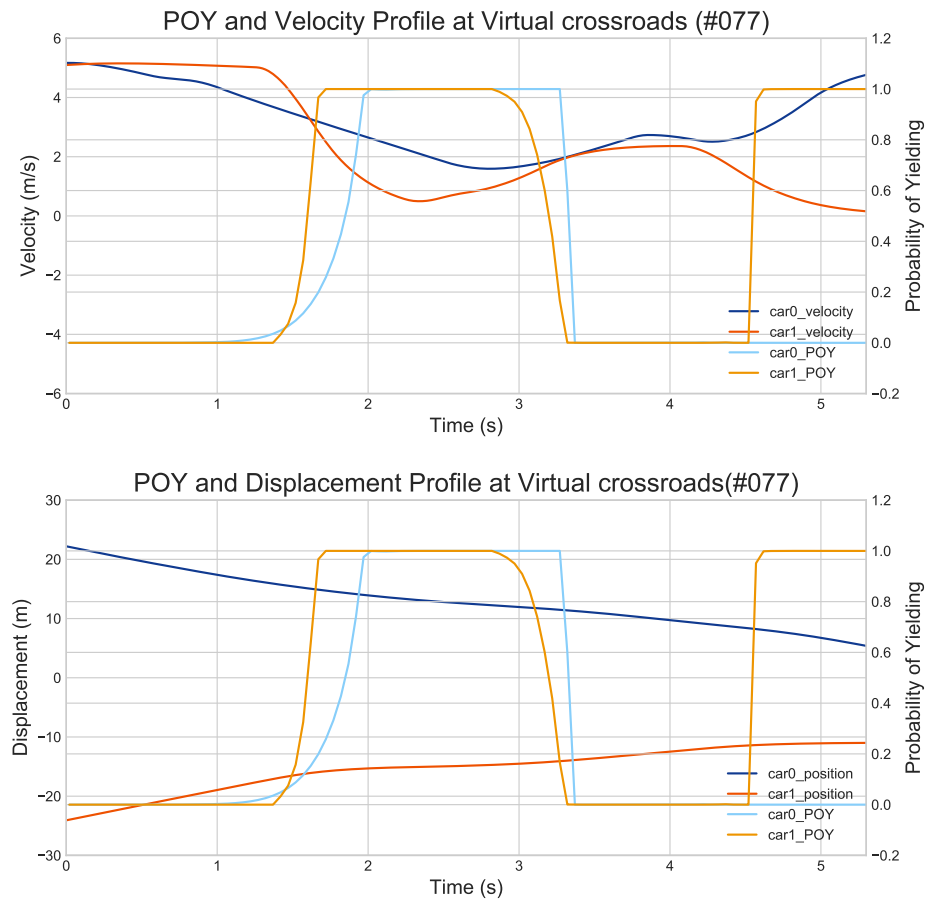


Figure 3.30: Trial #077 where car_0 and car_1 were confused about what action the other one might take.

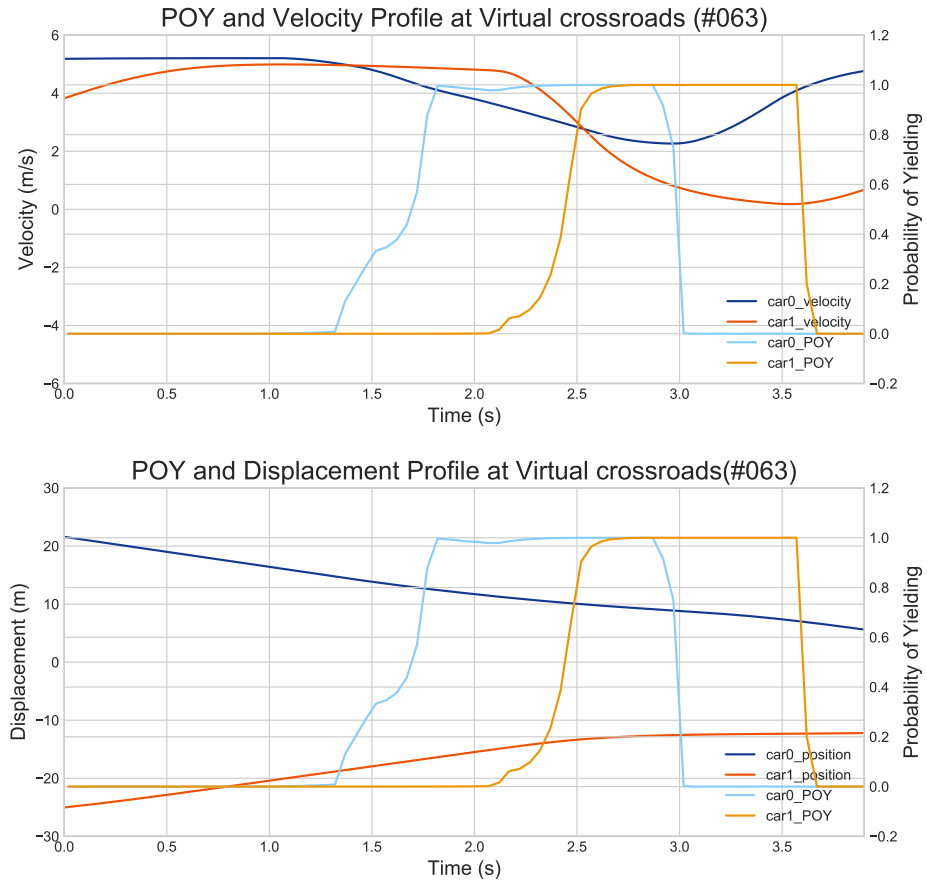


Figure 3.31: Trial #063 where car_0 yielded first but then passed due to the deceleration of car_1 .

3.4.3 Validation for Experiments in Simulated Environment

In Section 3.4.2, the proposed model is proved to be comparable to human drivers' prediction and the decisions of human drivers are managed to turn into some probabilistic values, which can be perceived by autonomous vehicles. In this section, the accuracy of the proposed model will be examined.

$$CARate = \frac{\text{number of correctly classified situations}}{\text{number of all situations}} \quad (3.21)$$

The Classification Accuracy Rate (CARate) is used to evaluate the classification accuracy of the proposed model. Due to the fact that the time spans for all interaction trials are different, the time line is be reversed and denoted as T_{minus} , i.e., $T_{minus} = 0$ denotes the time at the end of the process and $T_{minus} = 1$ denotes the time 1 sec earlier than that, and so on. Note that the end of the process is defined as the moment which the node is reached by one of the participants. The calculation of CARate is rather straight forward as shown in Eqn. 3.21. In the total of 168 cases of driver behaviors at the crossroad, the denominator of the CARate at each T_{minus} is then 168. The CARate results of the proposed model are shown in Fig. 3.32.

Results using the average parameters listed in Table. 3.1 are plotted in solid blue line while the trend line is plotted in dashed blue line. The reason for the drop from 0.0 to 1.5 T_{minus} is that, people tend to behave more aggressive in our simulated environments. During the experiment, participants who yielded for the other driver accelerated before the end of the process which is the moment when the node is reached. The example is shown in Fig. 3.33.

Comparing to other few behavior prediction model, the CARate of the proposed model is comparable to the state-of-the-art. In the work of Graf et al. [18], the CARate reached 0.81 at around $T_{minus} = 3$, while in the proposed model 0.81 is reached at $T_{minus} = 1.5$. This is owing to the relatively short interaction time span

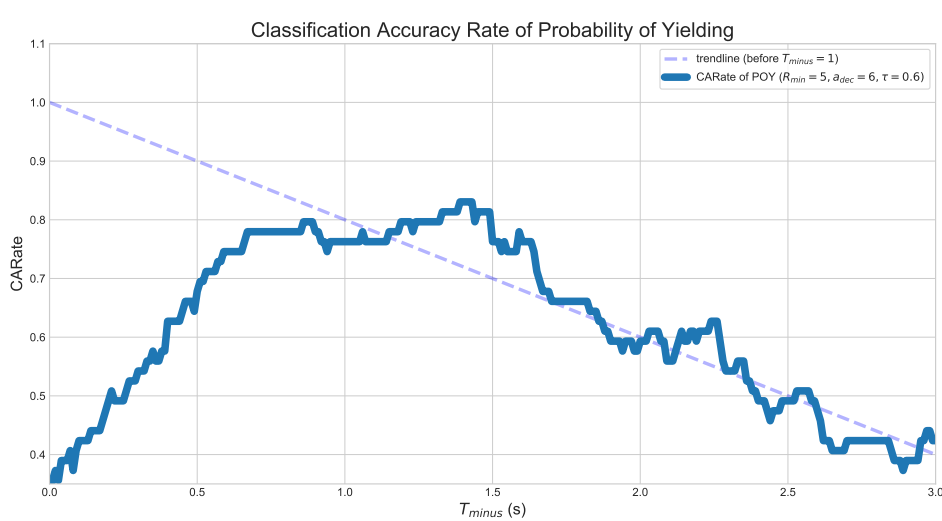


Figure 3.32: CARate of the POY using all data sets.

in the simulated environment, where participants are using joysticks sending out maximum command velocity. In the literature, interactions at real crossroads takes about 6 secs to cross a 12 to 18 meters long distance, yet at the simulated crossroad, it only takes about 3.5 secs to cross 20 meters. Furthermore, the method proposed in the literature requires pre-trained model for a specific where in POY no training steps are needed. The proposed POY also has the potential of generating better predictions if the parameters characterizing his or her driving pattern is known.

In this chapter, a novel driver behaviors model at crossroads was proposed. Driver intentions were predicted based on the parameter TTC, which is an important and well developed risk estimation method in traffic safety assessment. Derived from the concept, the TFA distribution was shown to be an innovative and effective driver intentions indicator that can be used to predict the driver behaviors. The normally distributed TFA distribution was then formulated and proven to be an unerring approximation. At last the driver behaviors model was finally proposed and validated at the simulated crossroad where prediction accuracy was comparable to the state-of-the-art driver behaviors prediction method.

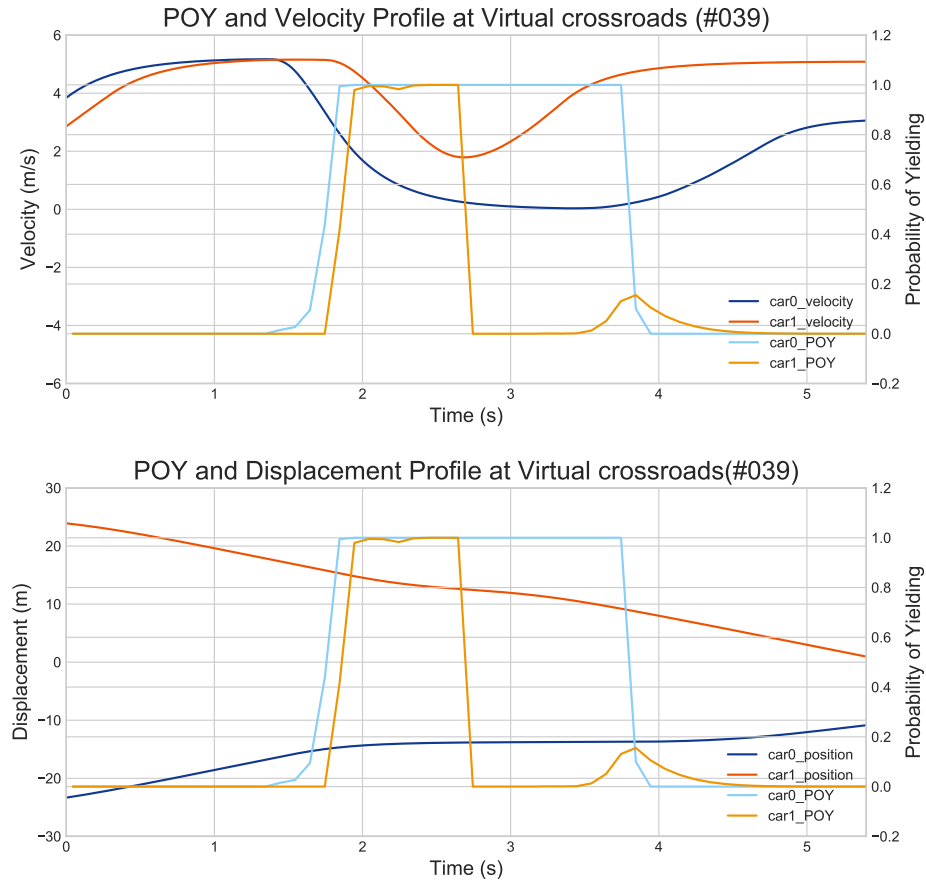


Figure 3.33: Trial #039 where car_1 begun to accelerate before car_0 passed the node, causing the false prediction.





CHAPTER IV

Model Parameters Identification

In Chapter III, a model providing a probabilistic way to evaluate the possible behaviors of other traffic participants was proposed. The concept of the fact that TFA distributions are different among people was also elaborated and formulated in Eqn. 3.8. Then, the average parameter of participants were found and used to estimate the POY in the experiment at the simulated crossroad. In this chapter, the characteristic parameters of drivers will be attempted to identify.

4.1 Characteristic Parameters

The way people drive is different from person to person, some are aggressive, while others are more conservative. This also applies to the decision on braking moment. In Section 3.2, the mean value of TFA distribution of drivers is formulated in Eqn. 3.8, where three parameters including R_{min} and a_{dec} are introduced. The R_{min} , standing for the minimum distance left when the vehicle is fully stopped, being a parameter known as a function of velocity of the vehicle, is also changing with different characters. To put it another way, two different driver driving two identical vehicles under same speed would have different mean distance left before the vehicle and the obstacle when the vehicle stops moving. This is a rather instinctive results since a more aggressive people tend to brake as late as possible which contributes to

the smaller R_{min} . Similarly, drivers who make traffic offense are having higher a_{dec} than those more conservative.

What can be learned from Eqn. 3.8 is that, each of these parameters can put effect on the value of TTA_{est} , in other words, they decide the value of TTA_{est} and the results of POY. In Fig. 4.1 and Fig. 4.2, the POY using the average parameters and the driver's parameters are compared. As we can see in these cases, the POYs of the vehicle (car_0 in Fig. 3.27) are higher using the characteristic parameters belonging to the driver.

This phenomenon is owing to the closer estimation of the TFA distribution. Bringing a set of average parameters into Eqn. 3.8 will only give an rough whereabouts of the TFA of the driver at the moment (considering velocity, displacement to the node and so on). Using the specific characteristic parameters, on the other hand, could effectively narrow down the TFA of the driver to within the consequential TFA distribution. Still, chances are that the estimated TFA distribution using the characteristic parameter might be different from the real TFA under the circumstance, given that both of them are distributions. However, given a large enough database, the average POY acquired using characteristic parameters should be higher than that using average parameter.

To identified the corresponding characteristic parameters of participants, experiments same as the one used in Chapter III are conducted for each participants. Here, experimental results and characteristic parameters of Participant 1 and 3 are shown in Fig .4.3, Fig .4.5, Fig .4.4 and Fig .4.5.

Similar to the result using combined data of all participants in Chapter III, the characteristic parameter of each participant can be approximated linearly and both R_{min} and a_{dec} are positively related to the velocity at the moment. Different values of slopes, as denoted as $C1_{Rmin}$ for linear approximated R_{min} or $C1_{a_{dec}}$ for a_{dec} in Eqn. 3.13 and Eqn. 3.14, are found on different participants. The values of R_{min} ,

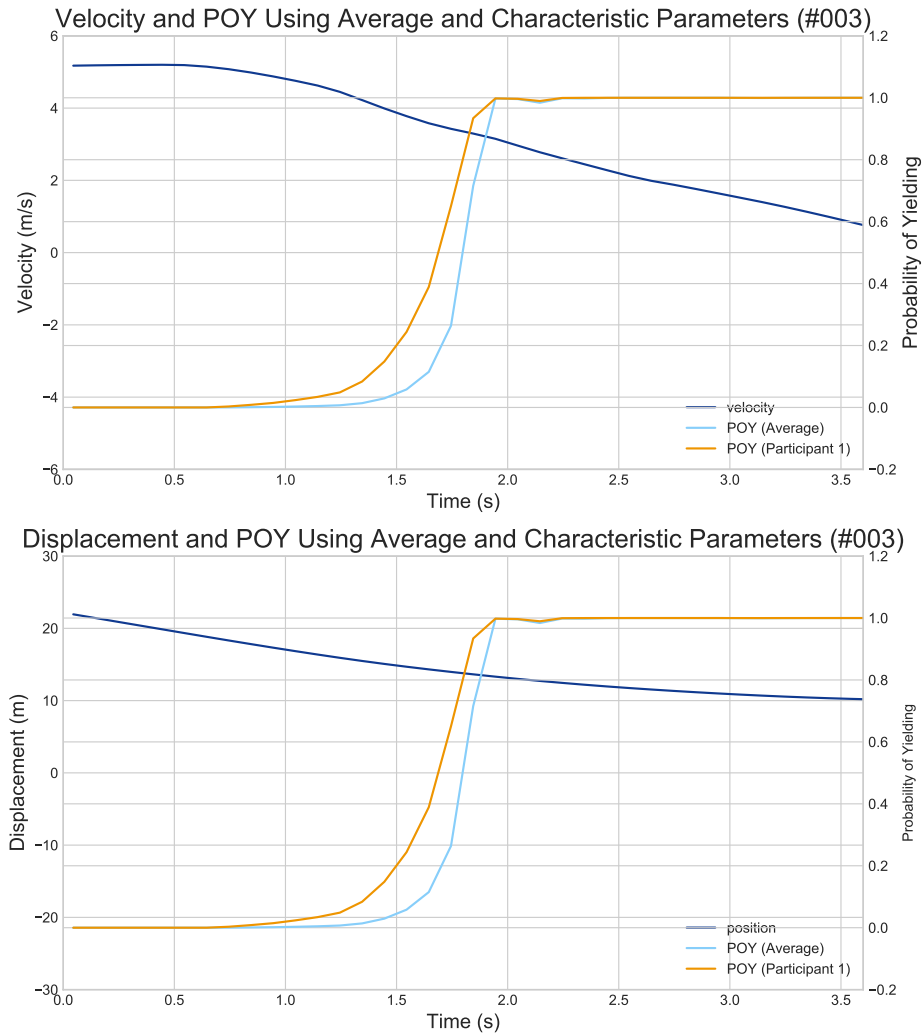


Figure 4.1: Trial #003 with POY using average parameters and parameters of Participant 1.

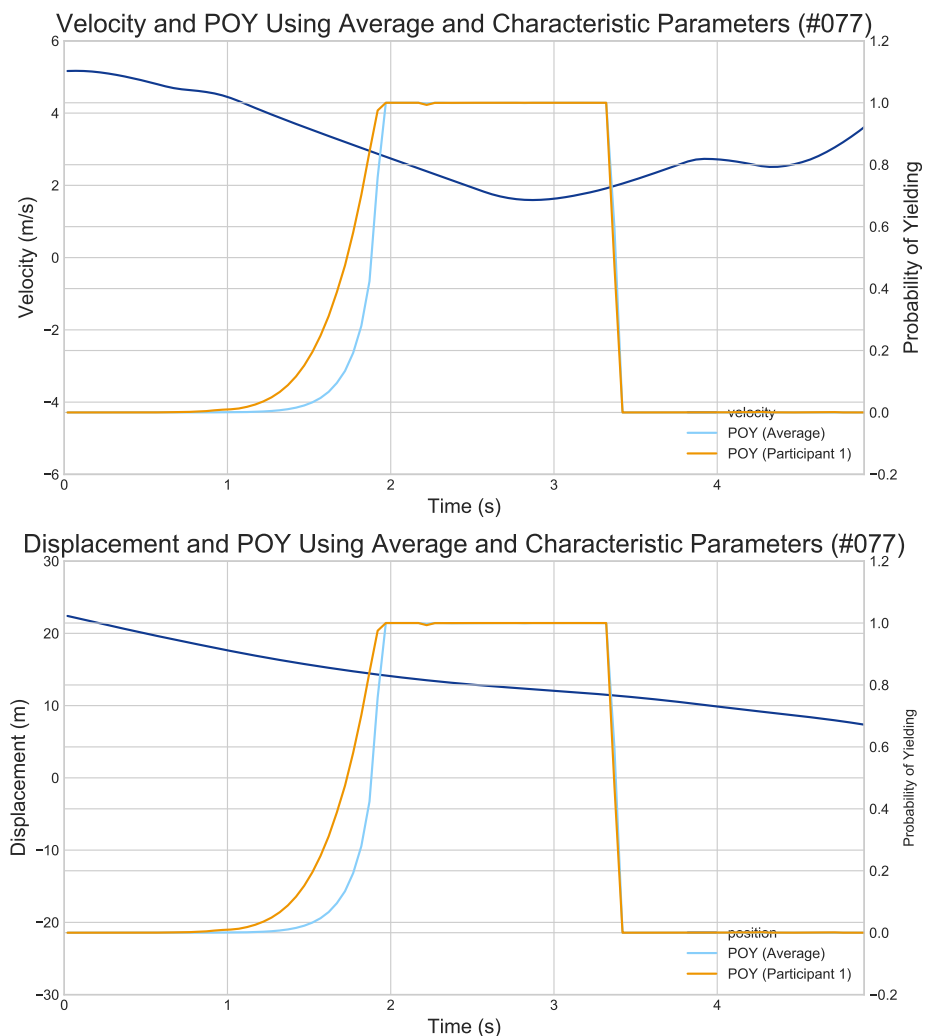


Figure 4.2: Trial #077 with POY using average parameters and parameters of Participant 1.

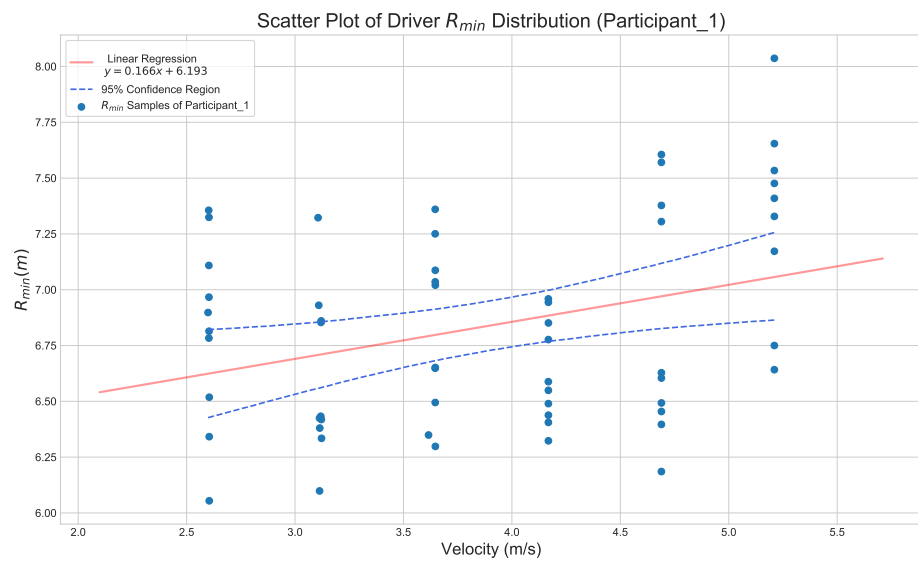


Figure 4.3: The R_{min} scatter plot of Participant 1 under various velocities.

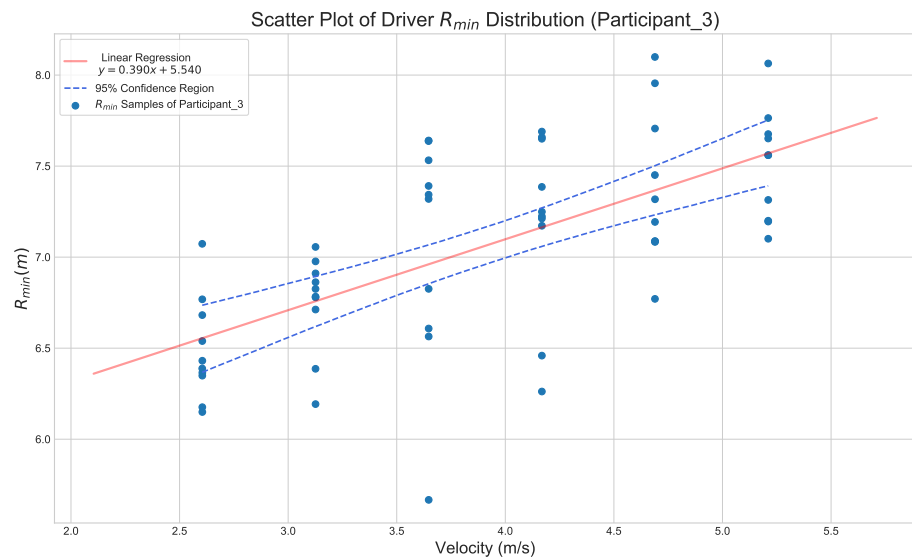


Figure 4.4: The R_{min} scatter plot of Participant 3 under various velocities.

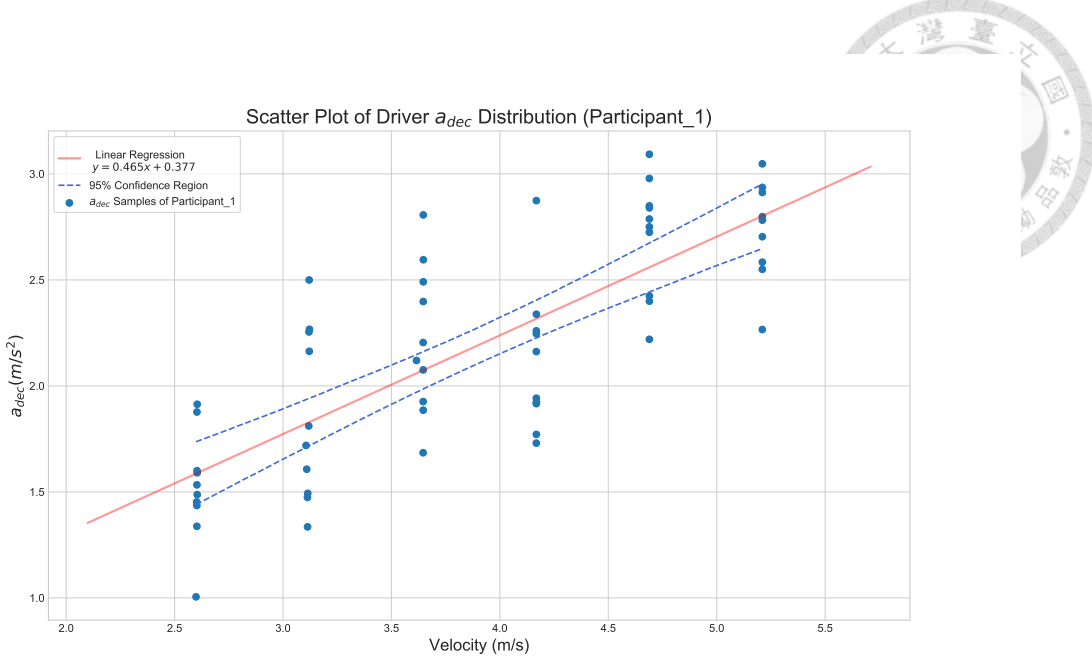


Figure 4.5: The a_{dec} scatter plot of Participant 1 under various velocities.

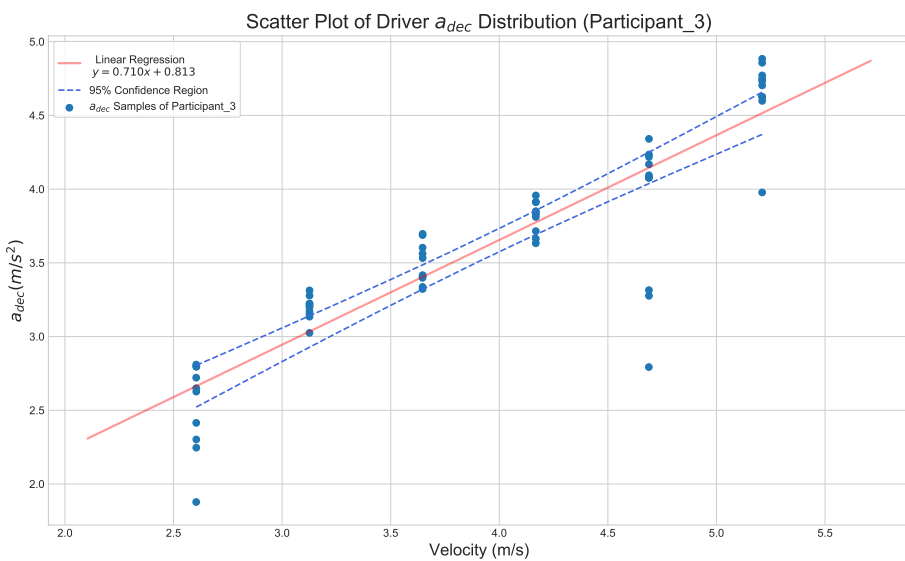


Figure 4.6: The a_{dec} scatter plot of Participant 3 under various velocities.

after the intersection at velocity around 3 m/s, those of Participant 3 have higher R_{min} from 3 to 5 m/s. As for a_{dec} , the line of Participant 3 is always above that of Participant 1.

The results can be suggested that Participant 3 is a more cautious driver than Participant 1, since there are larger distances (R_{min} values) left between the vehicle and the obstacle. Combining that with the large a_{dec} values, it is likely that Participant 3 is a new driver (in the simulated traffic environment) since more abrupt brakes are often applied. The characteristic parameters of these two participants are compared with average parameters in Table 4.1.

Table 4.1: Table for characteristic and average parameters.

Parameters	Average	Participant 1	Participant 3
Safe Margin Coefficient ($C1_{Rmin}$)	0.295	0.166	0.390
Safe Margin Constant ($C2_{Rmin}$)	5.47	6.19	5.54
Deceleration Coefficient ($C1_{a_{dec}}$)	0.458	0.465	0.710
Deceleration Constant ($C2_{a_{dec}}$)	0.877	0.377	0.813
Standard Deviation Parameter (γ)	0.148	0.115	0.102

When the characteristic parameters are identified, it is not only the driving style could be found, the right parameters for the proposed model can also be applied to have a better prediction of the next possible behaviors coming from other traffic participants. In the next section, the CARate curve of average and characteristic parameters will be compared for verification and optimization for the CARate curve will also be employed to identify the matching characteristic parameters.

4.2 Objective Function and Constraints for Optimization

In Section 4.1, the POY curves of the same trial using different variables sets are found to be different, because a more accurate approximation to the TFA dis-

tribution is generated using the characteristic parameters of the driver. To compare the characteristic parameters of a particular driver to average parameters, the trials involving that driver are specified and used as the database for the CARate curves using two sets of parameters. Results are plotted in Fig. 4.7.

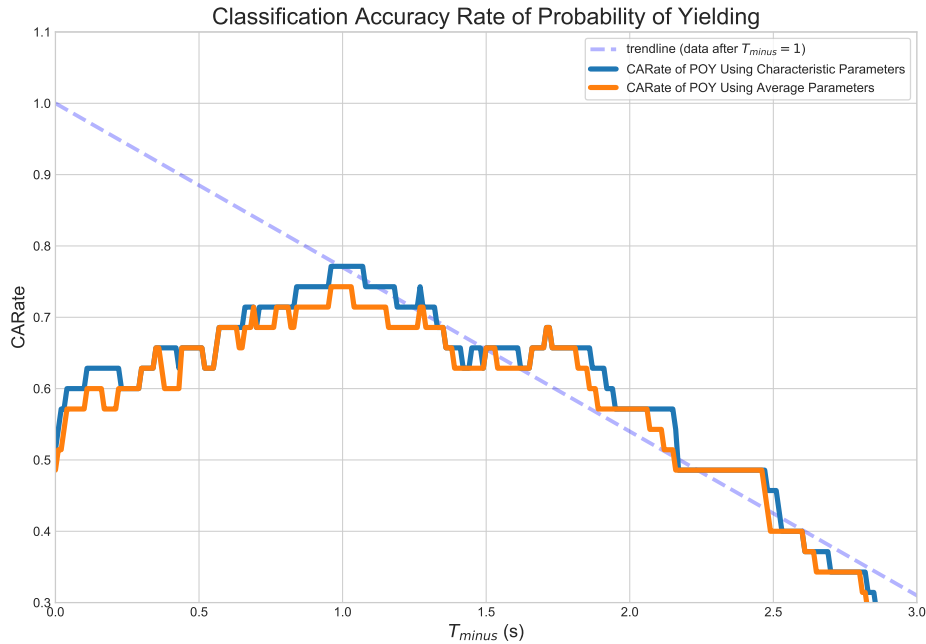
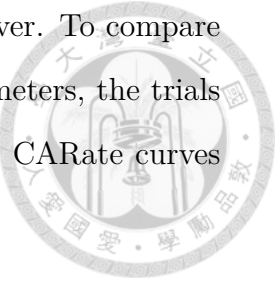


Figure 4.7: CARate curve of POY using average parameters and characteristic parameters are compared.

In the figure, the solid blue line indicates the CARate curve of POY using characteristic parameters (blue line for short) while the orange line represents the CARate curve of POY using average parameters (orange line for short). The highest CARate of the blue line is around 0.78, which is higher than that of the orange line around 0.74. Despite the non-significant difference between two highest points, it is noticeable that blue line is above the orange line throughout the whole T_{minus} span, which gives the evidence to the supposition that the closer parameters set can give rise to larger area under the resulting CARate curve. If a more far off set of parameters are ap-

plied, e.g. the parameters set of another participant, the gaps between the resulting CARate cure of POY should be larger, owing to the more imprecise estimation for the TFA distribution. The comparison between the characteristic parameters and the parameters set of another participants are made in Fig. 4.8.

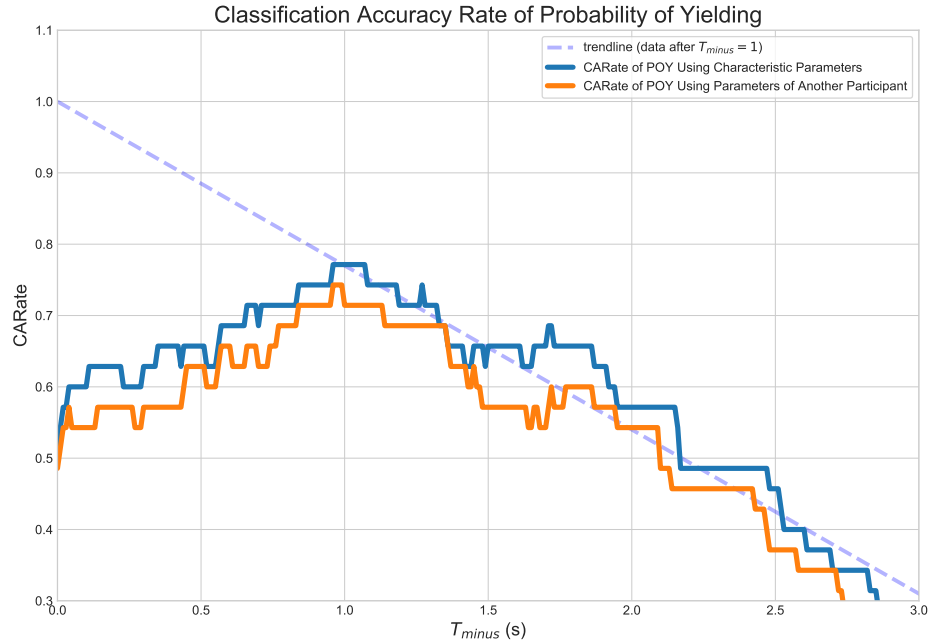


Figure 4.8: CARate curve of POY using characteristic parameters and the parameters set of another participant are plotted.

It is not hard to observe that the differences between two CARate curves are more distinct than that in Fig. 4.7, for that the values of average parameters set is closer to characteristic parameters than that of another participant.

Up to the present, the differences between the resulting CARate curves using different sets of parameter are identified. Based on this idea, creating a procedure using collected traffic data at crossroad to identify the characteristic parameters representing the driving behaviors of that area is possible. So the problem now would be, how to optimize the CARate curve so as to find the most possible parameters set

representing the driver.

To solve the problem using optimization, the objective function and constraints are defined as

$$\begin{aligned}
 & \underset{w}{\text{minimize}} \quad \frac{1}{M} \sum_{j=1}^M \sum_{i=1}^{N_j} -f(POY_j(t_i, w)) \\
 & \text{subject to} \quad 2.0 \cdot C1_{Rmin} + C2_{Rmin} \geq 4.48, \\
 & \quad 5.2 \cdot C1_{Rmin} + C2_{Rmin} \leq 12.0, \\
 & \quad 2.0 \cdot C1_{adec} + C2_{adec} \geq 0.01, \\
 & \quad 5.2 \cdot C1_{adec} + C2_{adec} \leq 3.5, \\
 & \quad 0.01 \leq \gamma \leq 0.5
 \end{aligned} \tag{4.1}$$

where the function POY_j in the optimization problem is

$$f(POY_j) = \begin{cases} 1 & \text{if } POY_j(t, w) \geq 0.8 \text{ and yielded} \\ 1 & \text{if } POY_j(t, w) \leq 0.2 \text{ and passed} \\ 0 & \text{otherwise} \end{cases} \tag{4.2}$$

The objective function in Eqn. 4.1 indicating the total area underneath the CARate curve, where the w is the parameters set $(R_{min}, a_{dec}, \gamma)$ maximizing the area (minimizing the negative area), i.e., bringing the parameters set into the proposed POY model could have the highest accuracy on predicting the behaviors of the driver from the experimental data. The constants M and N_j stand for the number of the trials in the collected data and the number of time steps in each trial with the resolution of 0.01 sec.

Due to the linearity of R_{min} and a_{dec} , the maximum and minimum value of both parameters should occur at the maximum and minimum velocity right before braking which are 5.2 and 2.0 m/s respectively. While the definition of the R_{min} is calculated

from the center of one vehicle to another, the minimum distance under 2.0 m/s is also bounded by the physical model built in the simulated world, which is 4.48 meters. The maximum is then bounded by the longest between vehicles one could possibly have, which is 12 meters, the maximum distance they can see each other. As for the minimum and maximum in the constraint of a_{dec} , they are also restraint within the boundary set for the command velocity sent from the joystick, which are 0.01 and 3.5 respectively.

4.3 Optimization Using Simulated Annealing

In this research, the Simulated Annealing (SA) is chosen for this optimization problem due to the non-smooth and time-consuming properties of the objective function. First published by Kirkpatrick et al. [25], SA is an efficient method to approximate the global optimization without using the derivative information. Despite being a global optimizer, it is not guaranteed that the solution found is an global optimum, however, the close enough variables set within limited time could be discovered.

The process of SA is an inspiration from the annealing process in material science, where the ductility is increased during the cooling process. The key idea applied to the optimization problems is the process of the temperature dropping, which is redefined as the lowering probability of accepting a worse variables set as the solution in the optimization problem. Four essential elements in the SA optimization problem are listed below :

- **Energy function :**

Usually denoted as E_i , representing the value of objective function using the best solution (set of variables) at the moment. In this situation, the sign of ΔE is then defining the current *move()* to be an uphill or a downhill move.

- **Random number generator :**

The function `move()` update the solution for the optimization problem. Despite the Monte Carlo method is applied, a well defined update procedure can solve the optimization problem with efficiency.

- **Worse case accepting probability :**

Defining the probability P_i that whether to accept a worse solution is the essential element for the SA to jump out of the local minimum. It is usually in the form of

$$P_i = \exp \frac{-\Delta E}{T_i} \quad (4.3)$$

where the ΔE represents the difference between the objective function value generated by the new solution and the best one so far. When a worse solution is generated, the value P_i is compared to a random number, and the worse solution is accepted if P_i is greater than the random number. Hence, larger the ΔE values will reduce the chance a worse solution being accepted. On the contrary, higher the current temperature indicating a higher chance of adopting the worse solution.

- **Annealing (cooling) schedule :**

Within the SA, the temperature drop is governed by equation

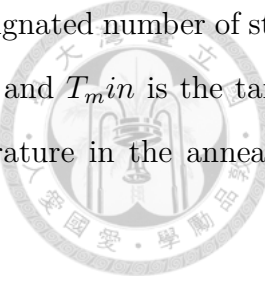
$$T_{i+1} = T_i \cdot \exp \frac{T_{factor,i} \cdot i}{N} \quad (4.4)$$

where the T_{factor} is defined as

$$T_{factor,i} = -\ln \frac{T_i}{T_{min}} \quad (4.5)$$

The temperature decay is based on the Newton's law of cooling with little

modification to end the optimization process within designated number of steps N . In the equation, the T_i is the current temperature and T_{min} is the target temperature of cooling (i.e. the environment temperature in the annealing process).



In our case, the energy function E_i is defined by the objective function in Eqn. 4.1, where the ΔE is found in every iteration by calculating $(E_{i+1} - E_i)$ after the new set of variables are generated by function *move()* and examined to satisfy the constraints. If a better solution is found (meaning that $\Delta E < 0$), the best solution is replaced with the new one. Otherwise, the probability P_i is then compared to a random number to decide whether to accept the worse solution. The process then iterate N times (until the temperature drops to the environment temperature), or one of the termination conditions is reached.

The results of the optimization are shown in Table 4.2, and the parameters used for the SA in the optimization problem are listed in Table 4.3.

Table 4.2: Table for results of the proposed optimization problem.

Optimization Number	$C1_{Rmin}$	$C2_{Rmin}$	$C1_{a_{dec}}$	$C2_{a_{dec}}$	γ	Area
1st Optimization	0.362	7.91	0.0460	0.954	0.460	-205.40
2nd Optimization	0.401	7.86	0.224	0.563	0.443	-205.37
3rd Optimization	0.322	7.91	0.106	0.941	0.434	-205.23
4th Optimization	0.456	7.49	0.102	0.824	0.444	-205.37
5th Optimization	0.346	7.95	0.145	0.812	0.448	-205.37
Characteristic	0.166	6.19	0.465	0.377	0.114	-183.89

The optimized parameters for R_{min} and a_{dec} are shown in Fig. 4.9 and Fig. 4.10. While in Fig. 4.11, the CARate curves using optimized parameters listed in Table 4.2 are plotted together with the CARate curves using characteristic parameters. In Fig. 4.9 and Fig. 4.10, the corresponding lines representing the linear equation using $C1$ and



Table 4.3: Table for parameters used in the Simulated Annealing.

Parameters	Values
Start Temperature	120
End Temperature	0.02
Steps	100000

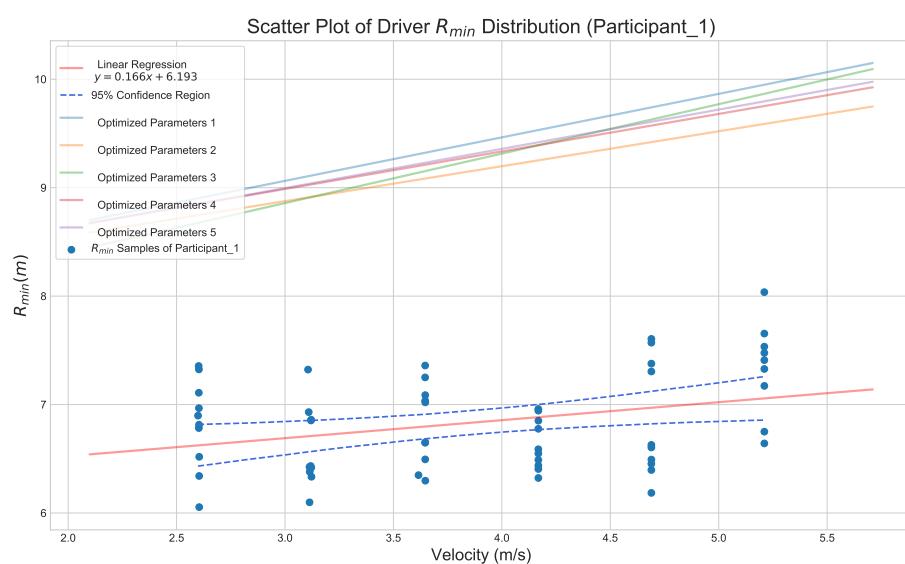


Figure 4.9: Optimized parameters of R_{min} are compared with characteristic parameters.

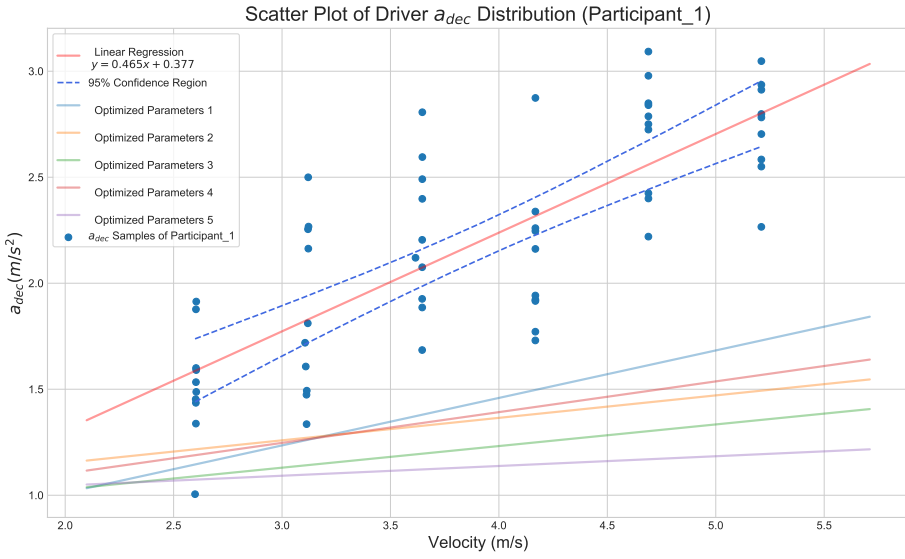


Figure 4.10: Optimized parameters of a_{dec} are compared with characteristic parameters.

$C2$ as the coefficient and constant are forming a cluster in plots of R_{min} . While in a_{dec} , the lines are not as ordered at higher velocities.

However, when looking into Fig. 4.11, all of the optimized CARate curves are overlapped and the area under the curves are larger than the characteristic parameters. Some might wonder, does this implied that the optimized parameters are a better set of parameters that can explain the behavior of the driver? To answer this question, first, the POY curves using the optimized parameters should be examined.

As shown in Fig. 4.12 and Fig. 4.13, the POY curves of the optimized parameter (here the parameters set Optimized 1 is chosen) rose way earlier than using the characteristic parameters. This implies that the the POY with optimized parameters is very sensitive to all the accelerations, so at the instance the vehicle begins to decelerate, the action is considered as having the intention to yield. Yet, being too sensitive to accelerations will result in the bumpy curves, making the meaning of POY curves not understandable, and will sometimes generate false results. For example,

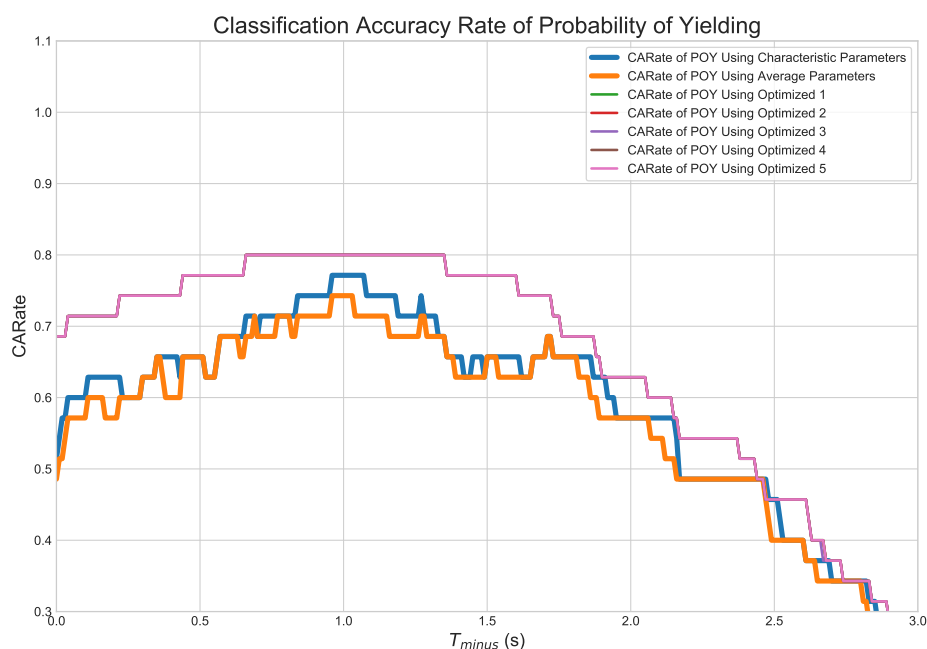


Figure 4.11: CARate curve of POY using characteristic parameters and optimized parameters are plotted.

the rises of POY curves using optimized curves in both figures are way early than the interactions begin, which happen around the distance to the node is about 15 meters. The optimized parameters do have a better CARate curve, but this does not suggest a more accurate prediction. Some modifications for the objective function are required, so the characteristic parameters could be identified more accurately.

In this chapter, a characteristic parameters identification procedure was developed. From the examinations of the POY curves using the characteristic parameters of the driver and the average parameters, the idea of using the results of POY curves and CARate curves to identify the characteristic parameters was generated. After proving it using the CARate curve, an optimization problem was constructed with the area under the CARate curve as the objective function. Despite some improvements are needed to have a more precisely parameters identification, this procedure provides a preliminary method for characteristic parameters recognition.

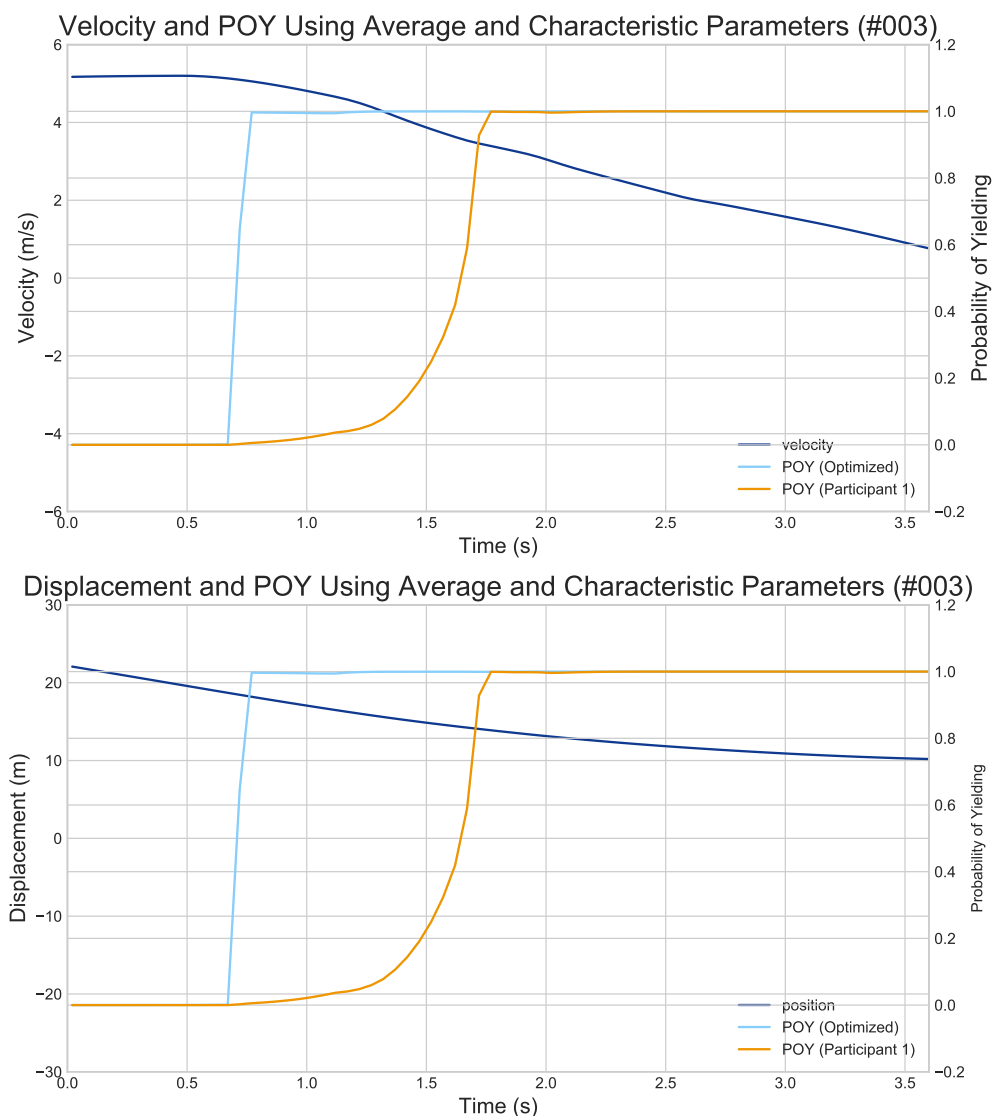


Figure 4.12: Trial #003 using the optimized parameters and the characteristic parameters.

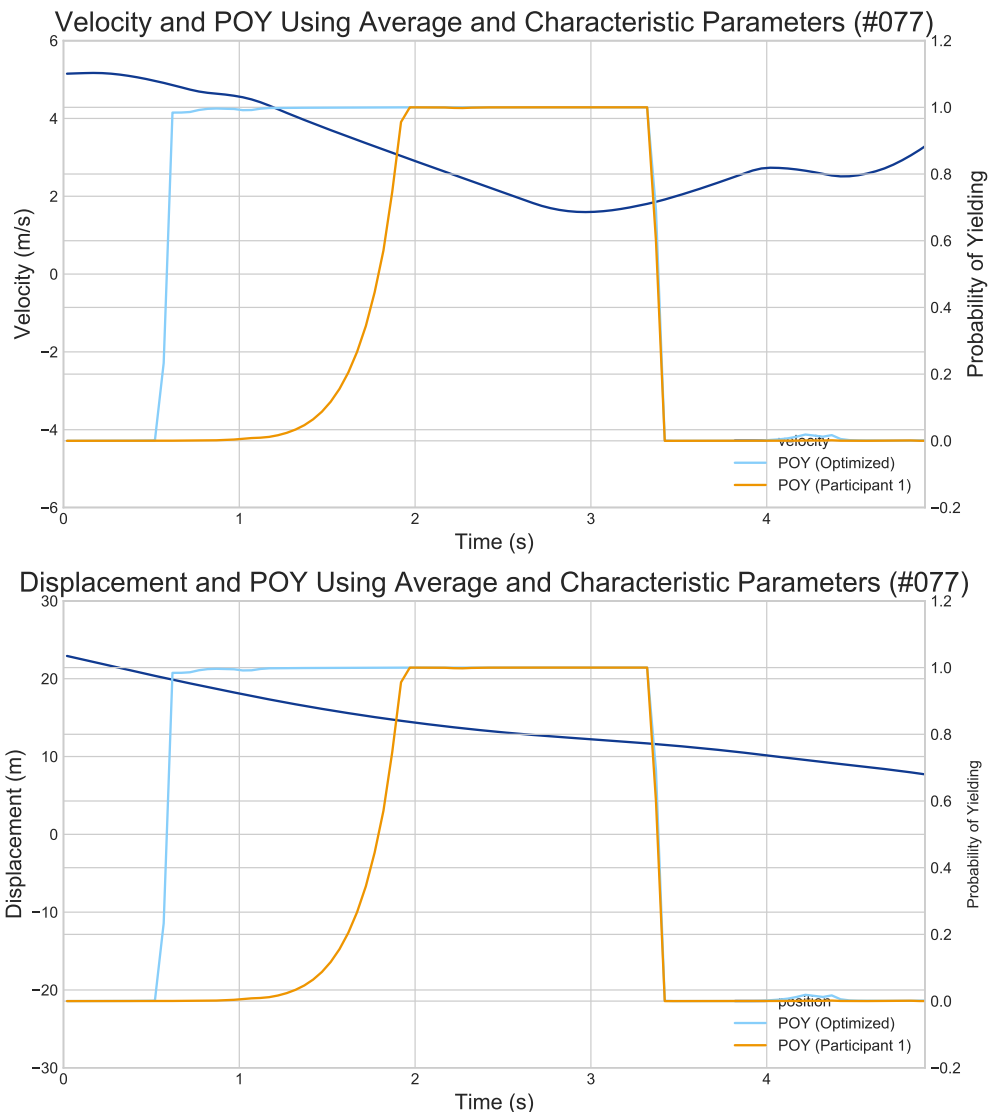


Figure 4.13: Trial #077 using the optimized parameters and the characteristic parameters.





CHAPTER V

Applications

In this chapter, the applications of the proposed driver behavior model are presented. In the first application, the relationship between certain driver behaviors and crashing cases are identified. Then, the proposed model is applied to predict the behaviors of drivers at an urban crossroad in real world where the performance is also evaluated. For the second application, considering that in the near future, it will be urgent for autonomous vehicles to handle the stnad-off situation where both participants are having the intention to yield (or to pass). To provide evidence that the proposed method is able to identify such situation and allows drivers (both computer and human) to make reasonable reactions accordingly, a simulated autonomous vehicle is constructed to predict the behavior of human driver based on the proposed POY model. Finally, the driver parameters at various crossroads in real world are also identified using the proposed model. Despite only the average parameters are acquired, these values are important factors for autonomous vehicles to travel through different crossroads.

5.1 Crash Examinations in the Simulated Crossroad

During the experiments in the simulated crossroad in Gazebo, few cases failed to cross the intersection safe and sound. In these cases, the participants either did not

notice the oncoming vehicle from the left (or right) or misjudged the arriving time of the other vehicle (i.e. its TTC) and led to the crashes. To examine the cause of the accidents, first the TFA distributions of both participants and the average distribution are shown and explained. Then, POYs are also shown together with the TTC difference for further explanation.

There are considerable number of reasons that can lead to crashes which seemly happen in a random pattern. However, there do exist some regions and intersections where traffic accidents happen more frequently. Reasons behind the high accident number might be the light conditions, the design of the road layouts or even the driving pattern of drivers in the neighborhood. In this section, these regions are attempted to be identified using the concept of the proposed TFA distribution. Then, the likelihood of accidents happening could also be estimated.

5.1.1 Crashing Likelihood Using TFA Distributions

In Chapter III, the TFA distribution is defined as the probability density function of the driver taking actions (e.g. braking) under different TTC. The closer the current TTC to the mean TFA of the driver, more likely the driver will brake at this TTC. As a consequence, in the **normal** cases (where vehicles passed or yield without collisions), drivers brake at TTCs within the TFA distribution to avoid potential collisions and most of the TTCs that drivers brake at are those closer to the mean value of the TFA distribution (those with higher likelihood). What can be noted here is that, as long as the TTC while braking is within the bound of the TFA distribution, greater the TTC value while braking stands for the more conservative driving pattern despite the smaller likelihood, and smaller the TTC value while braking represent the more aggressive driving pattern. To clarify the idea, let us look at the TFA distributions of a normal case where no accident happened (as shown in Fig. 5.1 and Fig. 5.2).

The velocities and displacements of both vehicles participated in this case is shown

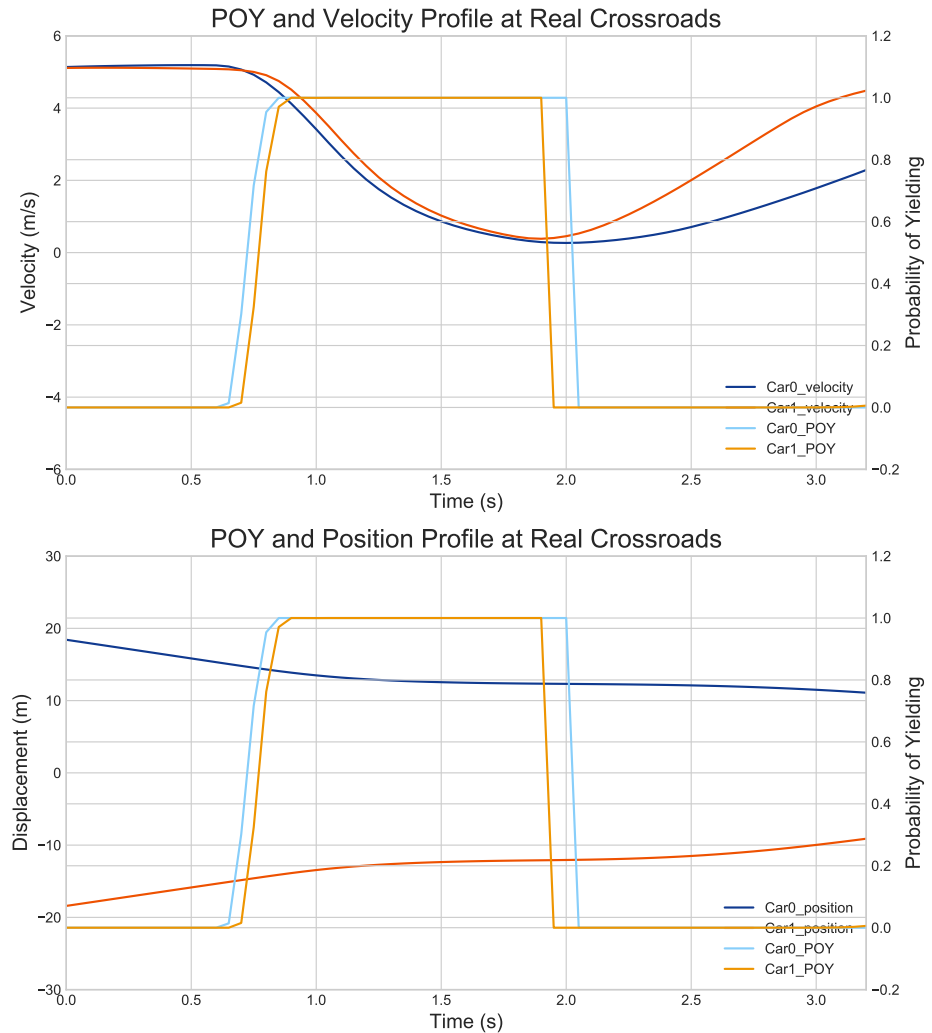


Figure 5.1: The velocities and displacements versus POYs of a normal case where no collision happened.

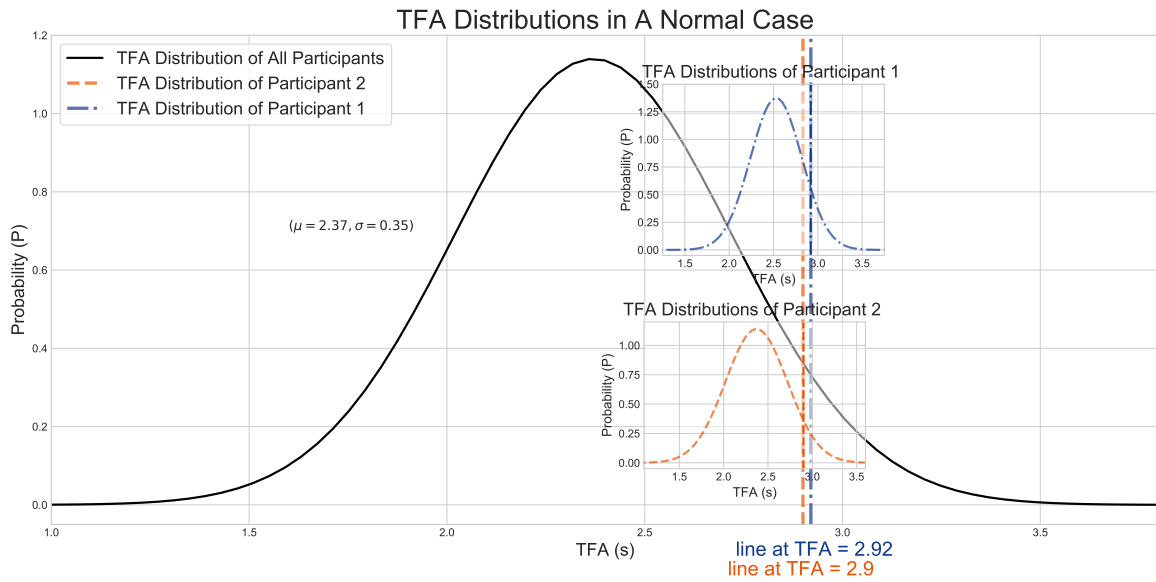


Figure 5.2: TFA distributions of Participant 1, 2 and average of a normal case where no collision happened.

in Fig. 5.1, where both vehicles yielded at around sec to avoid potential collisions from happening. When looking closer at the point of braking of both vehicle, the situation at this moment could be described using the concepts of TFA distributions as shown in Fig. 5.2. The TFA distribution in black solid line is the average TFA distribution of all people, as illustrated and identified in Chapter III. Two vertical dash lines (all-dash and dash-dot) indicate the TTCs of Car_0 (the driver is Participant 1) and Car_1 (the driver is Participant 2) at braking, which are 2.92 and 2.90 respectively (brakes were applied at around 0.7 sec in Fig. 5.1). Sub-figures with dashed TFA distributions are the TFA distributions of Participant 1 and 2 (drivers of Car_0 and Car_1 respectively). In this case, both drivers brake at the TTC with relatively high likelihood (around 0.4) in the average TFA distribution.

Then, a case where collision happened is shown in Fig. 5.6 and Fig. 5.4. Similarly, the velocities and displacements of both vehicles participated in this crashing case is shown in Fig. 5.6, however this time, two vehicles collided with each other.

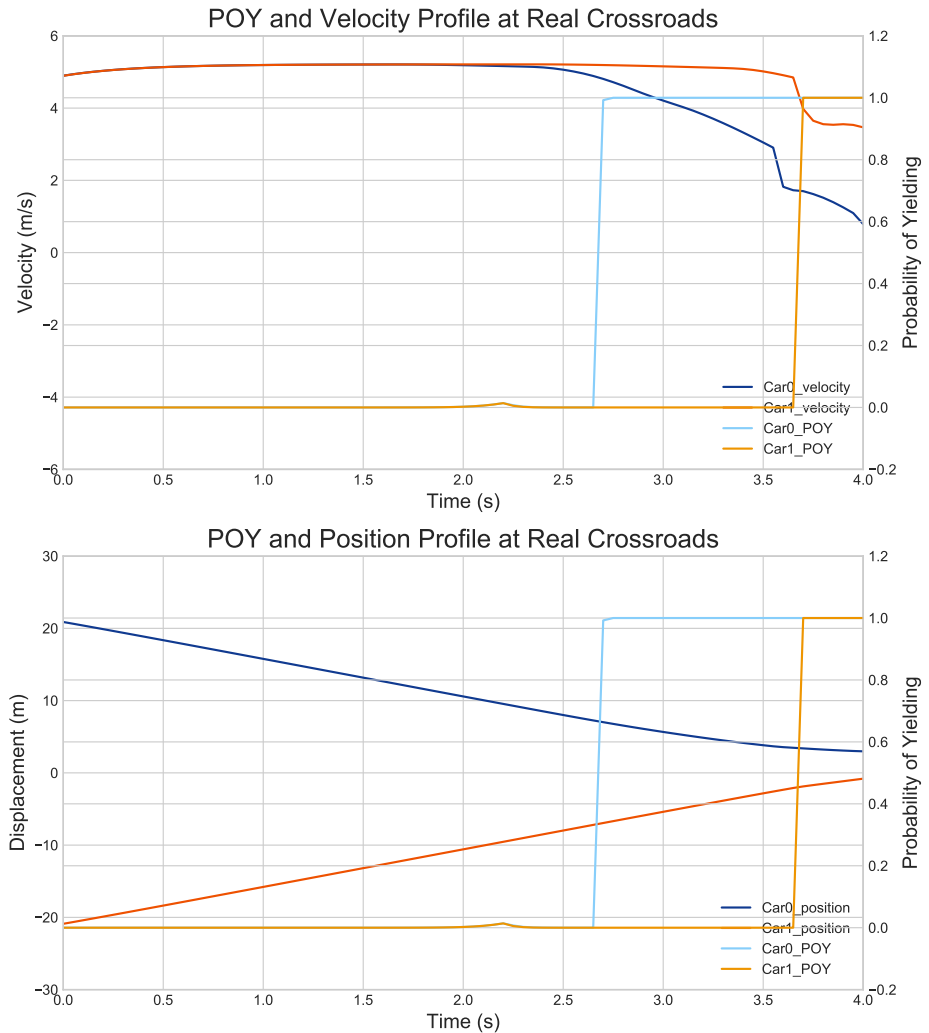


Figure 5.3: The velocities and displacements versus POYs of a normal case where a collision did happened.

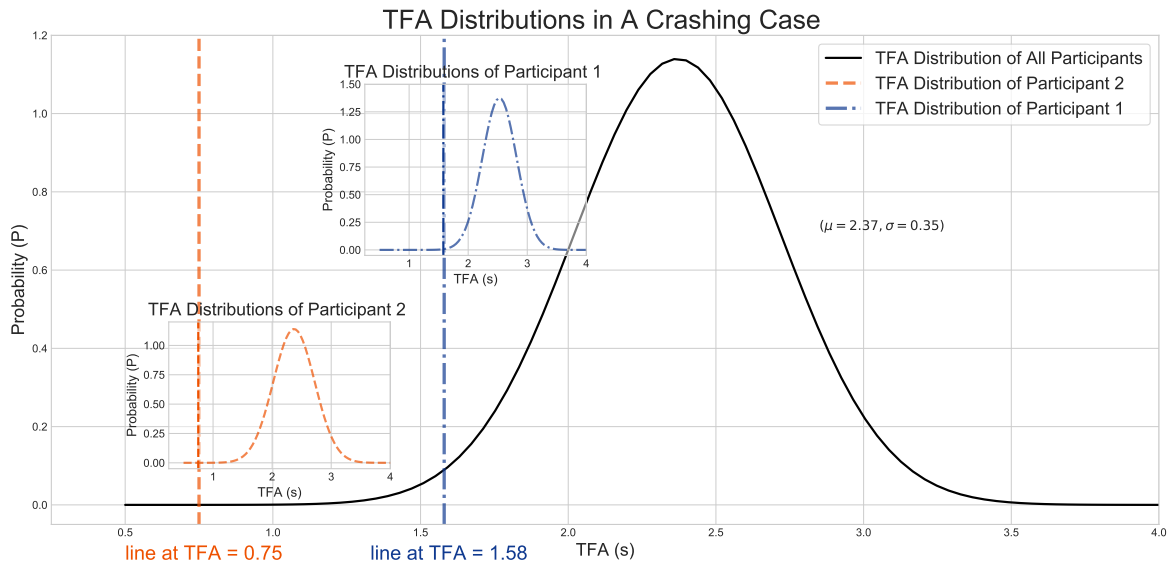


Figure 5.4: TFA distributions of Participant 1, 2 and average of a normal case where a collision did happened.

In Fig. 5.6, driver of Car_0 (i.e. Participant 1) believed that the other driver would yield to him, while driver of Car_1 (i.e. Participant 2) did not even noticed Car_0 (possibly due to the lack of concentration and obstructions of his view), so they both approached to the intersection with max speed. At around 2.5 sec, Participant 1 finally braked because he realized that the collision was going to happen, and Participant 2 braked at aroundd 3.5 sec, right before the collision. Still, the late braking did not prevent the collision at around 3.6 sec from happening. Then, again, the examination of this scenario using TFA distributions is conducted, as shown in Fig. 5.4. The figure shows the average TFA distribution in the solid black normal distribution while the TFA distributions of Participant 1 and 2 are shown in dash-dot blue curve and all-dash orange curve respectively. The two dashed lines again indicate the TTCs at the moment of braking for two drivers, which are 0.75 for Participant 2 and 1.50 for Participant 1 respectively. At these TTCs, the likelihoods are both below 0.1, which suggested it is less likely for drivers to brake at these TTC. And the

low TTCs also represent aggressive behaviors (brake at shorter distances under the same speed).

Comparing this crashing case (Fig. 5.4) to the normal case where no collision happened (Fig. 5.2), we can easily see that in the crashing case, behaviors of drivers tend to be more aggressive (the TFAs of drivers are very low, i.e. they brake at very low TTCs) and they are also less likely to happen (very low likelihood). This finding not only shows that the concept of the proposed model is effective, but also provides a different way to examine the likelihood of accidents happening under some particular behaviors. For example, when drivers at certain crossroads are found to have braking TTCs on the far-left side of the average TFA distribution, it is reasonable to argue that the possibilities of accidents happening in these crossroads are higher due to the more aggressive braking which are also less likely to happen in a normal braking process (the TFA distribution).

5.1.2 TTC differences and POYs

The differences between the normal and crashing cases can also be distinguished using the TTC differences and the proposed POY. The TTC difference is the difference of the arriving time between two vehicles attempting to cross the intersection at the same time, so smaller the time difference, higher the risk that two vehicles might collide with each other. If either of the vehicles brakes to yielded, the TTC difference will start to expand due to the increasing of the TTC value of the braking vehicle (because the decreasing of the vehicle speed).

Moreover, the proposed POY can be treated as an index if the weighting term A_t is not applied. Without the weighting term, the POY then rises only when the area under the TFA distribution and right to the current TTC is expending, which indicating that under current TTC, the chances for drivers to brake at that moment is higher. The reason for not using the weighting term A_t is that instead of predicting

the behavior of the driver based on his or her current states, only how likely the driver will brake is considered (i.e. whether the driver should brake or not at that TTC).

Combining the TTC difference and the POY without the weighting term, differences between the normal crossing cases and those ending up with collisions at the intersection could be identified. In Fig. 5.5 and Fig. 5.6, the figure at the top is the velocities of the both vehicles shown together with the POY curves without the weighting term, while the figure at the bottom includes the POY curves without the weighting term and the TTC difference indicated in red dashed line. For the cases where pairs of vehicles crossed the intersection without any collision, as shown in Fig. 5.5, the POYs without weighting term rose as both vehicles were drove toward the node which means that more and more drivers will brake at this moment to avoid potential collisions. And about 0.5 second before the rise of POYs, the TTC differences rose due to the brake of Car_0. This rising continued before Car_1 passed the node. The larger the value of the TTC difference indicating more buffer time and less chance for the collision.

When it comes to the cases where two vehicles end up colliding with each other, as shown in Fig. 5.6, the TTC difference were kept low and did not rise as the POYs were rising. It rose way after the rise of POYs and about 0.8 second before the collision happen owing to the emergency brake was applied. Note the cluttered segments on the velocity lines representing the collision coming right after the emergency brake. In the crashing cases, both vehicles did not notice each other or believed the brake would be applied by the other vehicle, which all end up with crashing at the intersection.

Hence, combining what are observed in both the pass-and-yield cases and the crashing ones, the late-rising TTC difference is highly relevant to the crashing cases. Despite the insufficient data of crashing cases to determine a more accurate TTC difference values and timing that will lead to the crashing, this finding is crucial for identifying the safety index at traffic scenarios. Using this method, it is possible

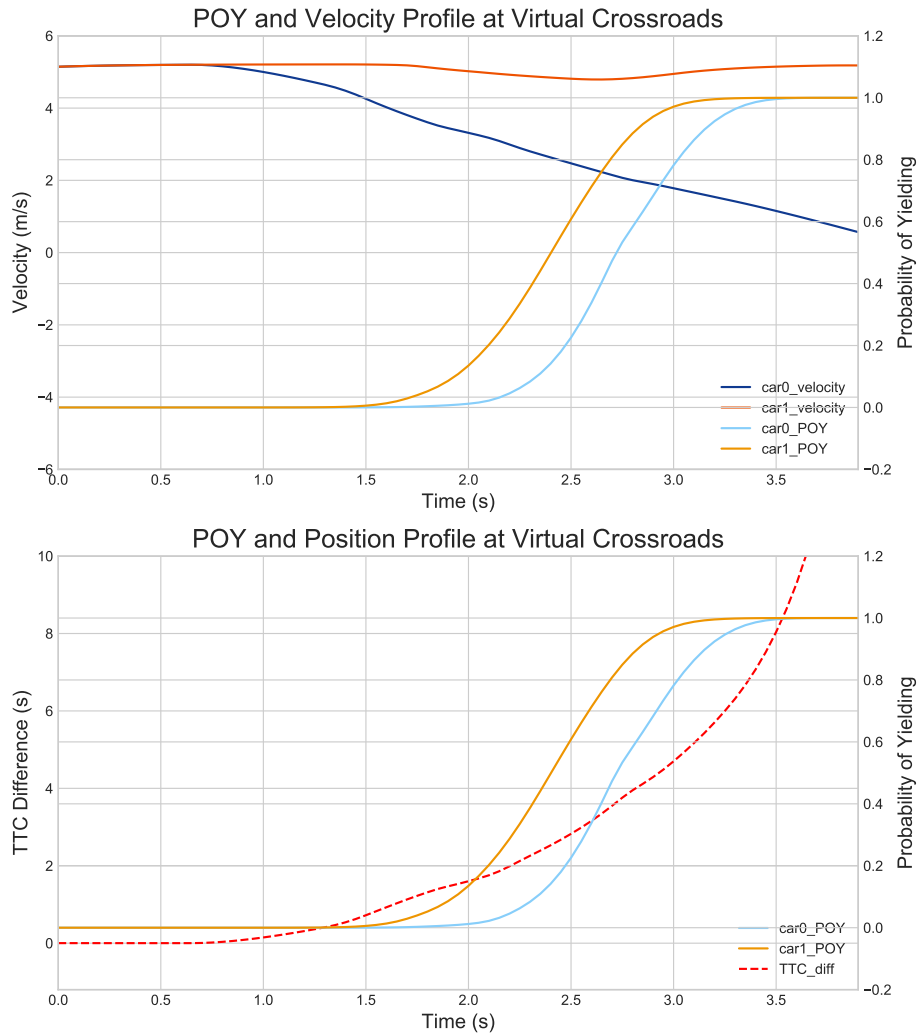


Figure 5.5: Situation where vehicles attempting to cross the intersection passed without any collision. Note that the TTC differences rose before POYs.

to estimate the risk of accidents according to the driving patterns of the drivers in certain area.

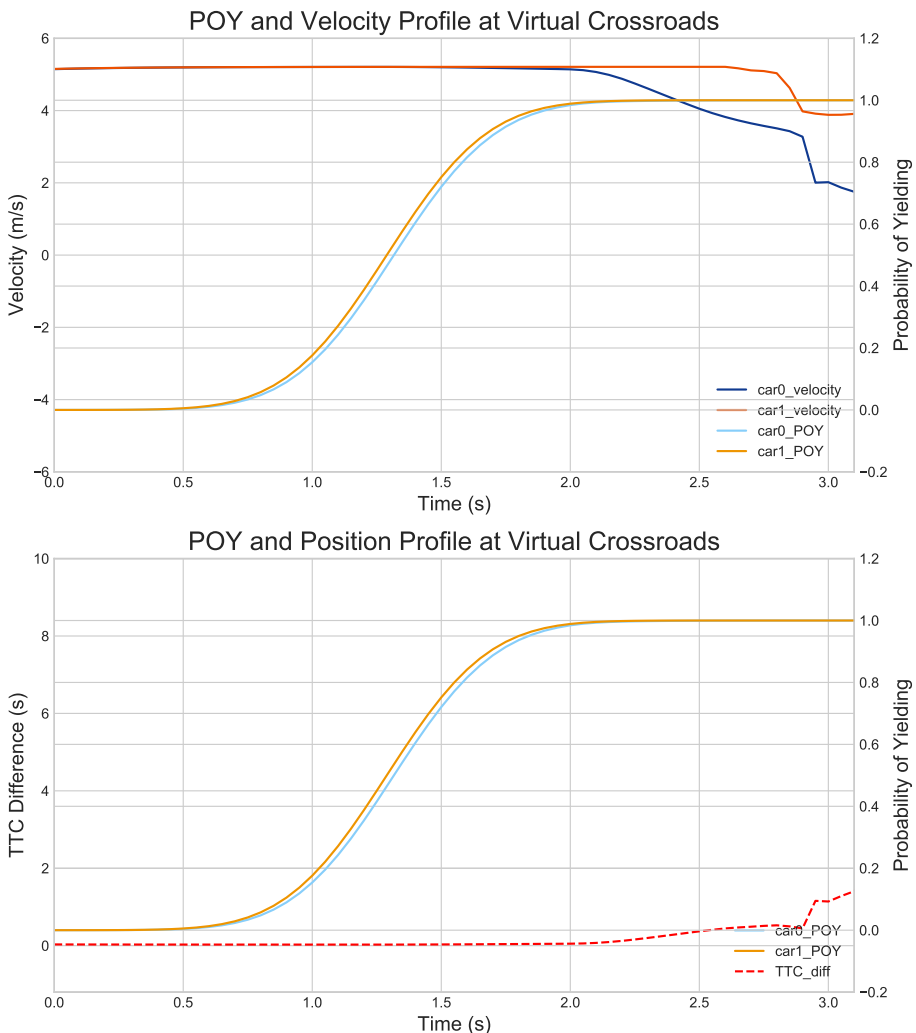
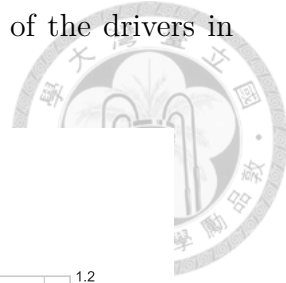
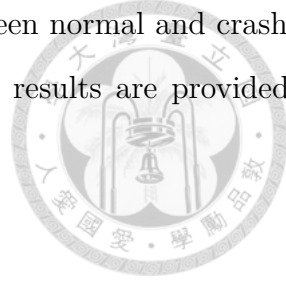


Figure 5.6: Situation where vehicles attempting to cross the intersection collided with each other. Note that the TTC differences rose way after POYs.

In this section, possible measures to estimate the possibility of accident happening is proposed. The method uses the TFA distributions to identify the likelihood and the aggressiveness of driver behaviors in certain areas. Then, the TTC differences and the

proposed POY are used also to explain the differences between normal and crashing cases. Despite further validations are required, convincing results are provided in both methods and ready to be extended.



5.2 POY Estimation at Urban Crossroads

The experiments are conducted to verify whether the proposed POY model can also count for the driver behaviors at the crossroads in real world. In the previous chapter, the importance of characteristic parameter is shown on how the resulting POY curves are affected by different sets of parameters. However, in the complex and stochastic world, to identify the characteristic parameters of all people is impractical and almost impossible, so the average parameter of the participants in the virtual crossroads experiments are adopted in the following experiments, before a more accurate set of parameters that can represent the observed crossroad is identified.

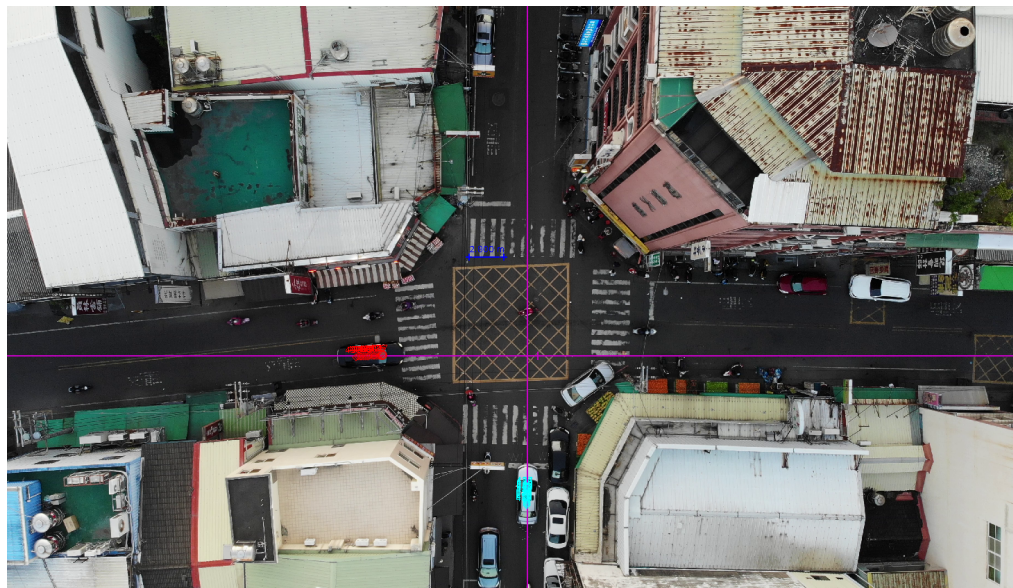


Figure 5.7: Using video analysis tool to track vehicles driven by humans.

To collect the related data, the drone for aerial filming is used at the crossroad in

urban environment (*Bo’ ai Rd.93-85, Yuanlin City, Changhua County 510, Taiwan* (23.958606, 120.573283)). This crossroad is an uncontrolled intersection, where no traffic signal available. To simplify the scenario, cases similar to the assumptions of the proposed model are observed. No turning is allowed and only two participants are involved in the interaction. After the interaction is over, the video analysis tool "tracker" is used to collect and analyze relevant variables (e.g. velocities and displacements). The image from the recorded films is shown in Fig. 5.7. Note that the angle of the road on the left hand side (about 6.7°) could be ignored since it only results in approximately 0.1% difference in velocity. Red and cyan circles indicate the position history of the vehicles at that moment, and the node is set at the intersect of two courses. Interval between every two frames is 0.042 second (24 fps). With the position and the time, the velocity is calculated. To better evaluate the driving behavior, we choose clips with maneuvers of two vehicles that are likely to cause a collision.

Two of the interaction are shown in Fig. 5.8 and Fig. 5.9 where the POY curves are similar to those example trials in the virtual crossroads. Owing to the measurement errors for the collected velocity and position profiles, the data shown are smoothen by the means of averaging every 5 collected data. Hence, the derived time step becomes 0.05 sec, which does not exert any influence to the POY estimation.

In the Fig. 5.8 (case I), the speed of car_0 was slightly above car_1 while the displacements to the node were exactly the same at the beginning of the interaction. At around 1.6 sec, the rise of the POY curve of car_0 was due to the estimated TFA being approached by the lowering TTC. However, this intention was not perceived by the driver of car_1 because of the subtle difference in their velocities and displacements. After about 1 second later, car_1 decelerated and decided to yield, causing the rise of the POY curve. The POY of car_0 then drop to 0 about 1 sec after the car_1 started to yield.

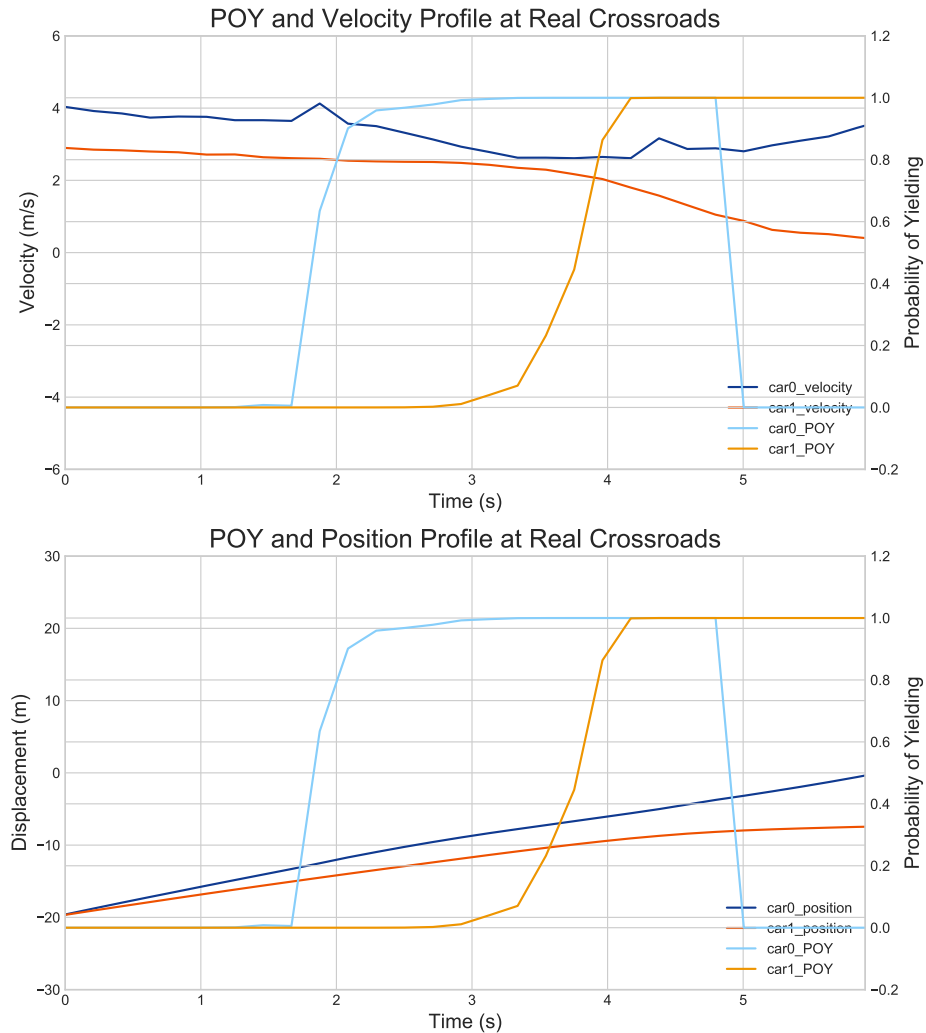
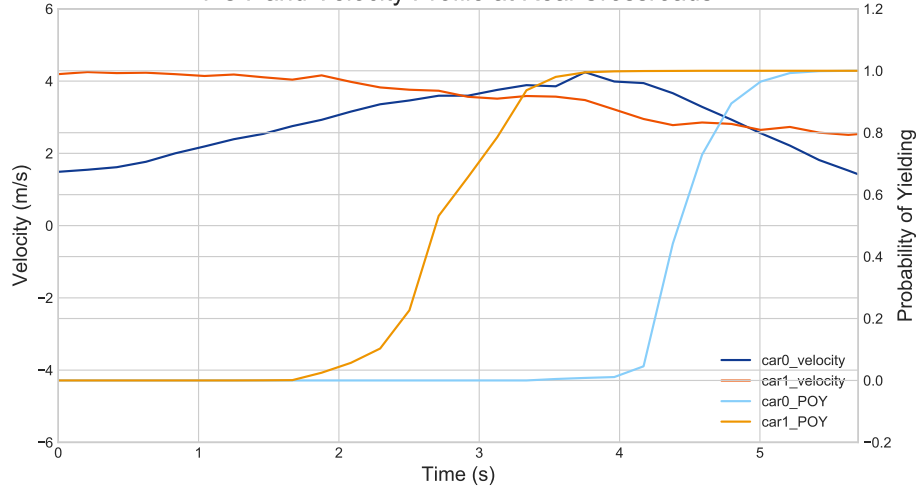


Figure 5.8: The corresponding POY curve at a crossroad in real world (Case I). car_0 had the dominance position and passed at the end.



POY and Velocity Profile at Real Crossroads



POY and Position Profile at Real Crossroads

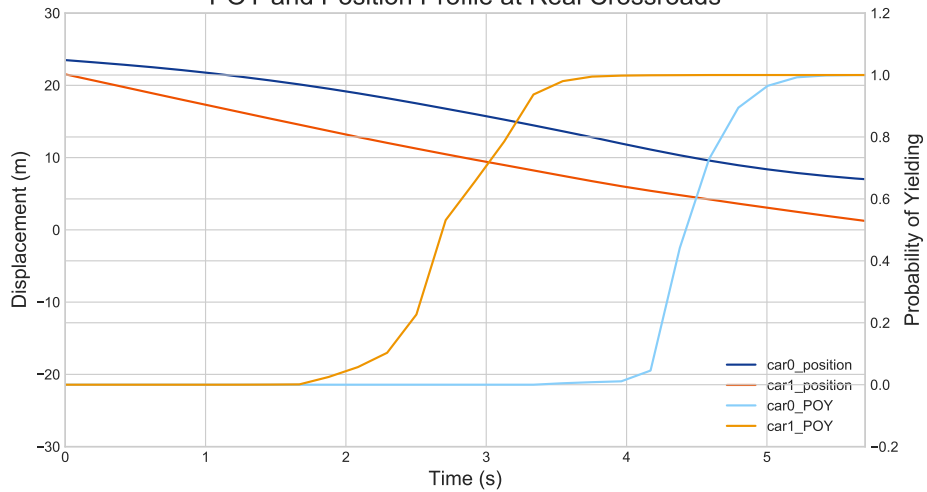


Figure 5.9: The corresponding POY curve at a crossroad in real world (Case II). car_1 had the dominance position but yield at the end.

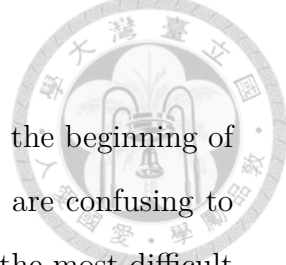
There are two possible reasons that car_1 did not choose to pass at the moment car_0 begun to yield. First reason is that the intention of the driver of car_0 was not perceived because of the subtle velocity difference it made. Second reason would be the closer position of car_0 to the node, which is about 3 meters at the moment car_1 yielded. So the driver of car_1 was observing the next decision made by the other driver during 2 to 3.5 sec. But the car_0 did not make any more obvious move, so car_1 yielded to avoid possible collision.

In Fig. 5.9 (case II), car_1 had faster speed and closer position to the node, but it started decelerating from around 2 sec owing to the acceleration of car_0. The POY of car_1 ascended as it decelerated and the TTC had gone closer to the estimated TFA distribution. Till it reached the node, the POY was kept at 1. The possible explanation for this is that car_1 was much closer to the node (about 6 meters) than car_0 was, so despite the intention to yield, it did not fully stopped, but was braking very slowly and prepared to yield to the end.

What can be learned form these two cases are that both cases show similar probabilistic pattern during the observation, which is also comparable to human drivers' prediction. Faster vehicles or vehicles closer to the node (the intersection of the cross-road) are in dominance of crossing over, so despite the intention to yield, they often pass at the end.

From these two cases, the decisions of human drivers are managed to be turned into probabilistic values and the results are similar to what was done in Chapter III. However, what the virtual environment can improve to approximate the real one more accurately is that the acceleration values should be set lower or some penalty measures should be taken to keep the participants from driving too recklessly.

5.3 Procedures for Autonomous Vehicle



Situations are that both driver at the crossroad both yielded at the beginning of the interaction. As we can see in Fig. 5.10, this kind of situations are confusing to human drivers and also autonomous vehicles. For humans, even in the most difficult situation, the solution to this scenario could be a gesture or flashing in the head light. For autonomous vehicles, however, to identify the situation where the other driver is yielding itself poses a problem already.

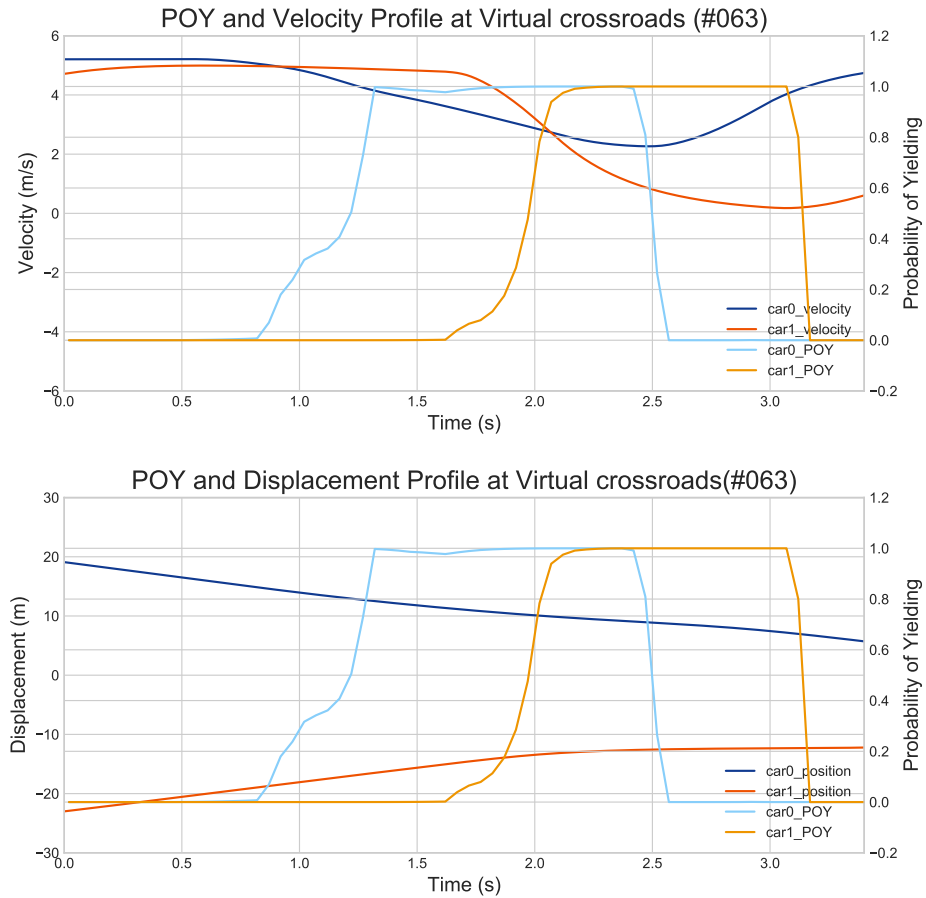


Figure 5.10: Both drivers yielded at the beginning of the interaction.

The strategy for autonomous vehicles nowadays to handle the interaction with human is yielding all the time, regardless of the real intentions of the other traffic participant. This kind of behaviors, as mentioned in the Chapter I, might lead to collisions since it is not what human drivers usually do. This is where the proposed driver behaviors model comes in handy. With the capability of perceiving the intentions of other traffic participants and present it in a probabilistic way, the POY could be used as a safety measure to handle the situations.

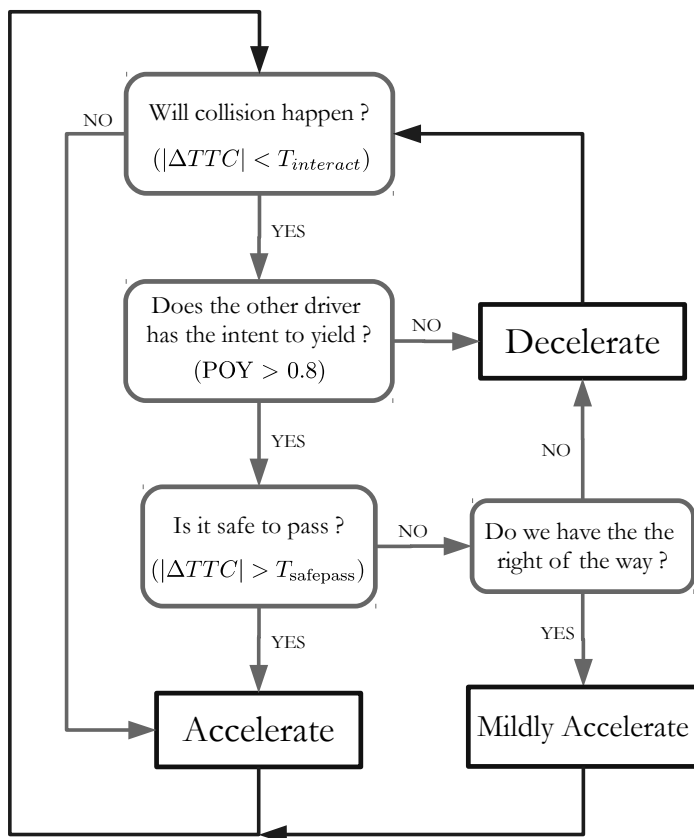


Figure 5.11: Flow chart for autonomous vehicle to deal with the interactions with human drivers.

When facing complex interactions such as both are yielding, which is similar to

the one shown in Fig. 5.10, or when the other vehicle insists on yielding after the autonomous vehicle yield, the process of interaction might take a while, since it is often that both drivers accelerate and decelerate together, leading to a stand off like situation. To allow autonomous vehicle to handle this, a procedure for them to follow is shown in the the flow chart (Fig. 5.11).

When another traffic participant is detected, the possibility of potential collision happening is first checked. Note that the $|\Delta TTC|$ stands for the absolute value of the difference of TTC between two vehicles. Due to the definition of TTC is the time it takes to arrive at the node, if this difference is smaller than a threshold $T_{interact}$, a collision might happen if no action is taken. Then the POY is checked, where it is defined as yielding if the POY is greater than 0.8 (which is an empirical value). The autonomous vehicle will brake if the other driver intends to pass and will check the $|\Delta TTC|$ again if the other driver intends to yield to make sure the passing is not threatening anyone. At this stage, it is guaranteed for collision-free even if the autonomous vehicle passes without checking the condition $|\Delta TTC| > T_{safe_pass}$. However, the smaller the $|\Delta TTC|$, the more dangerous the other driver might feel, hence the threshold T_{safe_pass} is defined. For the $|\Delta TTC|$ that might be terrifying to others, the right of the way is then checked, and there will be mild acceleration if the autonomous vehicle has the right of the way. Otherwise the situation will become both yielding, which would spend both parties a considerable amount of time.

This procedure is applied to the navigation system of one of the simulated vehicle in Gazebo. In Fig. 5.12, the POY curves during the interaction between human driver and autonomous vehicle (computer driver) are plotted. In this case, both vehicles yielded in the beginning, but as the human driver kept yielding, the computer driver decided to pass. Note that computer driver waited until ($|\Delta TTC| > T_{safe_pass}$) before it accelerated.

A few more trials were also conducted to examine the similarity between hu-

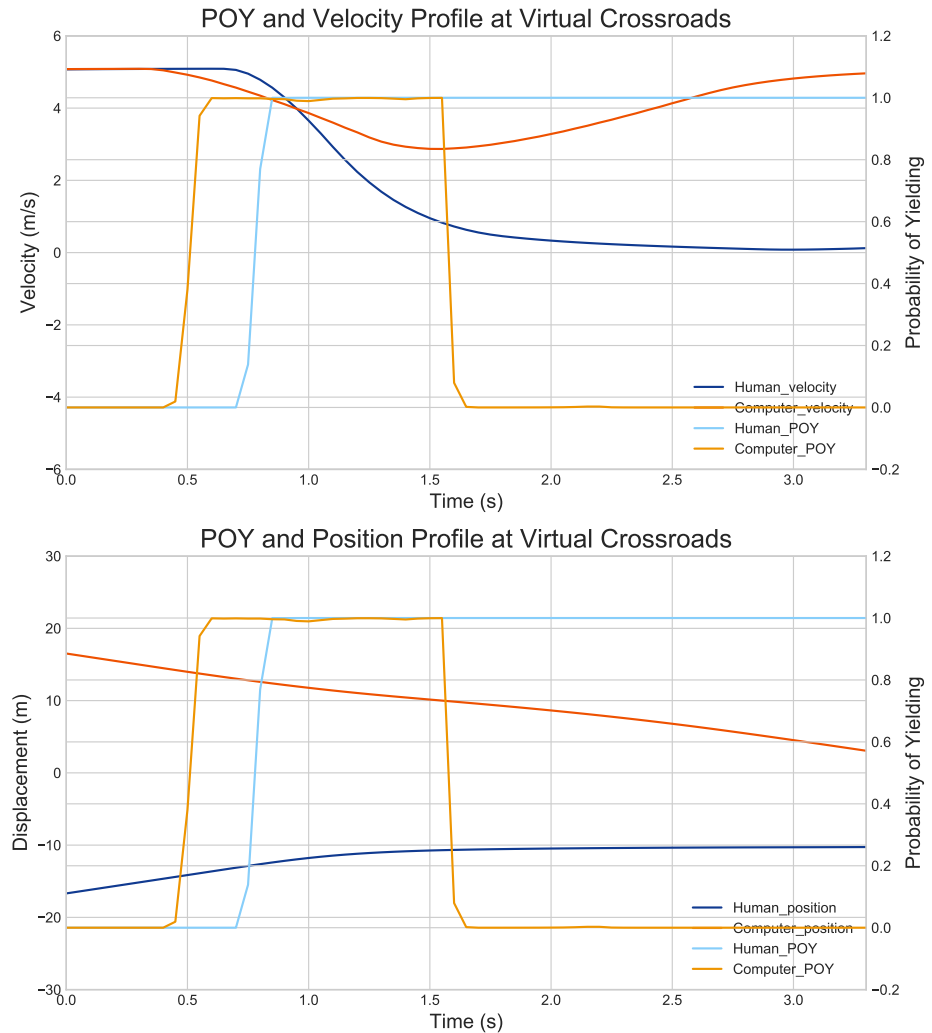


Figure 5.12: The POYs during the interaction between human driver and autonomous vehicle (computer driver) in the simulated environment.

man drivers and autonomous vehicles following this procedure. Human contestants were asked to drive across the virtual crossroad as in the previous experiments without knowing that the other vehicle was actually an autonomous vehicle with the proposed navigation system. Almost all the contestants did not realize it was the autonomous vehicle they were interacting. Even though the experiments were not assessed thorough enough, it is an initiation to make autonomous vehicles drive more like human.



Figure 5.13: The scene of interaction between human driver and autonomous vehicle with navigation algorithm in the simulated environment.

In this chapter, the possible applications for the proposed model are explored. First, the crashing cases were identified to be highly related to certain aggressive driver behaviors. Then, proposed POY was used to evaluate the intentions of drivers at crossroads in real world. The result are similar to those observed and verified in the simulated environment. Then, a procedure was defined to allow autonomous vehicle to have a more efficient and smooth interaction process when facing difficult situations. These applications will be further extended to finally apply on a real autonomous devices.



CHAPTER VI

Conclusions and Future Works

6.1 Conclusions

In this thesis, the behaviors of human drivers were modeled in a probabilistic way based on the cognitive information. In Chapter III, the fundamental concepts used in the proposed method were introduced. These concepts include: 1) the definition of TTC with its role to human drivers in cognitive science and the simplified crossroad model; 2) the presupposition of TTA distribution being normally distributed and the verification of it. Then the proposed POY was finally formulated and the required parameters in the model were also identified. In the last section of the chapter, the experiments were conducted in the virtual environment for the purpose of validation, and the results suggested the prediction accuracy rate being comparable to the state of the art method with more applicability.

Following the core model, the characteristic parameters identification was proposed using optimization method in Chapter IV. First the objective function was formulated with the area under the corresponding CARate curve using a set of parameter. Constraints were also listed according to the boundaries set in the simulated environment. Despite the set of parameters identified was not accurate enough, the proposed procedure is a preliminary method for characteristic parameters recognition.

Possible applications using the proposed model were explored in Chapter V. The

proposed model was applied at the crossroad in urban area, where no traffic signal was at the scene. The outcomes showed almost identical POY curves as in the simulated environments, providing evidence for the usefulness of the proposed model in real world. Then, a procedure was also developed to help autonomous vehicles handling the complex situation. Finally in this chapter, after the summary of this thesis, the possible extensions and directions for the proposed model and applications will be discussed.

6.2 Future Works

For the simulated experiments in the virtual world, some enhancements could be done to generate better results. Firstly, the database for the average parameters in the simulated environment could be extended to find a closer average parameters, so the performance could be improved when estimating the intention of an unknown driver. Secondly, using joystick to imitate the throttle and the brake of a real vehicle makes confusion for a licensed driver. The angles of views from the simulated environment are also quite different from that in a real vehicle. Despite these defects would not affect the prediction using the proposed model because the parameters used in the model are also gathered in the simulated environment, a more realistic virtual crossroad can make the data gathered in virtual world more applicable in the real world. In Chapter IV, some improvements are required for the characteristic parameters identification. Adding penalty functions to the optimization problem could be a possible direction to make modification since the over sensitive results consistent in the overrated POY values. When the parameter identification become reliable and robust, the average parameters of the urban crossroads can then be identified. The average parameters of the area can not only gives us the average driving styles of the area, but can also be applied to autonomous vehicles around that area to let them make better judgements of the possible behaviors of the surrounding vehicles.



BIBLIOGRAPHY





BIBLIOGRAPHY

- [1] S. Thrun, M. Montemerlo, H. Dahlkamp, D. Stavens, A. Aron, J. Diebel, P. Fong, J. Gale, M. Halpenny, G. Hoffmann, et al. Stanley: The robot that won the darpa grand challenge. *Journal of field Robotics*, 23(9):661–692, 2006.
- [2] P. Bansal and K. M. Kockelman. Forecasting americans’ long-term adoption of connected and autonomous vehicle technologies. *Transportation Research Part A: Policy and Practice*, 95:49 – 63, 2017.
- [3] US Department of Transportation. Preparing for the future of transportation: Automated vehicles 3.0 (av 3.0). Technical report, sep 2018. Accessed: 2019-06-23.
- [4] Todd Litman. Autonomous vehicle implementation predictions: Implications for transport planning. Technical report, Victoria Transp. Policy Inst., Victoria, BC, Canada, 2015.
- [5] California DMV. Report of traffic collision involving an autonomous vehicle (ol 316), 2019.
- [6] B. Paden, M. Čáp, S. Z. Yong, D. Yershov, and E. Frazzoli. A survey of motion planning and control techniques for self-driving urban vehicles. *IEEE Transactions on Intelligent Vehicles*, 1(1):33–55, March 2016.
- [7] S. Lefèvre, D. Vasquez, and C. Laugier. A survey on motion prediction and risk assessment for intelligent vehicles. *ROBOMECH Journal*, 1(1):1–14, 2014.
- [8] S. Ammoun and F. Nashashibi. Real time trajectory prediction for collision risk estimation between vehicles. In *2009 IEEE 5th International Conference on Intelligent Computer Communication and Processing*, pages 417–422, Aug 2009.
- [9] P. Fiorini and Z. Shiller. Motion planning in dynamic environments using velocity obstacles. *The International Journal of Robotics Research*, 17(7):760–772, 1998.
- [10] W. Zhan, C. Liu, C. Chan, and M. Tomizuka. A non-conservatively defensive strategy for urban autonomous driving. In *2016 IEEE 19th International Conference on Intelligent Transportation Systems (ITSC)*, pages 459–464, Nov 2016.

- [11] M. Ruf, J. Ziehn, B. Rosenhahn, J. Beyerer, D. Willersinn, and H. Gotzig. Situation prediction and reaction control (sparc). In B. Färber, K. Dietmayer, K. Bengler, M. Maurer, Ch. Stiller, and H. Winner, editors, *9. Workshop Fahrerassistenzsysteme (FAS 2014)*, pages 55–66, Walting im Altmühltaal, Germany, March 2014.
- [12] S. Lefèvre, C. Laugier, and J. Ibañez-Guzmán. Evaluating risk at road intersections by detecting conflicting intentions. In *2012 IEEE/RSJ International Conference on Intelligent Robots and Systems*, pages 4841–4846, Oct 2012.
- [13] Ismail Dagli, Michael Brost, and Gabi Breuel. Action recognition and prediction for driver assistance systems using dynamic belief networks. In Jaime G. Carbonell, Jörg Siekmann, Ryszard Kowalczyk, Jörg P. Müller, Huaglory Tianfield, and Rainer Unland, editors, *Agent Technologies, Infrastructures, Tools, and Applications for E-Services*, pages 179–194, Berlin, Heidelberg, 2003. Springer Berlin Heidelberg.
- [14] T. Gindele, S. Brechtel, and R. Dillmann. Learning context sensitive behavior models from observations for predicting traffic situations. In *16th International IEEE Conference on Intelligent Transportation Systems (ITSC 2013)*, pages 1764–1771, Oct 2013.
- [15] A. Foka and P. Trahanias. Probabilistic autonomous robot navigation in dynamic environments with human motion prediction. *International Journal of Social Robotics*, 2(1):79–94, Mar 2010.
- [16] C. Hubmann, J. Schulz, M. Becker, D. Althoff, and C. Stiller. Automated driving in uncertain environments: Planning with interaction and uncertain maneuver prediction. *IEEE Transactions on Intelligent Vehicles*, 3(1):5–17, March 2018.
- [17] M. Liebner, M. Baumann, F. Klanner, and C. Stiller. Driver intent inference at urban intersections using the intelligent driver model. In *2012 IEEE Intelligent Vehicles Symposium*, pages 1162–1167, June 2012.
- [18] R. Graf, H. Deusch, F. Seeliger, M. Fritzsche, and K. Dietmayer. A learning concept for behavior prediction at intersections. In *2014 IEEE Intelligent Vehicles Symposium Proceedings*, pages 939–945, June 2014.
- [19] A. Kemeny and F. Panerai. Evaluating perception in driving simulation experiments. *Trends in Cognitive Sciences*, 7(1):31 – 37, 2003.
- [20] J.K. Caird and P.A. Hancock. The perception of arrival time for different oncoming vehicles at an intersection. *Ecological Psychology*, 6(2):83–109, 1994.
- [21] J. Hayward. Near miss determination through use of a scale of danger. *Report TTSC-7115*, 1972.
- [22] J. Tresilian. Visually timed action: time-out for ‘tau’ ? *Trends in Cognitive Sciences*, 3(8):301 – 310, 1999.

- [23] V. Cavallo and M Laurent. Visual information and skill level in time-to-collision estimation. *Perception*, 17(5):623–632, 1988. PMID: 3249670.
- [24] W. Winsum and W. Brouwer. Time headway in car following and operational performance during unexpected braking. *Perceptual and Motor Skills*, 84(3_suppl):1247–1257, 1997. PMID: 9229443.
- [25] S. Kirkpatrick, C. D. Gelatt, and M. P. Vecchi. Optimization by simulated annealing. *Science*, 220(4598):671–680, 1983.